Universidad de Valladolid

ESDUVa
Escuela de Doctorado Universidad de Valladolid

PROGRAMA DE DOCTORADO EN INGENIERÍA TERMODINÁMICA DE FLUIDOS

TESIS DOCTORAL:

"AMPLIACIÓN Y MEJORA DE LA CAPACIDAD DE MEDIDA Y CALIBRACIÓN DE HIGRÓMETROS DE PUNTO DE ROCÍO CON EL PATRÓN NACIONAL DE HUMEDAD EN EL MARGEN DE -10 ºC A 95 ºC"

Presentada por D. Tomás Vicente Mussons para optar al grado de Doctor/a por la Universidad de Valladolid

Dirigida por:

Dr. Robert Benyon Puig y Dr. José Juan Segovia Puras

ÍNDICE

1. INTRODUCCIÓN 3
2. OBJETIVOS 6
3. METODOLOGÍA Y RESULTADOS OBTENIDOS 7
3.1. Estudio de estabilidad a largo plazo y cociente de temperatura de higrómetros de punto de rocío. (Benyon R, Vicente T, Hernandez P, De Rivas L and Conde F. "Evaluation of the Long-Term Stability and Temperature Coefficient of Dew-Point Hygrometers". Int. Journal of Thermophysics (2012). Vol. 33, Issue 8-9, pp 1758-1770). 7
3.1.1. Magnitudes de influencia. 9
3.1.2. Estabilidad a largo plazo 11
3.2. Estudio de la influencia de la presión. Desarrollo de sistemática (Mitter H, Böse N, Benyon R and T. Vicente, "Pressure drop considerations in the characterization of dew-point transfer standards at high temperatures". Int. Journal of Thermophysics (2012), Vol. 33, Issue 8-9, pp 1726-1740). 13
3.2.1. Configuración de medida 14
3.2.2. Caída de presión en función del caudal volumétrico (gas seco) 15
3.2.3. Caída de presión en condiciones de gas húmedo 17
3.2.4. Comparativa de configuraciones de muestreo 17
3.3. Relación entre termometría de contacto y realización de temperatura de punto de rocío. (Benyon R, Böse N, Mitter H, Mutter D, Vicente T "An Investigation of the Relation Between Contact Thermometry and Dew-Point Temperature Realization". Int. Journal of Thermophysics (2012), Vol. 33, Issue 8-9, pp 1741-1757). 19
3.3.1. Caracterización y selección de TRP 19
3.3.2. Comparativa entre termometría de contacto y medida de punto de rocío 23
3.4. Consistencia de las realizaciones de punto de rocío de los patrones nacionales de humedad. (Benyon R and Vicente T "Consistency of the national realization of dew-point temperature using standard humidity generators". Int. Journal of Thermophysics, (2012) Volume 33, Issue 8-9, pp 1550-1558). 26
3.4.1. Estado del arte antes de la nueva sistemática 26
3.4.2. Comparación con la nueva sistemática 28
3.5. Comparación clave internacional de temperatura de punto de rocío en el margen de 30 ºC a 95 ºC (CCT-K8) 32
3.5.1. Protocolo 32
3.5.2. Resultados preliminares 34
4. CONCLUSIONES 36
5. REFERENCIAS 38
6. SÍMBOLOS Y ABREVIATURAS 41
7. ANEXOS 42

1. INTRODUCCIÓN

En España, se cuenta con una infraestructura metrológica distribuida y coordinada por el Estado. Esta estructura se ha conformado de manera natural por la propia historia y trayectoria científica de las instituciones y organismos que la constituyen, con vista a optimizar recursos, no repetir instalaciones singulares, así como aprovechar y rentabilizar el conocimiento y talento existente en las mismas.

La Infraestructura Española de Metrología es coordinada por el Consejo Superior de Metrología (CSM), creado por el artículo 11 de la Ley 3/1985, de 18 de marzo, de Metrología. Es el máximo órgano consultivo y de coordinación del Estado en el campo de la metrología científica, técnica, histórica y jurídica. Forma parte de la Secretaría General de Industria y de la Pequeña y Mediana Empresa del Ministerio de Industria, Energía y Turismo. No puede atribuirse estrictamente el estatuto de organismo comparable a una comisión interministerial, ya que coordina las actividades de los departamentos ministeriales relacionados con la metrología. Sin embargo, su función está orientada a cumplir este objetivo, teniendo en cuenta el gran impacto que las mediciones tienen en las actividades cotidianas, informando y proponiendo al Ministerio de Industria, Energía y Turismo ya través de éste al Gobierno, según sea el caso, las acciones para un sistema nacional de medida coordinado.

Las realizaciones prácticas de las unidades de medida que constituyen los patrones nacionales y su diseminación al resto de usuarios de la metrología son realizadas por el Centro Español de Metrología (CEM) y sus seis laboratorios asociados (LL.AA.), en función de lo establecido en los artículos 4 y 17 de la Ley 32/2014, de Metrología de 22 de diciembre. La figura **1.1** muestra la infraestructura metrológica nacional.

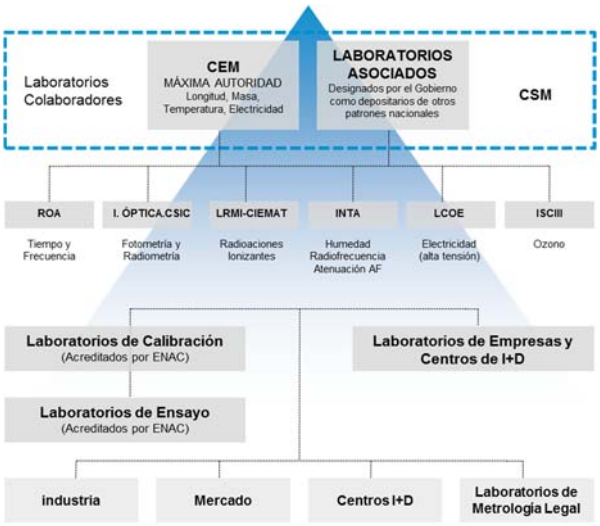

Fig. **1.1** Infraestructura metrológica nacional

El Instituto Nacional de Técnica Aeroespacial, “Esteban Terradas” (INTA) es depositario de los patrones nacionales de humedad y laboratorio asociado al CEM, de acuerdo con lo establecido en el Real Decreto 346/2001, de 4 de abril. En su doble carácter de laboratorio asociado al CEM y depositario del mencionado patrón nacional, el INTA es responsable, en nombre del Estado, de la custodia, conservación, mantenimiento y difusión del patrón nacional de las unidades derivadas citadas. El R.D. establece que esta responsabilidad se llevará a cabo bajo la supervisión y coordinación del Centro Español de Metrología.

La humedad es una de las unidades derivadas definidas en la Orden ITC/2581/2006, de 28 de julio. En esta orden se declara que: “el patrón nacional de la magnitud humedad, cuya unidad es el ºC de punto de rocío (ºCpr), es mantenido, conservado, custodiado y diseminado, bajo la supervisión y coordinación del Centro Español de Metrología, por el Laboratorio de

Temperatura y Humedad del Instituto Nacional de Técnica Aeroespacial «Esteban Terradas». Está materializado mediante generadores de humedad de precisión, utilizando el principio de saturación de un gas a una temperatura y presión conocidas y su posterior expansión. Estos generadores cubren el campo de temperatura de punto de rocío de -75 ºC a -10 ºC con saturación sobre una superficie de hielo, y de -10 ºC a + 75 ºC para saturación con respecto a agua, así como el campo de humedad relativa equivalente en el campo de temperatura ambiente de 5 ºC a 75 ºC. Este patrón se conserva mediante la comparación periódica efectuada con patrones de humedad de organismos metrológicos de otros Estados."

La incertidumbre expandida de medida de la temperatura de punto de rocío (para k=2) del INTA en el margen de interés de esta Tesis, es de 0,05 °C en el intervalo de -10 °C a 50 °C, de 0,10 °C hasta 60 °C y de 0,15 °C hasta 75 °C.

La temperatura de punto de rocío se materializaba en este margen con un generador comercial, Thunder Scientific modelo 9000, adquirido en el año 1994 y con un margen nominal de temperatura de punto de rocío -10 ºC a 70 ºC. Este generador fue optimizado mediante modificaciones del sistema de control del nivel del saturador, introducción de un purgado de líneas de medida de presión, instalación de un bypass del presaturador y el uso de instrumentación de medida independiente que permitía asegurar la trazabilidad metrológica de la medida de temperatura y presión absoluta al más alto nivel requerido. Este generador fue caracterizado en un margen ampliado hasta 75 ºC.

La creciente demanda de trazabilidad de higrómetros de punto de rocío con menor incertidumbre y a temperaturas más altas, fomentado por las mejoras de especificaciones declaradas por los fabricantes de instrumentación, ha impulsado la puesta en marcha de un nuevo generador patrón de humedad alta, ampliando el rango actual hasta 95ºC, según se describe en esta Tesis.

Los trabajos documentados en las cuatro publicaciones que conforman esta Tesis [2-4], tienen como propósito la ampliación de la capacidad de medida y calibración (CMC), con un estudio de las magnitudes de influencia, condiciones de medida y comparaciones que permiten materializar un nuevo patrón nacional de humedad [1] como se detalla a continuación:

En el primer trabajo [2] se analizan y documentan las dos características importantes de los patrones de transferencia que se emplearán en la caracterización del nuevo patrón nacional: la estabilidad a largo plazo y el cociente de temperatura. Se estudian las calibraciones realizadas en el laboratorio de temperatura y humedad del INTA, investigando todo el histórico de deriva las calibraciones realizadas por el laboratorio y aportando relevancia en el histórico de deriva. El propósito de este trabajo es establecer el estado del arte de las medidas en el INTA con trazabilidad al anterior patrón nacional en todo su campo de medida, y demostrar los valores límite a aplicar a las contribuciones de incertidumbre debido a la estabilidad a largo plazo y el cociente de temperatura de la medida de temperatura de punto de rocío. Esta publicación contiene trabajos realizados íntegramente en el INTA.

El segundo trabajo [3] tiene como propósito desarrollar y establecer una sistemática para asegurar que se establecen las condiciones de caudal de gas de muestreo de los patrones de transferencia para minimizar la contribución de incertidumbre debido a la influencia de la caída de presión resultante entre el punto de materialización de la unidad en el saturador del patrón y el punto de medida (espejo) del patrón de transferencia. Esta investigación se realiza debido a que durante el análisis del primer trabajo se detectó que por encima de 50 °C la corrección de los patrones de transferencia experimentaba un rápido cambio de tendencia. En un principio se pensó que tenía que ver con una limitación del generador patrón y por tanto la CMC debía incluir esta variación en la determinación de la incertidumbre de medida asociada. Posteriormente, durante una investigación con un medidor de presión diferencial y una modificación en la cabeza de medida del patrón de transferencia, consistente en sustituir el endoscopio por una toma de presión mecanizada en acero inoxidable con las mismas dimensiones exteriores, se pudo observar que la caída de presión incrementaba con el punto de rocío medido. La experiencia en ese momento era solo hasta 75 °C, pero en cuanto se hicieron las primeras medidas a 95 ºC el problema tomó una dimensión totalmente inaceptable

para la CMC necesaria para el nuevo patrón nacional. El error se debía a que se mantenía constante el caudal medido con un rotámetro situado tras una trampa de vapor, pero no se tenía en cuenta el caudal en las condiciones de medida de temperatura y presión del higrómetro. Por tanto, el caudal volumétrico (y la caída de presión asociada) en las condiciones de medida era muy superior al medido, ya que incorporaba el volumen correspondiente al vapor de agua que se había condensado en la trampa de vapor previo a la medida de caudal. Este hecho no se había detectado en comparaciones internacionales previas porque todos los participantes midieron de la misma manera, manteniendo constante el caudal medido tras la trampa de vapor. Este trabajo se realizó en colaboración con el Physikalisch-Technische Bundesanstalt (PTB) y E+E Elektronik Ges.m.b.H. (BEV/E+E), Instituto Nacional de Metrología (NMI) e Instituto Designado (DI) responsables de los patrones nacionales de humedad de Alemania y Austria, que aportaron históricos de sus medidas y que permitió realizar un estudio más universal de identificación del problema. El trabajo conjunto fue fundamental porque los investigadores involucrados habían determinado el protocolo de la comparación europea EURAMET-T.K8 de temperatura de rocío y habían participado en el mismo, junto con el autor. El INTA fue el laboratorio de enlace (link) midiendo los dos patrones viajeros de forma simultánea y el PTB y BEV/E+E eran los pilotos de la comparación. Los demás participantes solo midieron un patrón viajero en uno de los dos bucles de la comparación.

El tercer trabajo [4] se desarrolla con el propósito de determinar el estado del arte del uso de higrómetros de punto de rocío y establecer las contribuciones debido al flujo de calor y el gradiente de temperatura resultante en el espejo, entre la temperatura de la superficie donde se realiza la condensación y la posición del sensor de temperatura insertado en el espejo. Este trabajo se realizó también en una colaboración internacional, incluyendo no solo las determinaciones realizadas por el autor en el margen de interés de esta Tesis, sino también los resultados de las medidas realizadas en el PTB, BEV/E+E y el DI de Suiza, MBW Calibration AG (MBW). Este último es además el fabricante de los higrómetros estudiados y que se usarán en los siguientes trabajos de esta Tesis.

El alcance de la caracterización de la histéresis, estabilidad y calibración final de los sensores de temperatura integrados en los instrumentos investigados en el campo de medida aplicable a esta Tesis han sido definidos y estudiados por el autor y realizados en el INTA. Así mismo, las medidas de temperatura de punto de rocío han sido realizadas por el autor en el INTA. Los resultados obtenidos permiten establecer la clara relación entre la realización de temperatura de punto de rocío y la temperatura de referencia establecida por el sensor de temperatura (termómetros de resistencia de platino) para distintos tipos de encapsulado y tamaños de espejo del higrómetro. Los resultados obtenidos son fundamentales para la determinación de las contribuciones de incertidumbre por reproducibilidad del patrón al nivel requerido para la caracterización posterior.

Este trabajo se realiza en colaboración con los dos laboratorios nacionales para ampliar el alcance del trabajo a otros campos más de los de aplicación de esta Tesis e incluye al fabricante que colaboró facilitando la información de los sensores y construcción de los espejos y la integración de los mismos.

El cuarto trabajo [5] consiste en la determinación de la consistencia de la realización de punto de rocío de los dos generadores patrón nacional de humedad en su margen de solape de temperatura de punto de rocío de -10 ºC a +75 ºC. Este trabajo tiene dos finalidades:

La primera es asegurar que los laboratorios que han obtenido su trazabilidad metrológica a través del patrón nacional antiguo no van a sufrir ningún cambio en su histórico de deriva. Manifestando que los valores de referencia proporcionados por los dos patrones nacionales son totalmente equivalentes dentro del estado del arte de medida con higrómetros de punto de rocío. Cabe reseñar que con las técnicas desarrolladas en los anteriores trabajos se ha podido establecer correctamente la consistencia de los dos generadores. En la primera comparación [1] debido a los errores en la determinación del caudal volumétrico se siguieron detectando diferencias de hasta 0,041 °C, mientras que con la nueva sistemática se ha demostrado que la diferencia es menor de 0,001 ºC.

La segunda es demostrar la capacidad del INTA alineada con el estado del arte en la intercomparación de generadores de punto de rocío en el margen de interés. El INTA es el piloto y coordinador de la comparación clave internacional CCT-K8 de temperatura de punto de rocío que a fecha de redactar esta memoria ya ha sido lanzada tras la caracterización extensa y formal usando todo el conocimiento desarrollado en los cuatro trabajos publicados. Debido a motivos de confidencialidad impuesto por las normas aplicables a las comparaciones, no se pueden publicar los resultados de las mismas hasta su finalización y comprobación del primer borrador del informe por todos los participantes. No obstante, en el apartado de resultados se avanza la información relevante de la caracterización previa de los patrones de transferencia para demostrar el avance en el estado del arte, salvaguardando los valores de referencia exactos para no incumplir con el reglamento de la comparación. No obstante, se analizan los resultados relativos de los pilotos y el laboratorio de enlace (*link*) para estimar posibles derivas en los patrones, sin aportar valores absolutos.

La prueba concluyente de la equivalencia del nuevo patrón solo es posible con la realización de ambas comparaciones internacionales. Se describen los aspectos relevantes del protocolo desarrollado, teniendo en cuenta las técnicas nuevas desarrolladas y que ha sido evaluado por los comités de expertos de humedad del CCT/WG.Hu y de comparaciones clave, CCT/WG.KC, con resultado satisfactorio.

Con el fin de facilitar un avance con respecto a la equivalencia y validación de los resultados, se han incluido en esta memoria los resultados de la comparación bilateral que ha realizado el autor de forma periódica con el DI de Austria, BEV/E+E en el margen del nuevo patrón, empleando como patrón de transferencia el higrómetro monitor usado con el generador patrón.

2. OBJETIVOS

El principal objetivo de la tesis es la La ampliación y mejora de la capacidad de medida y calibración de higrómetros de punto de rocío con el patrón nacional de humedad en el margen de temperatura de punto de rocío de -10 ºC a 95 ºC.

Para la concesión de este objetivo los hitos perseguidos con la Tesis consisten en:

- Estudio de la estabilidad a largo plazo y el cociente de temperatura de generadores de humedad de precisión.

- Desarrollar y establecer una sistemática para asegurar las condiciones de caudal de gas de muestreo de los patrones de transferencia que minimicen la contribución de incertidumbre debido a la influencia de la caída de presión.

- Determinar el estado del arte del uso de higrómetros de punto de rocío con el objetivo de establecer las contribuciones debido al flujo de calor y el gradiente de temperatura resultante en el espejo, entre la temperatura de la superficie donde se realiza la condensación y la posición del sensor de temperatura insertado en el mismo.

- La demostración de la consistencia de las realizaciones primarias de temperatura de punto de rocío de los dos generadores patrones en su margen de solape, de -10ºC a 75ºC.

- Permitir la realización de comparaciones internacionales de temperatura de punto de rocío como CCT-K8, una vez demostrado el alineamiento con el estado del arte en la medida de temperatura de punto de rocío en el margen de interés.

3. METODOLOGÍA Y RESULTADOS OBTENIDOS

La metodología empleada en la ampliación y mejora de la capacidad de medida y calibración de higrómetros de punto de rocío con el patrón nacional de humedad en el margen de -10 ºC a 95 ºC queda patente en la justificación de relación de los trabajos de las cuatro publicaciones en las que se basa esta Tesis, indicado en el capítulo 1.

Se ha aplicado el método científico en el campo específico de la metrología: la realización primaria de temperatura de punto de rocío y diseminación de la unidad derivada de la humedad. El autor ha determinado el estado del arte previo a los trabajos y ha buscado un desarrollo progresivo de sus conocimientos y capacidades de medida, desarrollando las técnicas necesarias para culminar en la determinación de la consistencia de los dos patrones nacionales de humedad que aseguran continuidad en la trazabilidad metrológica obtenida por los laboratorios, organismos e industrias en el campo de medida objeto de la Tesis.

En la estimación de incertidumbre se han aplicado los métodos reconocidos internacionalmente [6] así como las buenas prácticas de medida y muestreo de humedad desarrollados en el laboratorio de temperatura y humedad del INTA a lo largo de más de dos décadas.

En el desarrollo del protocolo de la comparación CCT-K8 se han aplicado las buenas prácticas indicadas en [7].

3.1. Estudio de estabilidad a largo plazo y cociente de temperatura de higrómetros de punto de rocío. (Benyon R, Vicente T, Hernandez P, De Rivas L and Conde F. “Evaluation of the Long-Term Stability and Temperature Coefficient of Dew-Point Hygrometers”. Int. Journal of Thermophysics (2012). Vol. 33, Issue 8-9, pp 1758-1770).

Un generador patrón de humedad es básicamente un condensador en el que se requiere una eficiencia de saturación del 100 %. En el margen de temperatura de punto de rocío de interés en este trabajo, en el que la saturación se produce siempre a temperaturas por encima de 0 °C, se pude recurrir a técnicas de sobresaturación en relación con la temperatura del condensador y un posterior enfriamiento del gas hasta condensar el exceso de vapor de agua y asegurar de esta forma la saturación ideal. Para que un generador pueda ser considerado un patrón primario para realizar la magnitud de temperatura de punto de rocío, es necesario determinar las condiciones de operación en el que la humedad generada es independiente de las magnitudes de influencia que intervienen en el proceso.

En los generadores dinámicos en el que se satura un gas y no se recircula tras su paso por los instrumentos de medida, es necesario determinar que la temperatura de punto de rocío del gas está realmente correlacionada con la temperatura de saturación en el punto final de saturación. En contra de lo que podría pensarse, es necesario tener un gradiente de temperatura definido en el saturador para que realmente se obtenga la saturación completa en unas condiciones de presión y temperatura conocidas.

Por otra parte, necesariamente se produce una caída de presión en el propio saturador que es función no solo del caudal de gas húmedo, sino del nivel del condensado en el saturador, que produce una reducción en la sección del volumen interno por el que circula el gas, por encima de la superficie de agua en el mismo. Por otra parte, si se produce un exceso de condensación por una diferencia excesiva de temperatura del presaturador sobre la temperatura del saturador principal, el incremento de temperatura producido localmente a la entrada del saturador principal puede alterar el equilibrio termodinámico del sistema e incluso llevar, en condiciones de caudal alto, a un arrastre de gotas de agua que produciría una temperatura de rocío aparente, superior a la esperada por la temperatura medida en el saturador.

La única forma de determinar el funcionamiento idóneo del generador, es mediante la medida precisa de la humedad del gas generado, mediante un patrón de transferencia con una repetibilidad adecuada al nivel de incertidumbre requerido. Esto es complicado en la práctica si

se tiene en cuenta que el único instrumento con el que lo podemos hacer, es precisamente el que va ser calibrado usando el generador patrón. Esto parecería un dilema de difícil solución, si no se perfecciona una sistemática de uso del patrón de transferencia que permita realizar medidas relativas con mínima incertidumbre. Para esto es necesario primero conocer los límites del propio patrón de transferencia para determinar la incertidumbre combinada del generador y el patrón de transferencia y asignar el valor de incertidumbre típica a la reproducibilidad combinada del sistema.

Se caracterizaron los higrómetros de punto de rocío enumerados en la tabla 4.1.1. Estos miden la temperatura de condensación del vapor de agua en una muestra de gas en una configuración de flujo continuo.

ID	Marca	Modelo	Año de fabricación	Calibración
A92a	MBW	DP3-D-BCS-I	1992	2003 – 2009
A92b	MBW	DP3-D-SH-I	1992	2000 - 2005
A92c	MBW	DP3-D-SH-III	1992	1997 - 2010
A92d	MBW	DP3-D-SH-III	1992	2001 - 2010
A92e	MBW	DP3-D-BCS-I	1992	2004 - 2010
B99	MICHELL	DEWMET-TDH	1999	1999 – 2002
C99	GENERAL EASTERN	M2 (Sensor 1211H-XR)	1999	1999 - 2007
A01	MBW	DP30-BCS-K2	2001	2001 - 2009
D04	EDGETECH	DEWPRIME II (Sensor S)	2004	2004 - 2006
B05	MICHELL	OPTIDEW (Sensor ST1)	2005	2005
D05	EDGETECH	DEWPRIME II (Sensor S)	2005	2005 - 2009
A06	MBW	373HX	2006	2009 - 2010
A07	MBW	473	2007	2007 - 2010
B08a	MICHELL	OPTIDEW (Sensor ST2)	2008	2008 – 2010
C08	GENERAL EASTERN	OPTISONDE (Sensor 1211H-SR)	2008	2008 - 2010
B08b	MICHELL	OPTIDEW	2008	2008 – 2010

Tabla 4.1.1: Instrumentos caracterizados, indicando año de fabricación e histórico de calibración

La condensación en el espejo a medida que la temperatura se reduce de un valor por encima de la temperatura de punto de rocío produce una reducción en la señal de reflectancia detectada por un sensor óptico, en comparación con la señal superior correspondiente a un espejo limpio. Esta señal actúa sobre un bucle de control que ajusta la corriente que pasa a través de los enfriadores termoeléctricos para obtener un espesor constante de condensado. La temperatura del espejo se mide usando un termómetro de resistencia de platino industrial (TRPI) ubicado debajo de la superficie del espejo y se mide usando un indicador de temperatura incorporado. Además, en los patrones de transferencia de laboratorio de precisión, se puede disponer de una segunda TRPI para la medición directa utilizando dispositivos externos de medición de resistencia (p. ej puentes de resistencia). Para instrumentos con una sola TRPI en el espejo, también es posible medir el sensor utilizando un dispositivo de medición de resistencia externo en algunos instrumentos, mientras se mantiene conectada una resistencia de tara a la entrada del indicador de temperatura incorporado para no dejarla en circuito abierto. En algunos casos, el valor nominal de la temperatura indicada es utilizado por el instrumento para otros fines, como la selección de parámetros de control o como punto de consigna para el control de calefacción de la cabeza y el valor de la resistencia de tara debe ajustarse para proporcionar una indicación equivalente a la temperatura de punto de rocío nominal medida.

Las mediciones realizadas en el INTA se han obtenido utilizando generadores de humedad patrón o por comparación con higrómetros de temperatura de punto de rocío de precisión calibrados contra el primero. A menos que se especifique lo contrario, las calibraciones se realizaron bajo las siguientes condiciones: (a) el caudal volumétrico del gas en las condiciones del espejo se mantiene constante a 0,5 $L.min^{-1}$; (b) la temperatura de la cabeza y la temperatura del pre-enfriador (cuando corresponda) se mantuvieron a una temperatura nominal de 30 ºC por encima de la temperatura de punto de rocío medida; (c) el condensado se evapora y se vuelve a formar antes de cada medición; (d) la presión absoluta nominal de la cabeza es de 101,3 kPa; (e) las condiciones ambientales son la temperatura de (23 ± 1) ºC y la humedad relativa inferior al 70% de hr, y (f) las mediciones se tomaron para valores crecientes de humedad.

En las figuras incluidas en este documento todas las barras de error representan la incertidumbre expandida para un factor de cobertura k = 2, asignada en el momento de la calibración. Dependiendo de si las calibraciones se han realizado utilizando un generador patrón o por comparación con un patrón de transferencia de precisión que ha sido calibrado directamente con el generador patrón, la incertidumbre de medida asignada se corresponde con la CMC publicada en el KCDB [10] o por el Organismo de acreditación [11], respectivamente. Esta incluye todas las contribuciones debidas a los patrones de referencia (calibración, deriva, magnitudes de influencia), el método (ecuaciones de tensión de vapor, caídas de presión, factores de no idealidad, uniformidad de la temperatura de la cámara, donde sea aplicable, etc.) y el propio instrumento (resolución, repetibilidad, estabilidad durante la calibración).

En esta estimación de la incertidumbre, para la calibración de patrones de transferencia de precisión, las contribuciones dominantes son generalmente las incertidumbres de tipo B debido a los patrones y el propio método. Por otro lado, para los patrones de segundo nivel, las contribuciones dominantes son generalmente las atribuibles a los propios instrumentos, según lo esperado.

A lo largo de este trabajo, las barras de error incluidas en las figuras pretenden mostrar la variación del parámetro de interés (deriva a largo plazo o coeficiente de temperatura) en el contexto de la incertidumbre expandida asignada, extrayendo la información de las calibraciones realizadas durante un largo periodo de tiempo, y no de experimentos específicos para determinar estas magnitudes de influencia con una baja incertidumbre. Por lo tanto, las barras de error en todos los casos parecen sobredimensionadas con respecto a la dispersión de los resultados obtenidos.

Para el nivel de exactitud requerido en la validación del generador patrón nacional, nos centraremos en los resultados obtenidos sobre los instrumentos de mejores características metrológicas, a saber, los instrumentos empleados como patrones de transferencia de primer nivel.

3.1.1. Magnitudes de influencia.

Una de las magnitudes de influencia que afectan a la medición de la temperatura del punto de rocío es la diferencia entre la temperatura de la cabeza de medida y el espejo. Para las unidades en las que no hay pre-enfriamiento de la cabeza (es decir, su temperatura no puede controlarse por debajo de la temperatura ambiente), dependiendo de la construcción del mismo, puede haber una dependencia significativa de los gradientes cuando se activa el calentamiento de la cabeza para mediciones de temperatura de punto de rocío próxima a la temperatura ambiente. Uno de los primeros patrones de transferencia de alto rango del INTA, A92a, es un claro ejemplo de ello. La Figura **4.1.1.1(a)** muestra la corrección del instrumento en el margen de temperatura de rocío de -10 ºC a 70 ºC basado en la conversión de la resistencia del TRPI medida a la temperatura utilizando [8]. Los círculos representan mediciones con el sistema de calefacción de la cabeza apagada y los triángulos con la calefacción encendida. En ambos casos, la temperatura del gas entrante se acondiciona a 30 ºC por encima de la temperatura nominal de rocío, con un límite inferior de 30 ºC. Las líneas son un ajuste lineal de mínimos cuadrados a los datos en ambos casos. La excelente reproducibilidad del instrumento

se puede observar a partir de las mediciones repetidas a 10 ºC, 30 ºC y 60 ºC. El desplazamiento a 20 ºC es inferior a 20 mK. La figura **4.1.1.1(b)** muestra los resultados obtenidos en la versión moderna del instrumento, A06, donde existe una función lineal continua en el rango -10 ºC a 75 ºC sin ningún desplazamiento.

Una vez más, la excelente reproducibilidad puede verse a -10 ºC, 50 ºC y 65 ºC. Este offset se ha visto también en otros cuatro instrumentos de la misma construcción y edad similar. La causa más probable del desplazamiento tiene que ver con la construcción de la cabeza y en particular con la conexión del TRPI incluido bajo la superficie del espejo, que para minimizar la conducción de la vaina al espejo, tiene una sección corta con sólo dos hilos de platino en una zona de alto gradiente. Este valor no está compensado con la medida de resistencia de cuatro hilos. El offset se mantiene constante al mantener constante el diferencial de temperatura. Más información sobre las magnitudes de influencia se dan en [4] y en la sección **0**.

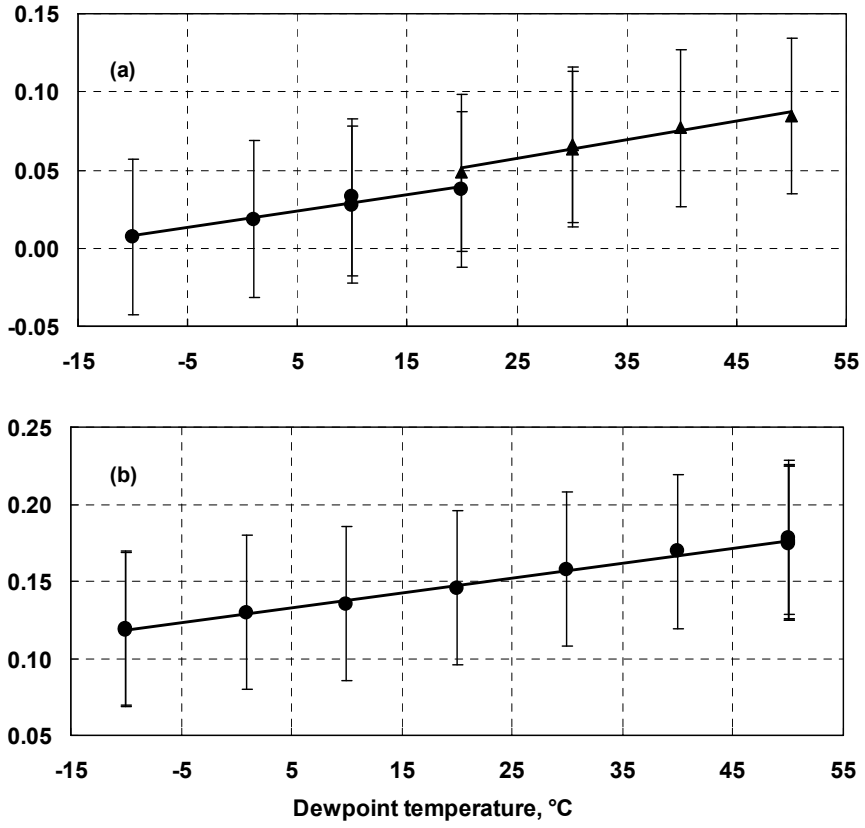

Figura 4.1.1.1 Corrección del instrumento en K, que muestra el efecto de la calefacción de la cabeza para instrumentos de gama alta en el rango de -10 ºC a 75 ºC. (a) para un instrumento más antiguo, A92a con espejo grande y calefacción de cabeza integrada. Los círculos y los triángulos están con la calefacción, apagada o encendida, respectivamente. La compensación a 20 ºC se puede ver claramente. (b) para un instrumento más moderno con espejo de tamaño mediano, A06, con calentamiento de la cabeza sobre el margen, y donde no se puede ver ningún desplazamiento. Las barras de error son la incertidumbre expandida de la medición (k = 2).

3.1.2. Estabilidad a largo plazo

La estabilidad a largo plazo se puede obtener a partir de calibraciones repetidas del instrumento. Sin embargo, se pueden obtener resultados muy diferentes si la unidad se calibra en términos de la lectura del instrumento o en términos de la medición directa del mismo TRPI usando un puente de resistencia externo. La figura **4.1.2.1** muestra la estabilidad a largo plazo del A92b, un instrumento diseñado para mediciones de hasta 60 ºC, que tiene un espejo medio y un enfriador termoeléctrico de una etapa.

La figura muestra la deriva observada a una temperatura de punto de rocío de 5 ºC con respecto a la corrección obtenida en la primera calibración en 2000, para la resistencia del TRPI medida con un puente externo y las correspondientes mediciones de la salida analógica (10 $mV.K^{-1}$), representadas por cuadrados y círculos, respectivamente. La incertidumbre expandida de la medición (k = 2) es 0,10 K.

Las líneas representan el ajuste lineal de mínimos cuadrados de los datos, cuya pendiente indica una deriva de 2,3 mK / año y 14,4 mK / año para las salidas TRPI y analógicas, respectivamente.

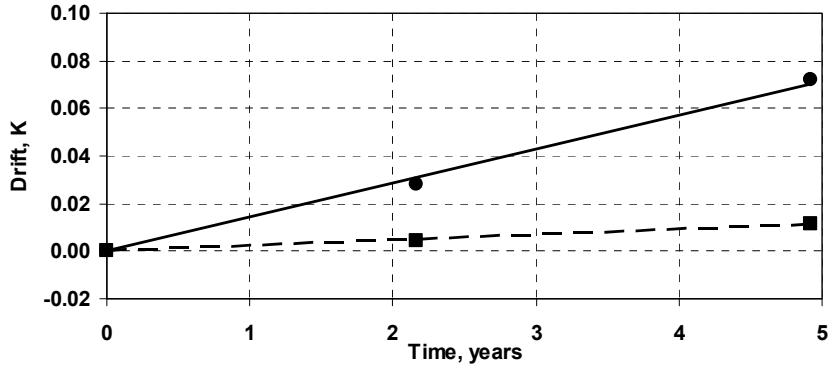

Fig. 4.1.2.1 Estabilidad a largo plazo de A92b con un espejo medio y un enfriador termoeléctrico de una etapa. Deriva relativa a la calibración en el año 2000. Medición de TRPI con puente externo y de salida analógica (10 mV.K-1), representada por cuadrados y círculos, respectivamente

La situación con un instrumento más moderno, A01, con un espejo medio y dos TRPI independientes instalados en el espejo, se puede ver en la figura **4.1.2.2(a)** y **4.1.2.2(b)** para resistencia y salida analógica, respectivamente. En el caso de la salida analógica, la deriva máxima en seis años está entre 1 mK a -30 ºC y 55 mK a 60 ºC y entre 8 mK a -30 ºC y 35 mK a 60 ºC para la medición de resistencia. Para esta unidad, la electrónica mejorada ha reducido significativamente la diferencia, aunque no hay suficientes datos para poder asegurar esta cuestión.

La principal ventaja de medir la TRPI directamente, es la falta de riesgo de perder información histórica si la electrónica tiene que ser reparada. Con unidades digitales más modernas, como A06, donde se ha realizado una selección previa de las TRPI insertados después del tratamiento térmico y de los ciclos, se pueden obtener mejores resultados para la deriva [4], [12].

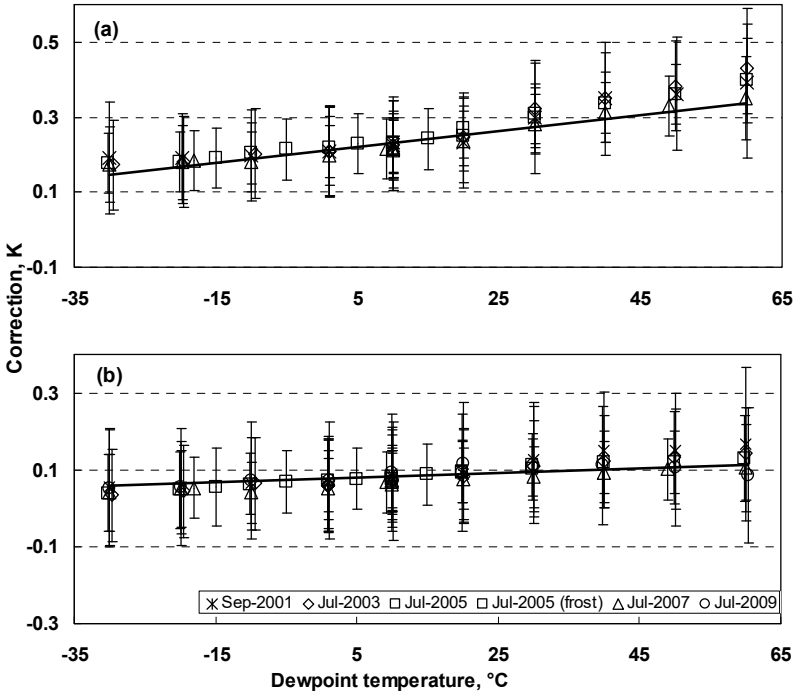

Figura 4.1.2.2 Estabilidad a largo plazo del instrumento A01, con espejo medio y enfriador termoeléctrico de dos etapas: a) Medición de TRPI con puente externo, y b) medición de la salida analógica (10 mV, K-1). Las barras de error son la incertidumbre expandida de la medición (k = 2).

La figura **4.1.2.3** muestra la estabilidad a largo plazo de los dos primeros patrones de transferencia adquiridos por el Laboratorio y que han sido utilizados como monitores de los generadores de humedad patrón. La unidad de rango bajo, A92c tiene una unidad de refrigeración de pre-enfriador, espejo pequeño, enfriador termoeléctrico de tres etapas y cabeza para una temperatura máxima de 60 ºC. Su estabilidad a largo plazo se muestra: (a) a -50 ºC y (b) a -20 ºC.

La estabilidad a largo plazo de la unidad de rango alto, A92b, con un espejo grande y un único enfriador termoeléctrico se muestra en (c) a 50 ºC. Como se puede ver, no se detecta deriva en la unidad de rango bajo durante 12 años y para la unidad de rango alto, la deriva durante 8 años es inferior a 20 mK.

Los gráficos también muestran el excelente nivel de reproducibilidad combinada de los higrómetros y generadores durante una década. La estabilidad observada se puede justificar, teniendo en cuenta que las TRPI integradas en el espejo son de un diseño cerámico encapsulado y por lo tanto han recibido un tratamiento térmico a temperaturas elevadas inherentes al proceso de fabricación, y se utilizan solamente en un intervalo de temperatura muy estrecho y con un límite superior de temperatura relativamente bajo.

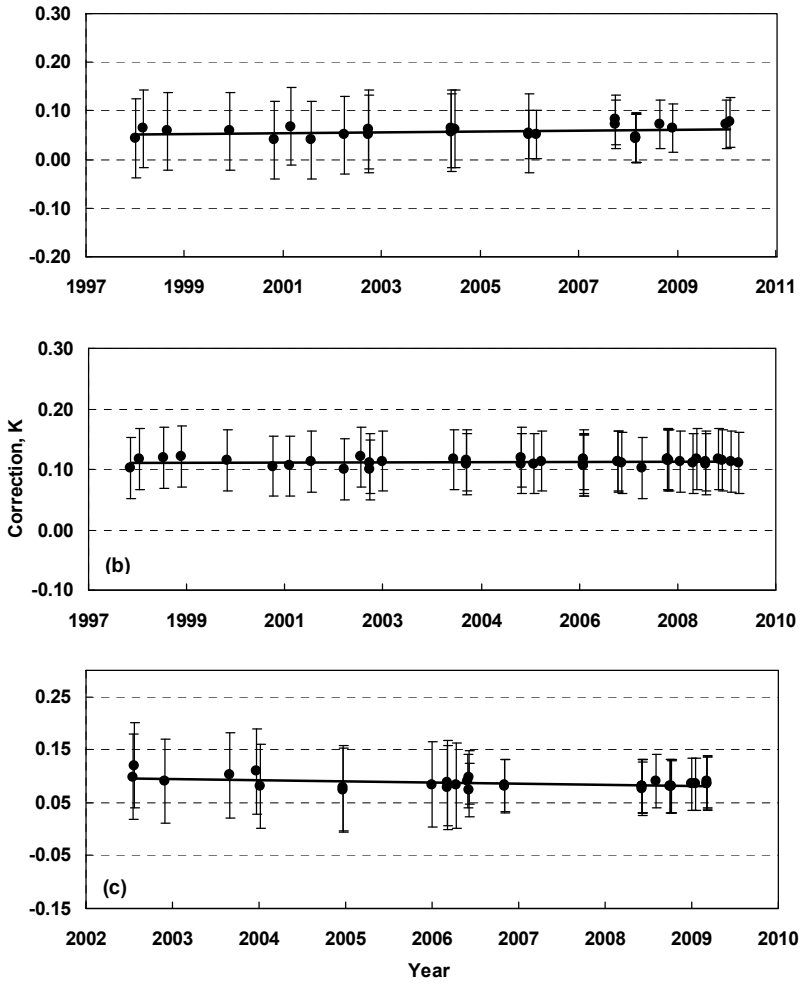

Figura 4.1.2.3 Estabilidad a largo plazo del instrumento A92c con espejo pequeño, refrigerador termoeléctrico de tres etapas y pre-enfriador a: (a) -50 ºC y (b) -20 ºC. Los resultados a +50 ºC para el instrumento A92b con un espejo grande y un único enfriador termoeléctrico, se muestran en (c). Las barras de error son la incertidumbre expandida de la medición (k = 2).

3.2. Estudio de la influencia de la presión. Desarrollo de sistemática (Mitter H, Böse N, Benyon R and T. Vicente, "Pressure drop considerations in the characterization of dew-point transfer standards at high temperatures". Int. Journal of Thermophysics (2012), Vol. 33, Issue 8-9, pp 1726-1740).

En la caracterización de patrones de transferencia de punto de rocío de alta temperatura, la caída de presión interna del instrumento es una de las magnitudes de influencia críticas. Esto es debido a qué dependiendo de la configuración de medida, puede existir una diferencia importante entre la temperatura de punto de rocío materializada en el generador patrón y la indicada por el propio instrumento. La tensión de vapor equivalente a la temperatura de rocío de referencia (la presión parcial debida a un componente del gas) se ve modificada de forma proporcional a la variación de la presión absoluta. Por tanto, el patrón de transferencia indicará una temperatura de rocío más baja que la de referencia, en función de la caída de presión debida al flujo de gas. En las medidas de punto de rocío en las que la contribución de la presión total debida al vapor de agua es significativa, para un mismo caudal de gas seco que entra al saturador del generador, el caudal volumétrico generado, y por tanto la caída de presión entre la salida del saturador y el instrumento, incrementará debido al aporte de vapor de agua. Lo mismo pasa entre el racor de entrada y el punto de referencia de higrómetro (el espejo donde se detecta la condensación).

Por todo lo anterior es fundamental desarrollar una metodología que permita establecer de forma reproducible y práctica, una caída de presión constante para temperaturas de punto de rocío en todo el margen de interés (30 °C a 95 °C). Esto formará parte de los protocolos de las comparaciones internacionales de temperatura de punto de rocío.

3.2.1. Configuración de medida

En las medidas realizadas se han considerado las dos posibles configuraciones de medida empleadas en los institutos nacionales de metrología e institutos designados; (a) Muestreando desde una cámara presurizada a una presión conocida (ver Fig. **4.2.1.1**), y (b) suministro del flujo de gas directamente desde la salida del saturador al instrumento y la medida de la presión aguas abajo (ver Fig. **4.2.1.2**).

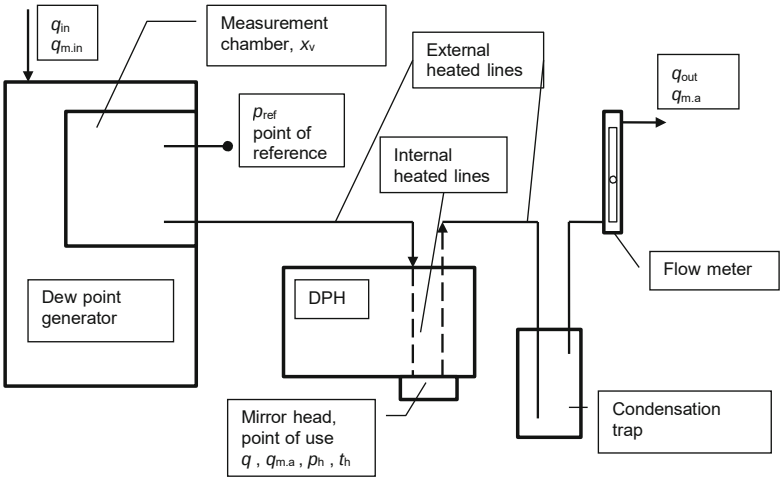

Fig. 4.2.1.1 Configuración para la calibración de un higrómetro de espejo refrigerado utilizando aire acondicionado con temperatura, muestreado en la cámara de prueba de un generador de dos presiones. La presión en el sensor de espejo refrigerado se calcula a partir de la presión medida en la cámara aguas arriba del higrómetro, teniendo en cuenta la caída de presión entre el punto de referencia (cámara de ensayo) y el punto de uso (cabeza de espejo del higrómetro).

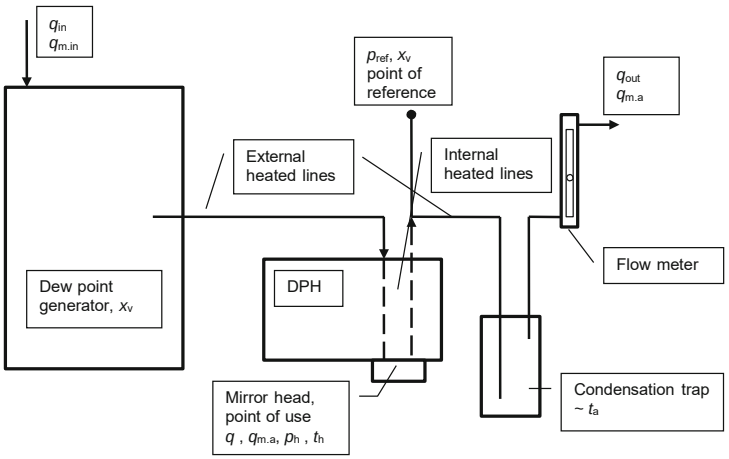

Fig. 4.2.1.2 Configuración para la calibración de un higrómetro de espejo refrigerado utilizando aire acondicionado con temperatura de un generador de punto de rocío de paso simple (dos presión o presión simple). La presión en el sensor de espejos refrigerados se calcula a partir de la presión medida aguas abajo del higrómetro tomando en cuenta la caída de presión entre el punto de referencia (higrómetro de salida) y el punto de uso (cabeza de espejo del higrómetro).

Independientemente del tipo de generador de humedad o higrómetro de punto de rocío utilizado, la diferencia relevante es la ubicación de la posición de la medición de presión para el punto de referencia. Estas configuraciones son representativas de las utilizadas en pruebas experimentales de los modelos de flujo de gas.

La temperatura del punto de rocío se mide en el espejo del higrómetro de punto de rocío (DPH en sus siglas en inglés), y luego el gas pasa del DPH a una trampa de condensación, donde el vapor de agua contenido en el gas húmedo que excede una temperatura de punto de rocío equivalente a la temperatura ambiente (o inferior si se enfría la trampa), se eliminará. El gas "seco" se conduce a través de una válvula de aguja y un conjunto de medidor de flujo para medir el caudal de gas muestreado, $q_{out.}$

En condiciones ideales, la presión de referencia, p_{ref}, necesitaría sería medida directamente en la cabeza de medida del DPH en el punto de condensación (el espejo). Sin embargo, esto resulta en dificultades técnicas, ya que no se puede asegurar que la medición de la temperatura de condensación no se vea afectada por la medición de presión debido a efectos de condensación o de zonas muertas. Por esta razón, la medición de presión se realiza en un punto no crítico de la trayectoria de gas de muestra. Como consecuencia, la presión p_h en el punto de uso (espejo del DPH) es distinta a la presión de referencia, p_{ref}, debido al caudal volumétrico entre los dos puntos. Esta diferencia de presión causa una diferencia en la temperatura del punto de rocío y debe ser corregida o tenida en cuenta en la estimación de incertidumbre de medición. Dependiendo de la configuración de medición, la presión de referencia se mide directamente en la cámara de medición del generador (véase la figura **4.2.1.1**) o inmediatamente después de la salida del DPH (figura **4.2.1.2**). para un caudal volumétrico en las condiciones de temperatura y presión de medida, de 0,5 $L \cdot min^{-1}$, la pérdida de presión entre el punto de referencia y el punto de uso es de alrededor de 1 hPa (Fig. **4.2.1.1**) o alrededor de 0,2 hPa (Fig. **4.2.1.2**) cuando se utiliza un tubo estándar de acero inoxidable con un diámetro interno de 4 mm en la longitud de uso común. La corrección resultante del punto de rocío es de aproximadamente 2 mK a 14 mK en el margen de interés.

Como es difícil medir directamente el caudal volumétrico de un gas caliente y muy húmedo, el flujo de gas se mide después de la trampa de condensación a temperatura ambiente. Este volumen de gas de volumen medido, q_{out}, después de la trampa de condensación se utiliza para determinar y establecer un caudal volumétrico constante, q, sobre el espejo del DPH para mantener la caída de presión constante entre "el punto de referencia" y "el punto de uso", independientemente de la temperatura de rocío aplicada.

Los valores típicos para las condiciones de la cabeza del espejo son:

- caudal volumétrico, q = 0,5 $L \cdot min^{-1}$,
- presión, $p_h > p_a$, generalmente varios hPa por encima p_a para mantener un flujo de gas suficiente por el DPH,
- temperatura de la cabeza del espejo y de la línea interna calentada: $t_v = t_h = t_d + 30$ °C.
  Debe tenerse en cuenta que un DPH comercial suele tener un límite de temperatura superior de la temperatura de la cabeza y la temperatura interna del tubo, que debe ser considerado en los cálculos del caudal de gas.

Para un caso de "punto de referencia" en la cámara de medición (figura **4.2.1.1**), la temperatura de la línea exterior calentada desde el generador hasta el DPH t_v debe ser igual a t_h.

3.2.2. Caída de presión en función del caudal volumétrico (gas seco)

La caída de presión se ha medido en función del caudal volumétrico de aire seco entre la entrada y la salida de un DPH de amplio margen (MBW 373-LHX). Este tipo de dispositivo permite que la temperatura interna de la línea de gas se ajuste en una amplia gama de ~ t_a a 115 °C. El instrumento es un diseño especial sin bomba de gas interna, por lo que la

alimentación de gas es simétrica entre la entrada y la salida en relación con el cabezal de medición y también produce una caída de presión simétrica para este DPH.

Se ha elegido el diseño especial sin una bomba de gas interna porque la bomba de gas provoca una interferencia adicional en el flujo de gas, lo que resulta en unas caídas de presión poco reproducibles y mayores en el área de la bomba de gas. La simetría de la caída de presión también se ha probado mediante una medición de presión directa en el cabezal de medición y comparación con la presión en la entrada y la salida para diferentes caudales volumétricos.

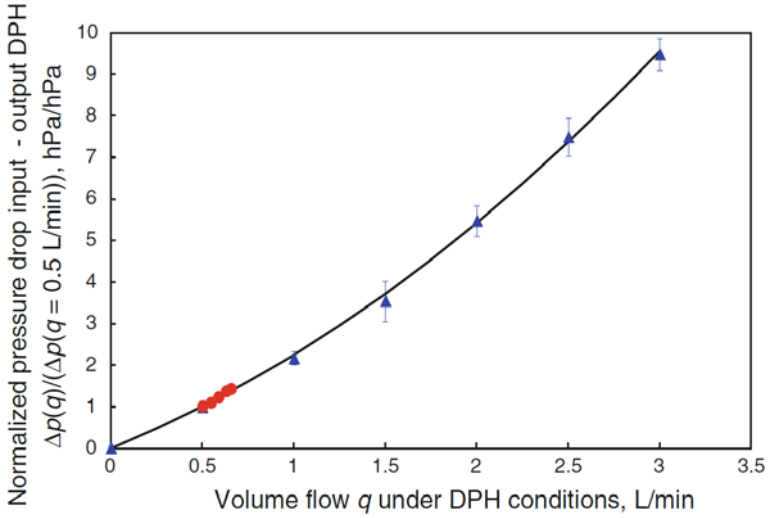

Fig. **4.2.2.1** Variación en la caída de presión normalizada desde la entrada a la salida de un MBH373 LHX, que resulta de variar el caudal interno directamente a temperatura ambiente (triángulos azules) o indirectamente mediante la variación de la temperatura interna del DPH (círculos rojos). La línea es un ajuste por mínimos cuadrados. Las barras de incertidumbre corresponden a la incertidumbre expandida de las mediciones de la diferencia de presión y la incertidumbre del ajuste del caudal para un factor de cobertura de k = 2.

El caudal volumétrico, q, en las condiciones de presión y temperatura de la cabeza de medición se ha variado de dos maneras diferentes:

q_{out} = 0,5 L·min^{-1} = const, variación de la temperatura interna de la línea de gas desde la temperatura ambiente hasta 115 °C y variación de q = q_{out} en el margen de 0 L·min^{-1} a 3 L·min^{-1} a temperatura interna constante.

Dependiendo de las condiciones de medición, se establece un flujo de volumen interno q que da como resultado una diferencia de presión correspondiente entre la entrada y la salida del DPH. Para un caudal volumétrico de q = 0,5 L·min^{-1}, se produce una caída de presión de aproximadamente 0,4 hPa entre la entrada y la salida del DPH; Correspondientemente, entre la cabeza de medición y la salida, hay una caída de presión de ~0,2 hPa.

Las mediciones de la diferencia de presión para los caudales volumétricos indicados anteriormente han sido normalizadas a la medida a q = 0, 5 L·min^{-1} y representadas en la Fig. **4.2.2.1**. La diferencia de presión normalizada dependiendo del caudal volumétrico q se puede describir mediante un polinomio de segundo orden. Con q = 0, la caída de presión es igual a 0 en línea con la definición.

3.2.3. Caída de presión en condiciones de gas húmedo

La caída de presión se midió entre la entrada y la salida de un MBW 373 LHX sin una bomba de gas interna descrito en la sección anterior, en condiciones reales de gas húmedo. Las mediciones de presión diferencial se realizaron usando dos transductores de presión absolutos Paroscientific 6000-200A con un conmutador para seleccionar el transductor 1 a la entrada y al transductor 2 a la salida y viceversa. La presión diferencial se calculó a partir de los valores de los transductores en ambas configuraciones para eliminar los desplazamientos de cero. Ambos transductores de presión se estabilizaron a 35 °C. El tubo de conexión a la muestra de gas se calentó suficientemente para evitar efectos de condensación. Se insertó en la línea una trampa de condensación para evitar la condensación en los transductores.

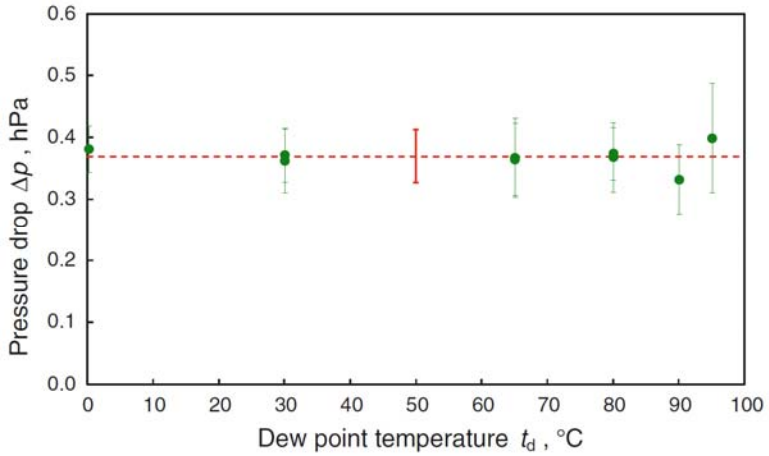

Fig. **4.2.3.1** Caída de presión en condiciones de aire húmedo entre la entrada y la salida de un MBH373 LHX sin una bomba de gas interna para evitar efectos adicionales por la bomba. El caudal en las condiciones de DPH se ha ajustado para caudal volumétrico constante. Las barras de incertidumbre indican la incertidumbre combinada de las mediciones de la diferencia de presión y la incertidumbre del ajuste del flujo con un factor de cobertura de k = 2. La línea discontinua indica el promedio de todas las mediciones con una barra de incertidumbre expandida (k = 2) a td = 50 ◦C

El punto de rocío se aplicó usando un generador de punto de rocío de un solo paso en una configuración de una presión (sin válvula de expansión), y el caudal volumétrico se ajustó para de mantener un flujo volumétrico constante, q = 0,5 L·min^{-1} en las condiciones de medida del DPH.

Los resultados obtenidos se ilustran en la Fig. **4.2.3.1**. Confirman un ajuste correcto del caudal volumétrico usando el método descrito. Esto asegura una caída de presión constante, dentro de la incertidumbre de medida, en todo el margen de temperaturas de punto de rocío aplicadas.

3.2.4. Comparativa de configuraciones de muestreo

Como parte de la puesta en marcha y validación del nuevo generador (antes de desarrollar esta sistemática) se observó que a temperaturas de punto de rocío crecientes se observaban diferencias entre los dos generadores patrón del laboratorio, a pesar d que se usaron las mismas referencias para la medida de presión y temperatura. A temperaturas de punto de rocío por encima de aproximadamente 50 ° C, las desviaciones se hicieron significativas, y a t_d = 75 °C, alcanzaron valores que eran muy superiores a los esperados para la incertidumbre de medida asociada. El generador antiguo (un Thunder Scientific 9000 optimizado) se empleó en la configuración indicada en la Fig. **4.2.1.1**, mientras que el nuevo generador se usó en la configuración de la Fig. **4.2.1.2**. Estas medidas eran las primeras medidas de comparación de

los generadores, antes de proceder a la comparativa detallada usando la nueva sistemática (véase la sección **3.4**).

Como DPH de transferencia, se utilizó un MBW 373 HX donde la bomba de gas interna se había retirado y reemplazada con un tubo de acero inoxidable para evitar los efectos de presión no deseados adicionales descritos anteriormente. Esto proporcionó al dispositivo una alimentación de gas ligeramente más larga después del espejo y no la caída de presión simétrica descrita en la sección **3.2.2**.

Al comienzo de las mediciones en ambos SHG, se midió la diferencia de presión entre el punto de referencia y el punto de uso por encima de la conexión del endoscopio del DPH usando un transmisor de presión diferencial de 10 hPa y usando con gas suficientemente seco con un rocío de aproximadamente 1 °C y un caudal volumétrico de 0,5 $L \cdot min^{-1}$. Sin embargo, al aumentar el punto de rocío, la operación del primer generador con un flujo de gas seco constante produjo un aumento significativo en el caudal volumétrico y, por lo tanto, un aumento de la caída real de presión entre el punto de referencia y el punto de uso, por lo que la corrección ya no era válida con la caída de presión medida y resultó en la desviación observada al comparar ambos generadores.

Cambiando el funcionamiento de ambos generadores a un caudal volumétrico constante q en las condiciones de medida del DPH, de acuerdo con la sistemática desarrollada, las diferencias entre los dos generadores desaparecen. La figura **4.2.4.1** muestra las diferencias entre los resultados de calibración en el intervalo de solape de ambos generadores después de cambiar a caudal volumétrico constante en las condiciones del DPH.

Las barras de error corresponden al doble de la desviación estándar combinada de las mediciones en cada valor nominal. Se puede ver claramente que los valores obtenidos son enteramente consistentes con los ± 20 mK actualmente asignados por el Laboratorio como la reproducibilidad combinada del DPH y del generador, basado en mediciones repetidas a largo plazo durante varios años con desviación insignificante, dentro de este semi-intervalo. Este valor incluye contribuciones debido a los efectos de la contaminación, histéresis y determinación de la caída de presión, representando el límite alcanzable actual con un DPH de última generación.

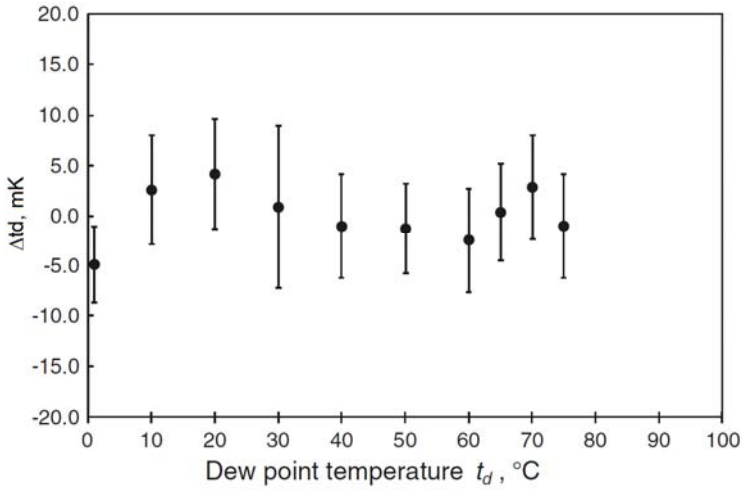

Fig. **4.2.4.1** Diferencia entre los resultados de calibración de MBW373-HX (SN: 06-1112) de acuerdo con las configuraciones de las Figs. **4.2.1.1** y **4.2.1.2** (generador de alto rango) en el rango de solapamiento de ambos generadores.

3.3. Relación entre termometría de contacto y realización de temperatura de punto de rocío. (Benyon R, Böse N, Mitter H, Mutter D, Vicente T "An Investigation of the Relation Between Contact Thermometry and Dew-Point Temperature Realization". Int. Journal of Thermophysics (2012), Vol. 33, Issue 8-9, pp 1741-1757).

La construcción de un higrómetro de punto de rocío (DPM) de espejo refrigerado gira en torno a la configuración básica de un espejo de cobre con un recubrimiento de oro o rodio con un termómetro de resistencia de platino (TRP) de miniatura insertado por debajo de la superficie del espejo en contacto con el gas. El espejo tiene su superficie pulida en contacto con el gas y la parte posterior en buen contacto térmico con un módulo termoeléctrico. Las principales magnitudes de influencia que afectan al rendimiento de los sensores de temperatura incorporados en el higrómetro de punto de rocío son el considerable flujo de calor y los efectos de conducción dentro de un conjunto con dimensiones reducidas y una configuración compacta.

En la fabricación de los DPM es necesario tener en cuenta estos factores para mitigar sus consecuencias mediante un cuidadoso diseño y selección de materiales. Para minimizar el flujo de calor entre el área de superficie de condensación y los componentes restantes y también reducir la carga térmica sobre los refrigeradores termoeléctricos utilizados para controlar la temperatura de la superficie de condensación, se emplean materiales de conductividad térmica específica comparativamente baja en los alrededores zona. Esto limita la disipación de calor a las conexiones, terminales y / o la carcasa del dispositivo.

La baja conductividad térmica específica del área alrededor de la superficie de espejo controlada por temperatura conduce a gradientes de temperatura significativos, por lo que la temperatura debe controlarse de manera que la condensación sólo se produzca cerca de la superficie de condensación, pero no en las áreas circundantes.

Por otra parte, se requieren materiales con una alta conductividad térmica para suministrar la energía térmica requerida a la superficie de condensación con un gradiente de temperatura lo más bajo posible, normalmente usando una capa de pasta conductora. Una cuestión clave para mantener los gradientes del espejo a un mínimo es el preacondicionamiento de la temperatura del gas antes de su contacto con el espejo. Una operación reproducible exitosa requiere que todos estos parámetros sean controlados.

Se presentan los resultados de la caracterización y selección de los TRP utilizados en una serie de patrones de transferencia y la comparación de la calibración de termometría de contacto con los resultados obtenidos en términos de temperatura de punto de rocío. Se han estudiado dos generaciones de patrones de transferencia con un margen amplio de temperatura de punto de rocío. Los instrumentos estudiados tienen dos TRP de 5 mm de longitud y 1.5 mm de diámetro que se insertan radialmente en el bloque del espejo.

3.3.1. Caracterización y selección de TRP

Antes de la calibración, los sensores se ensamblan en un bloque de cobre de miniatura sellado con una junta tórica, diseñado expresamente para alojar los sensores y anclar térmicamente los conductores finos que luego se llevan al conector a través de una vaina de acero inoxidable de pared fina. En las primeras medidas, se montaron cinco sensores de este tipo en un solo bloque (véase la figura **4.3.1.1**). En los últimos instrumentos, se han montado los sensores individualmente, en un formato más compatible con las células de punto triple de agua y la calibración por comparación con los termómetros de resistencia de platino patrón (TRPP) en baños de calibración de líquidos con bloques de cobre convencionales.

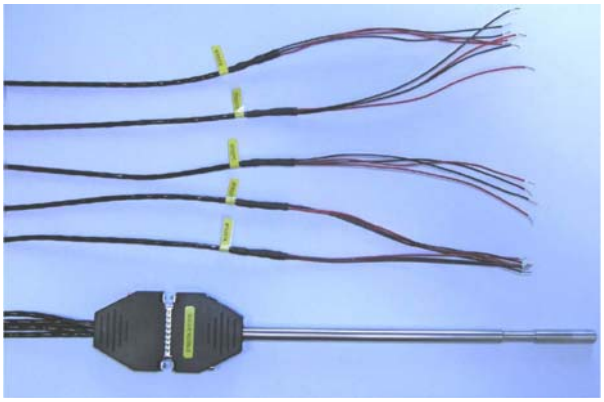

Fig. **4.3.1.1** Sensores montados en bloque de cinco para la caracterización y ciclos térmicos, 07-0227 a 07-0227E usados en la comparación clave EUROMET-T.K8.

Una vez montados, los TRP se someten a ciclos de temperatura entre los extremos del intervalo de calibración previsto hasta que se observa la estabilización o se rechazan los sensores. Después de cada temperatura, la resistencia se mide a un valor cercano a la mitad del rango, que en los casos reportados fue el punto triple del agua.

La figura **4.3.1.2** muestra la estabilidad en el punto triple del agua para un lote de cuatro TRP sometidos a ciclos térmicos entre -80 ºC y +60 ºC, para el instrumento del INTA NS: 97-1220. Los símbolos sólidos corresponden a las dos TRP seleccionadas para el instrumento. Los últimos tres puntos corresponden a los puntos triples inicial, medio y final durante la calibración, después de los primeros diez puntos. La escala vertical corresponde a 10 mK por división. Los valores de histéresis, definidos como el semi-intervalo alrededor de la media de los valores una vez que se observa la estabilización, se resumen en la tabla **4.3.1.1**. Para los TRP seleccionados para el patrón de transferencia (con sufijos B y D), el valor es inferior a 1 mK .

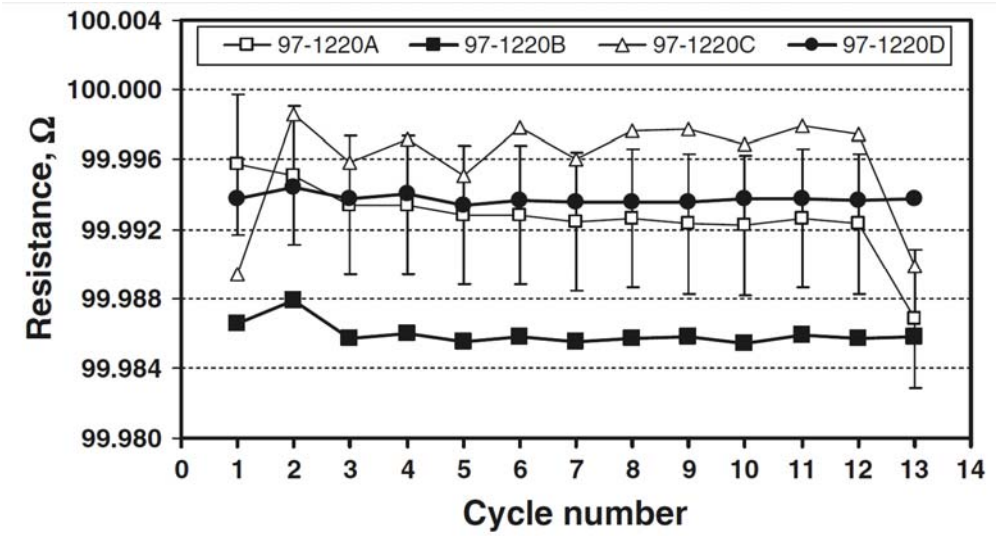

Fig. **4.3.1.2** Estabilidad en el punto triple del agua para un lote de TRP al ciclarse de -80 ◦C a +60 ◦C, para 97-1220, referencia de calibración TH400665 (INTA). Los puntos 11 y 13 son antes y después de la calibración de -80 ◦C a +60 ◦C

Tabla 4.3.1.1 Resultados de la evaluación de la histéresis de TRP para NS: 97-1220 a partir de ciclos de -80 ºC a +60 ºC, medido en el punto triple del agua.

Temperatura	Histeresis (ciclos -80 ºC / +60 ºC), mK			
ºC	97-1220A	97-1220B	97-1220C	97-1220D
0,01	1,5	0,8	3,6	0,8

A continuación se incluyen los resultados obtenidos sobre los TRP empleados en las dos comparaciones clave EUROMET-T.K8 (TRP encapsuladas en vidrio) y CCT-K8 (TRP sobre sustrato cerámico) que no se podían publicar para no invalidar las comparaciones. En este trabajo no se identifican los sensores finalmente seleccionados para las indicaciones digitales o para medida con puente externo.

En la figura **4.3.1.3** se muestra el resultado del ajuste del sensor 07-0227B. El cociente de sensibilidad es de aproximadamente 2,5 mK/mΩ, por lo que las líneas representan 12 mK. Se observa la excelente reproducibilidad en el punto triple del agua. Los residuos del ajuste son inferiores a ± 2 mK en el margen de -10 °C a 105 °C.

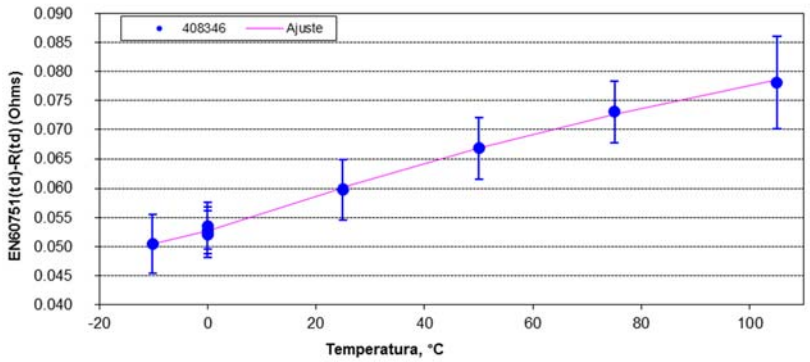

Fig. **4.3.1.3** Resultado del ajuste a la función de referencia de la Norma EN 60751:2008 para el sensor 07-0227B. Sensor del fabricante Netsushin encapsulado en vidrio. Ref: C-408346 / ENAC 16123.

En los preparativos para la comparación mundial CCT-K8, se hizo un estudio mucho más exhaustivo de los tratamientos térmicos de estabilización y cuantificación de la histéresis. Los resultados fueron muy sorprendentes. Se estudiaron dos lotes de nuevos sensores de Netsushin, con referencias MBW 09-0609A a 09-0609K (10 sensores) y tras los resultados obtenidos, se midieron otros cinco, con referencia MBW 09-0801A a 09-0801E (5 sensores).

Los resultados de la primera serie se muestran en la figura **4.3.1.4**. Se observa que el sensor B es muchísimo peor y que el sensor A se recupera, pero en general los sensores tienen una deriva totalmente inaceptable para su uso en los patrones de transferencia. Los resultados muestran la deriva con respecto a la primera medida. La diferencia se ha obtenido a 50 °C por comparación con dos TRPP Rosemount 162CE calibrados en puntos fijos de la EIT-90.

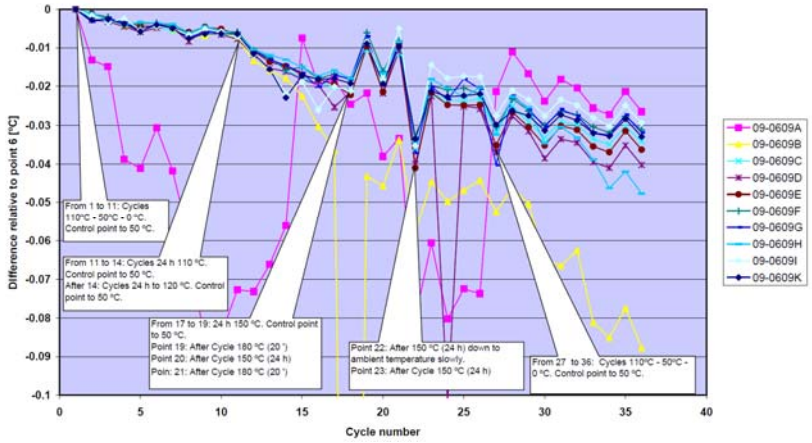

Fig. **4.3.1.4** Estabilidad relativa de los sensores encapsulados en vidrio de la serie 09-0609 a 50 °C, tras un total de 36 ciclos térmicos a distintas temperaturas entre 150 0 °C y 0 °C. Prueba de estabilidad tras ciclos de histéresis.

Los resultados de la segunda serie se muestran en la figura **4.3.1.5**. Aquí se observa un incremento inicial de 10 mK tras media hora a 105 °C y una progresiva reducción de la resistencia con una eventual estabilización a un valor de 15 mK por debajo del inicial, excepto para el sensor B.

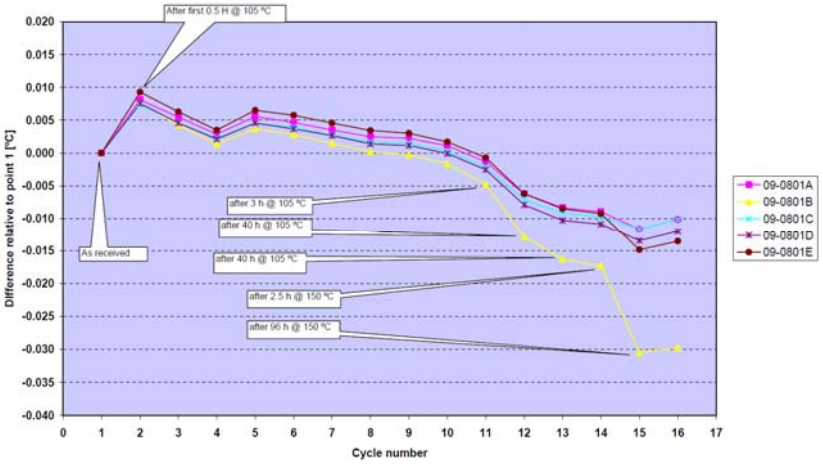

Fig. **4.3.1.5** Estabilidad relativa de los sensores encapsulados en vidrio de la serie 09-0801 a 50 °C, tras un total de 50 horas a temperaturas de 150 0 °C y 105 °C. Prueba de envejecimiento.

La tabla **4.3.1.2** muestra las pendientes de la deriva. Se observa la deriva mayor al subir a 150 °C y su progresiva reducción a medida que se produce el tratamiento térmico. A diferencia de la prueba de la serie anterior, aquí no se han producido ciclos térmicos.

	105 °C	**105 °C**	**105 °C**	**150 °C**	**150 °C**	**150 °C**	**150 °C**	**150 °C**	Drift rate
	Run1 (0 to 15 h)	Run1 (15 to 40 h)	Run2 (0 to 40 h)	Run3 (0 to 10 h)	Run3 (10-20 h)	Run3 (20-44 h)	Run4 (0-30 h)	Run4 (30 to 50 h)	
Max	-0.000450	-0.000190	-0.000110	-0.000930	-0.000400	-0.000230	-0.000088	-0.000055	K/hour
Min	-0.000330	-0.000130	-0.000070	-0.001300	-0.000540	-0.000110	-0.000154	-0.000092	K/hour
Max	-4.50	-1.90	-1.10	-9.30	-4.00	-2.30	-0.88	-0.55	mK per 10 hours
Min	-3.30	-1.30	-0.70	-13.00	-5.40	-1.10	-1.54	-0.92	mK per 10 hours

Tabla **4.3.1.2** Resultado de deriva de los cinco sensores de la serie 09-0801 tras tratamiento térmico a durante un total de 50 horas a distintos tiempos a temperaturas de 105 °C y 150 °C. Sin ciclos.

El laboratorio tenía muy buena experiencia con sensores encapsulados en cerámica que se habían usado en los higrómetros varias décadas antes. El fabricante había cambiado a sensores encapsulados en vidrio porque en los higrómetros de baja temperatura se habían producido roturas de los sensores por la condensación de agua ambiente sobre la cerámica porosa de los sensores y su rotura tras congelación por la expansión.

En base a los resultados expuestos, se solicitó el suministro de un lote de sensores cerámicos del mismo tipo nominal de los usados antiguamente. Estos sensores fueron sometidos a tratamientos térmicos de estabilización a 130 °C hasta observar la estabilidad y luego fueron calibrados en los puntos nominales de la comparación, en el margen de 0 °C a 95 °C. El valor del punto triple del agua fue medido también tras los tratamientos térmicos y durante la calibración. La figura **4.3.1.6** muestra la diferencia entre los valores medidos en el punto triple del agua relativos al valor medio de resistencia en el punto triple del agua, expresado en mK. Se observa que el valor se reduce inicialmente 7,5 mK tras el primer tratamiento y luego sube aproximadamente 1 mK tras el segundo y se mantiene dentro de 0,8 mK durante la calibración. El resultado del ajuste a la Norma EN 60751:2008 tiene solo residuos entre +0,3 mK y -0,6 mK.

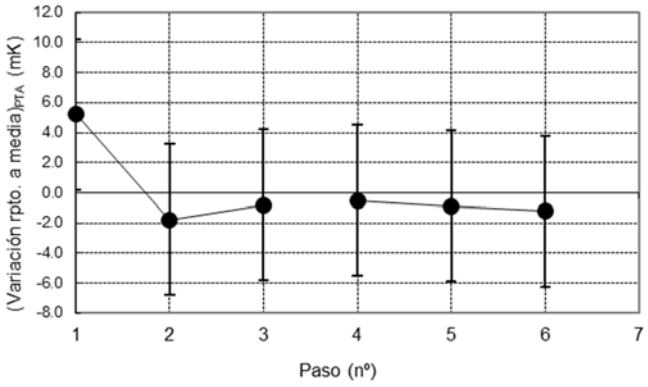

Figura **4.3.1.6** Deriva en el punto triple del agua del sensor cerámico Tx09-0901C (Ref C-410896 / ENAC 22457).

Otra de las pruebas realizadas a los termómetros es la medida del calentamiento propio de la resistencia a la intensidad nominal de medida (1 mA). El resultado de estos sensores fue de 8,9 mK.

3.3.2. Comparativa entre termometría de contacto y medida de punto de rocío

De la misma manera que se han analizado los residuos del ajuste a la Norma EN 60751:2008 en la sección anterior para la calibración TRP en términos de temperatura de contacto, se pueden realizar para las medidas en términos de temperatura de punto de rocío. La figura **4.3.2.1** muestra los residuos de tres calibraciones de humedad de 2005 a 2010 (símbolos huecos) realizados en el INTA de -75 ºC a 20 ºC. Los valores se sitúan dentro de ± 15 mK, un factor de 3 mayor que la calibración de temperatura (símbolos sólidos). El resultado es muy satisfactorio, teniendo en cuenta que en el peor de los casos esto sólo representa una quinta parte de la CMC asociada a los puntos de calibración individuales y es consistente con el criterio de aceptación de ± 20 mK establecido en el procedimiento de calibración.

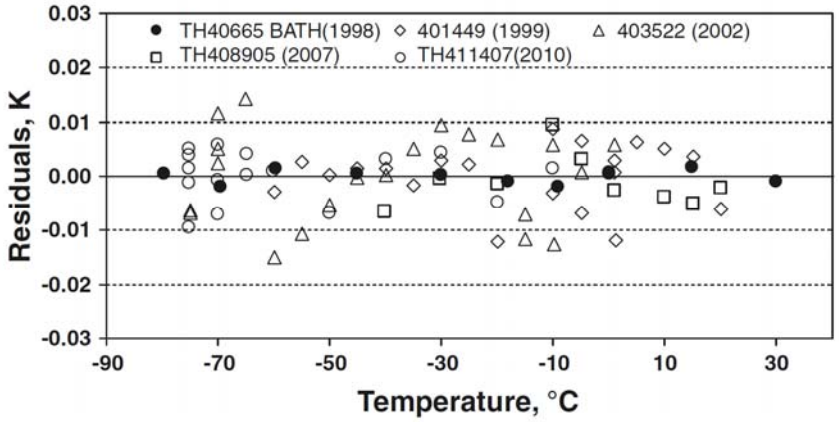

Fig. **4.3.2.1** Residuos de ajuste de mínimos cuadrados de las desviaciones de EN 60751: 2008 función de referencia para la calibración por comparación en baños de temperatura, para MBW DP30/K1806, NS: 97-1220 (TH40665) y tres calibraciones de 2005 a 2010. Los valores por encima y por debajo de -10 ºC son de Diferentes generadores.

Por otra parte, los resultados obtenidos por BEV/E+E con el generador en modo una presión (1P) y el INTA usando ambos generadores de alto rango en modo dos presiones (2P) en el margen -10 ºC a 95 ºC con el MBW373HX NS: 06-1112, representados en la Fig. **4.3.2.2**, muestran un excelente acuerdo entre los resultados en términos de temperatura de punto de rocío y la calibración en baños, con residuos de ± 5 mK.

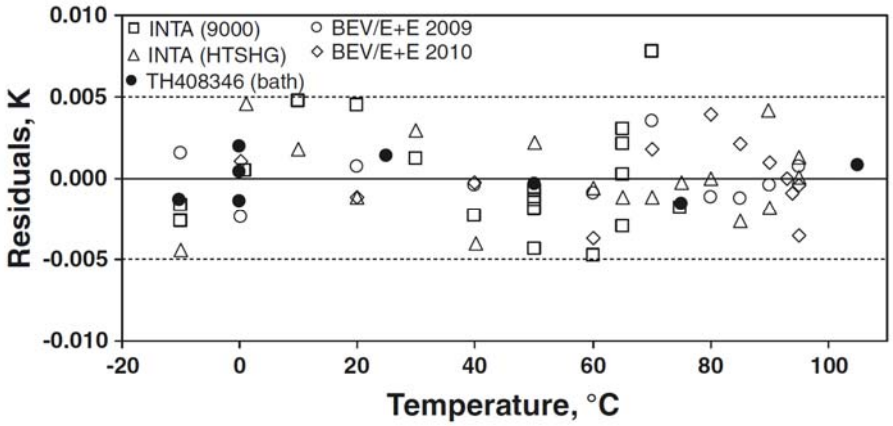

Fig. **4.3.2.2** Residuos de ajuste por mínimos cuadrados de las desviaciones de la función de referencia EN60751: 2008 para la calibración en comparación de TRP (TH408346E) en baños de temperatura (símbolos sólidos) y para calibraciones de temperatura de punto de rocío en INTA (generadores de alto rango) y BEV / E + E, para MBW 373HX NS: 06-112.

La figura **4.3.2.3** muestra la diferencia entre la temperatura de punto de rocío generada (INTA) y la correspondiente calibración en baño del TRP para SN: 97-1220 desde 1999 a 2010. El número de serie del TRP es 97-1220D, cuyos ciclos se representaron en la Fig.**4.3.1.2**. Debe tenerse en cuenta que los valores superiores e inferiores a -10 ºC son de generadores diferentes, con un solape de -10 ºC a 1 ºC (INTA). En el intervalo de -60 ºC a +20 ºC, donde la CMC es de 0,05 ºC, la diferencia media es de aproximadamente -50 mK, con una dispersión consistente con los residuos para estas calibraciones representadas en la Fig. **4.3.2.1** y el criterio de aceptación establecido para las medidas (± 20 mK). La disminución gradual de la magnitud de la diferencia a medida que la temperatura del punto de rocío disminuye a -75 ºC en aproximadamente 50 mK. , no puede atribuirse necesariamente al aumento del flujo de calor a medida que los tres enfriadores termoeléctricos son accionados con más fuerza ya que la incertidumbre expandida en este margen es tres veces mayor que en el rango precedente. Sin embargo, un efecto similar ha sido observado por BEV/E+E para un 373LHX de margen extendido, con un generador con una incertidumbre estimada menor [3].

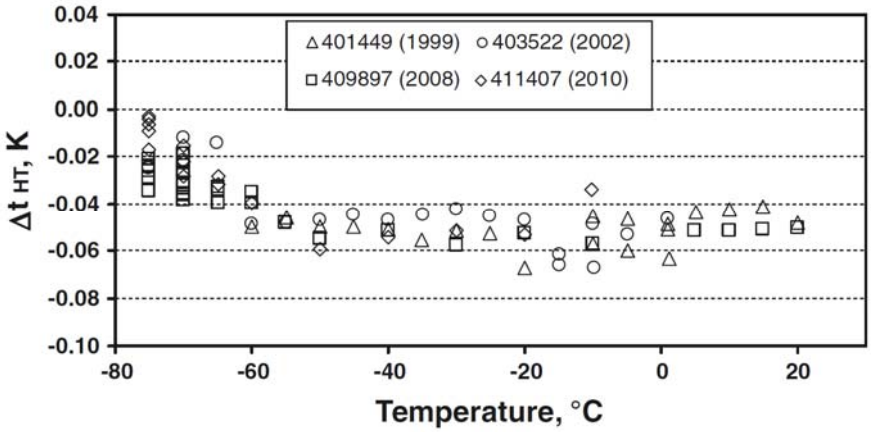

Fig. **4.3.2.3** Diferencia entre temperatura de rocío generada (INTA) y calibración en baño del TRP para 97-1220.

El higrómetro patrón de transferencia de alto rango MBW 373HX, número de serie 06-1112 ha sido estudiado exhaustivamente dentro de un proyecto de colaboración con BEV/E+E [9], que cubre la implementación de un generador patrón de humedad de alto rango en el INTA, su posterior validación y la optimización de la CMC. La figura **4.3.2.4** muestra la diferencia entre la temperatura de punto de rocío generada y la calibración en baño de TRP para las mediciones en BEV/E+E en 2009 y 2010 y la medición de INTA realizada con ambos generadores en 2009. La deriva del instrumento es despreciable A 80 ºC, y es un máximo de 15 mK a 95 ºC, dentro de la incertidumbre expandida de 50 mK asignada. La amplitud total del intervalo de los datos en un laboratorio en un año es de 20 mK en el margen completo de -10 ºC a 95 ºC, con los valores BEV/E+E más próximos al valor nominal producido por la calibración de la TRP. La diferencia entre las calibraciones BEV/E+E e INTA tiene una diferencia sistemática de 20 mK, y se mantiene durante todo el trabajo realizado. Las posibles causas de ello aún no se han identificado y son también parte del proyecto de colaboración entre ambos laboratorios. En cualquier caso, teniendo en cuenta toda la información disponible, la diferencia entre la realización de la temperatura de punto de rocío y la calibración en baño de la TRP está entre -40 mK y +10 mK en todo el margen.

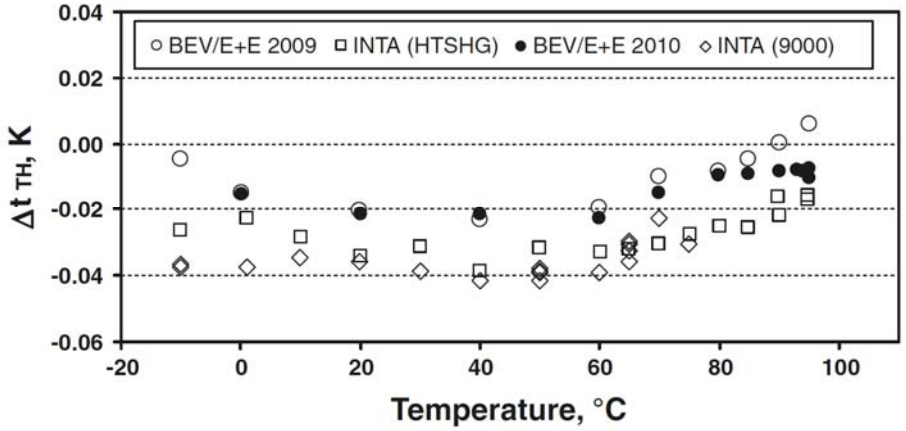

Fig. **4.3.2.4** Diferencia entre temperatura de rocío generada (BEV/E+E e INTA) y calibración en baño del TRP para 06-1112. BEV / E + E 2009 y 2010 e INTA con ambos generadores en 2009.

3.4. Consistencia de las realizaciones de punto de rocío de los patrones nacionales de humedad. (Benyon R and Vicente T "Consistency of the national realization of dew-point temperature using standard humidity generators". Int. Journal of Thermophysics, (2012) Volume 33, Issue 8-9, pp 1550-1558).

La robustez de la realización de temperatura de punto de rocío de los patrones nacionales se constata mediante la comparación de los dos generadores patrón en su margen de solape. Para poder comparar los generadores, se requiere la utilización de uno o más patrones de transferencia y el límite de incertidumbre de la comparación viene determinado, entre otros factores, por la repetibilidad y reproducibilidad combinada del generador y el higrómetro patrón. En este capítulo se resumen los resultados obtenidos, partiendo del estado del arte antes del desarrollo de la nueva sistemática y mostrando los nuevos resultados que mejoran la técnica en hasta un orden de magnitud.

3.4.1. Estado del arte antes de la nueva sistemática

Las primeras medidas de comparación entre los dos generadores fueron realizadas por el autor como jefe de sección técnica de patrones de humedad, bajo la supervisión del jefe del Laboratorio y presentadas en [1].

Las figuras **4.4.1.1** y **4.4.1.2**, presentan las medidas obtenidas en uno de los patrones de transferencia (DP3 N/S: 92-0322), para medidas sin y con calefacción, respectivamente. Los resultados se expresan en términos de la temperatura equivalente a la resistencia medida del TRP del espejo del patrón obtenida según la referencia y la temperatura de punto de rocío nominal, como ordenada; y la temperatura de punto de rocío de referencia como la abscisa. Los puntos indicados como cuadrados rojos, corresponden a las cuatro primeras series obtenidas con el generador antiguo y los círculos en azul corresponden a las medidas iniciales realizadas con el generador nuevo.

De estos resultados, el nivel de reproducibilidad de la realización de temperatura de punto de rocío en el INTA usando el generador antiguo y su coherencia con el nuevo generador puede ser establecida dentro de las limitaciones de los propios patrones de transferencia (un semi-intervalo de ± 15 mK hasta 60 ºC y ± 30 mK por encima).

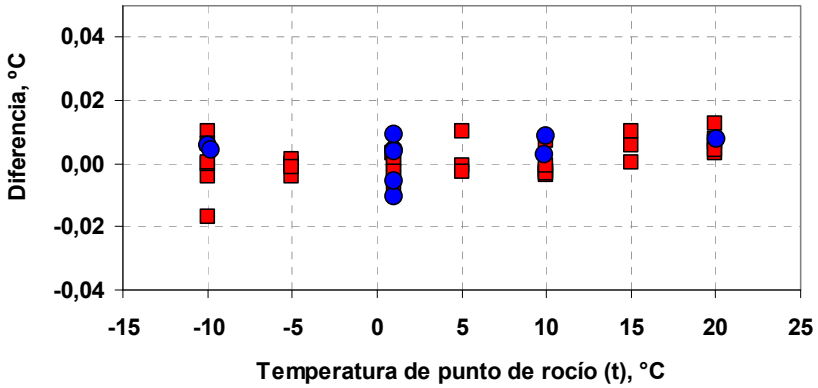

Figura **4.4.1.1**: Medidas realizadas en uno de los patrones de transferencia (Sin calefacción)

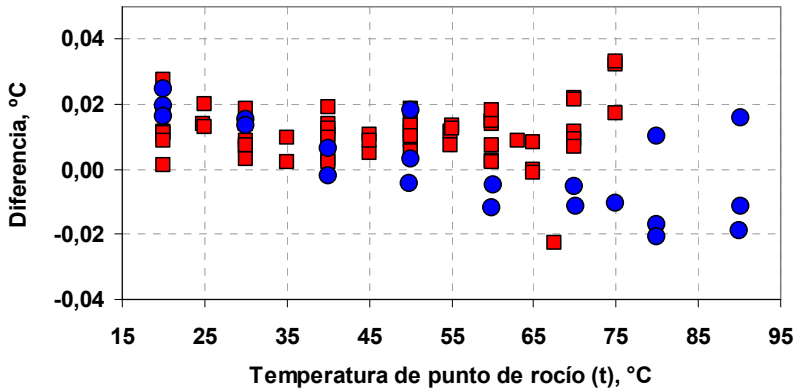

Figura **4.4.1.2**: Medidas realizadas en uno de los patrones de transferencia (Con calefacción)

La Tabla **4.4.1.1** muestra la diferencia entre los dos generadores obtenida de la media de los dos patrones de transferencia. Se observa que el nivel de acuerdo es excelente en el margen de -10 ºC a +60 ºC, donde los valores están dentro de la reproducibilidad combinada del generador y el patrón de transferencia. En el límite superior del generador, la diferencia aumenta hasta dos veces esta cantidad. Todos los resultados se encuentran dentro de los límites de CMC declarados por el INTA para ese generador (ver Tabla **4.4.1.2**), como se puede ver en la Fig**. 4.4.1.3**. El resultado es muy satisfactorio, teniendo en cuenta, que los dos generadores tienen saturadores de diseños completamente diferentes y que funcionan a caudales con un rango dinámico de 25:1.

Temperatura de punto de rocío (ºC)	Diferencia (Antiguo-Nuevo) (ºC)
-10	+0.005
1	-0.007
10	+0.002
20	+0.005
30	-0.004
40	+0.008
50	+0.015
60	+0.020
70	+0.021
75	+0.041

Tabla **4.4.1.1**: Diferencia entre los dos generadores patrón

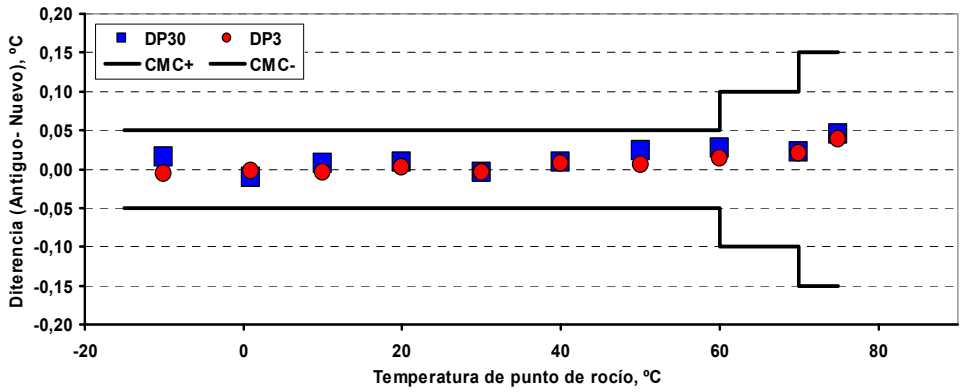

Figura **4.4.1.3**: Diferencia entre los dos generadores patrón comparados con las CMC basadas en el generador antiguo

Pos.	Nivel o margen del mensurando			Margen del mensurando		Incertidumbre expandida		Comparaciones que amparan la CMC
	Valor mínimo	Valor máximo	Unid.	Parámetro	Especificaciones	Valor	Unid.	
1	-60	<-10	ºC	Temperatura ambiente	(23 ± 1) ºC	0,05	ºC	EURAMET T-S19 Bilateral con NIST
2	-10	60	ºC	Temperatura cámara medida	(0 a 100) °C	0,05	ºC	EURAMET T-S19 Bilaterales con NIST y PTB
3	>60	70	ºC	Temperatura cámara medida	(0 a 100) °C	0,10	ºC	EURAMET T-S19 Bilateral con PTB
4	>70	75	ºC	Temperatura cámara medida	(0 a 100) °C	0,15	ºC	EURAMET T-S19 Bilateral con PTB

Tabla **4.4.1.2**: Resumen de la CMC de temperatura de punto de rocío para el generador antiguo

Con este nivel del estado del arte, se realizó una comparación bilateral con el patrón nacional austriaco dentro de un proyecto EURAMET [9], con resultados satisfactorios y que se resumen en la Tabla **4.4.1.3**.

Temperatura de punto de rocío (ºC)	Diferencia (BEV/E+E - INTA) (ºC)		Temperatura de punto de rocío (ºC)	Diferencia (BEV/E+E - INTA) (ºC)
-10	-0.006		50	0.029
1	-0.003		60	0.033
10	0.001		70	0.024
20	0.006		80	0.018
30	0.008		90	0.003
40	0.019			

Tabla **4.4.1.3**: Resultados de comparación bilateral BEV/E+E e INTA

3.4.2. Comparación con la nueva sistemática

En esta segunda comparación se han utilizado tres higrómetros de punto de rocío de última generación modelos 373HX de MBW CALIBRATION AG, de Suiza), todos ellos con endoscopio para poder observar las características del condensado sobre el espejo. Los detalles de los tres higrómetros se muestran en la Tabla **4.4.1.4**.

Generador			Patrón de Transferencia		
1	2	Márgen comparado	Fabricante	Modelo	Nº Serie
TSC9000 (Antiguo)	HTSHG (Nuevo)	-10 ºC a 75 ºC	MBW	373HX	06-1112
					08-0413
					08-0414

Tabla **4.4.1.4**: Detalle de los patrones de transferencia

Las medidas se tomaron en orden creciente de la temperatura de punto de rocío. En modo “dos presiones”, cada valor nominal fue generado con al menos dos combinaciones de presión y

temperatura diferentes, a fin de incluir la variación debida a los factores de corrección por no idealidad [1]. Los espejos de los instrumentos se limpiaron con alcohol isopropílico, seguido de agua desionizada de alta pureza a intervalos frecuentes durante todo el programa de medidas.

Antes del comienzo de cada secuencia de medida, a cada temperatura de baño, se aseguró la presencia de condensado suficiente en los dos elementos del saturador. En caso del generador antiguo, esto se realiza con sensores de nivel de líquido en el desagüe de saturador y en caso del nuevo generador, vaciando periódicamente el condensado de las dos etapas, en cada temperatura de baño.

A fin de establecer condiciones de referencia reproducibles y cuantificadas, el caudal de gas de muestreo de los higrómetros, medido después de la trampas de vapor aguas abajo de los instrumentos, fue ajustado para obtener un valor de caudal volumétrico constante en las condiciones de medida de la cabeza de higrómetro. Este valor fue fijado en 0,5 l/min. Las líneas de muestreo se mantuvieron 30 ºC por encima de la temperatura de punto de rocío generador, con un límite inferior de 30 ºC.

Todas las medidas de los patrones de transferencia se expresan en términos de la medida independiente del Termómetro de Resistencia de Platino (TRP) incorporado en el espejo del patrón de transferencia. Las condiciones de medida se resumen en:

a) el flujo volumétrico del gas sobre el espejo se mantiene constante en 0,5 $l.min^{-1}$;
b) la temperatura de la cabeza de medida y la temperatura del “pre-cooler” de los higrómetros (donde aplica) se mantuvo a una temperatura nominal de 30 ºC por encima de la temperatura de punto de rocío a medir;
c) el condensado sobre el espejo se evaporó y se formó antes de cada medida;
d) la presión absoluta nominal de la cabeza de medida fue de 1013 hPa;
e) las condiciones ambientales del Laboratorio se mantuvieron entre (23 ± 1) ºC y una humedad relativa en el ambiente menor del 70 %;
f) todas las medidas se realizaron en sentido creciente de niveles de humedad.

Las caídas de presión en las líneas de muestreo se midieron para cada configuración de medida y el flujo volumétrico se ajustó para cada temperatura de punto de rocío, según el procedimiento desarrollado y detallado en la referencia [3]. Los valores analizados están referenciados a las correcciones de las TRP según [8].

La comparación entre el generador antiguo (TSC9000) y el nuevo (HTSHG) se realizó en tres etapas de medida:

1 los tres patrones de transferencia 373HX (ver Tabla **4.4.1.5**) se calibraron utilizando el generador TSC9000 en el margen de – 10 ºC a + 60 ºC cada 10 ºC, y cada 5 ºC hasta el margen superior de + 75 ºC. En cada punto se realizaron dos medidas, salvo en los puntos 30 ºC, 50 ºC y 65 ºC, donde como mínimo se tomaron cuatro medidas;
2 se pasaron los tres patrones al generador HTSHG y se realizaron las medidas en los puntos de – 10 ºC, 1 ºC, 10 ºC, 20 ºC, 30 ºC, 50 ºC y 65 ºC con el mismo número de reiteraciones indicado anteriormente y cada 5 ºC hasta completar el margen superior de este generador (95 ºC);
3 las medidas en los puntos de 40 ºC, 60 ºC, 70 ºC y 75 ºC solo se realizaron para el DPM n/s: 06-1112.

Los resultados obtenidos se presentan en la Fig. **4.4.1.4** expresando la diferencia (en mK) entre los dos generadores, en función de la temperatura de punto de rocío medida en el espejo.

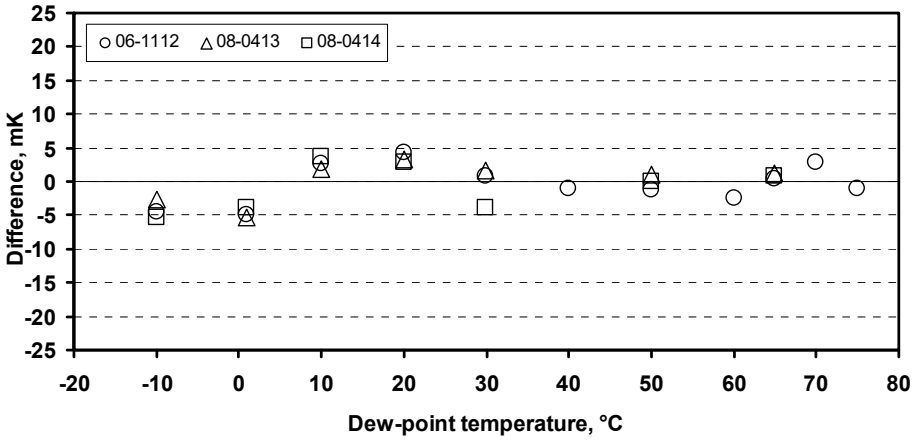

Figura **4.4.1.4**: Diferencia entre los generadores (TSC9000-HTSHG) entre -10 ºC a +75 ºC, expresadas en mK.

Como se puede observar el acuerdo en las medidas es excelente, encontrándose todas ellas dentro de ± 5 mK. La repetibilidad entre los valores medidos por los patrones de transferencia, en cada una de las temperaturas nominales de punto de rocío donde han coincidido, de nuevo se considera excelente ya que todas se encuentran dentro de 2 mK, excepto en el punto de 30 ºC donde la diferencia para el patrón de transferencia 08-0414 difiere 5 mK respecto de los otros dos higrómetros.

Con estos resultados se puede asegurar que no existe ninguna diferencia relevante entre los generadores y todos los valores se distribuyen simétricamente alrededor de cero. La media aritmética se ha considerado como valor adecuado para el análisis de los datos y se ha comprobado que el valor de la media y la desviación estándar obtenida individualmente para cada patrón de transferencia comparado con el análisis del conjunto de datos para los tres patrones posee un alto grado de acuerdo (ver. Tabla **4.4.1.5**) tienen un alto grado de acuerdo, con una diferencia media de – 0.3 mK y una desviación estándar de 3 mK si analizamos el total de los datos. El número individual de medidas para cada generador está indicado entre paréntesis. Es importante mencionar que las CMCs del Laboratorio para estos márgenes están entre:

50 mK y 150 mK para el TSC9000 y 50 mK para el HTSHG, con un nivel de confianza de aproximadamente el 95 %. En la Tabla **4.4.1.6** se presenta un ejemplo de cálculo de incertidumbre para la generación de temperatura de punto de rocío de 20 ºC.

Patrón de Transferencia	**06-1112**	**08-0413**	**08-0414**	**Todos**
	Diferencia TSC9000-HTSHG, mK			
Media	-0.4	0.1	-0.8	-0.3
Desv. Std.	2.9	3.0	3.6	3.0
nº (9000 / HTSHG)	(19/63)	(26/61)	(26/41)	(71/165)

Tabla **4.4.1.5**: Valores medios y desviaciones estándar de las diferencias obtenidas en las medidas de temperatura de punto de rocío/escarcha entre (TSC9000-HTSHG)

Se debe tener en cuenta, que en la investigación de la diferencia entre los dos generadores hay muchos términos que se anularían y que están altamente correlacionados (por ejemplo: misma trazabilidad en los medidores de temperatura y presión, mismos modelos de equipos, misma presión de vapor saturante y la incertidumbre de los "*enhancement factor*" son similares al utilizarse las mismas combinaciones de temperatura/presión). La deriva de los patrones de

transferencia es insignificante al realizar todas las medidas en un periodo de 8 semanas, por lo que básicamente, las contribuciones dominantes son atribuibles directamente a los patrones de transferencia y a las correcciones por caída de presión en ambos generadores, por las diferencias existentes entre el punto de medida de la presión al punto de referencia en el espejo.

Para el TSC9000 es aproximadamente, una caída de 2 hPa en la línea de gas hasta la cabeza de medida, y en el HTSHG es un incremento de aproximadamente 0.2 hPa aguas abajo de la medida de presión hasta la cabeza

(símbolo) Q_i		Incert. $u_{(Qi)}$		D.o.f. ν_i	**Coc.**	**Contrib. u_i en °C**
Temperatura saturación	*Termómetro:*					
	Incertidumbre de calibración (sensor e indicador)	0.002	ºC	50	0.927	0.0019
	Estabilidad a largo plazo (sensor e indicador)	0.005	ºC	50	0.927	0.0046
	Auto calentamiento y flujos de calor residual (sensor)	0.001	ºC	50	0.927	0.0009
	Resolución y especificaciones o linealidad (indicador)	0.001	ºC	50	0.927	0.0009
	Saturador:					
	Temperatura homogeneidad	0.012	ºC	50	0.927	0.0107
	Temperatura estabilidad	0.003	ºC	30	0.927	0.0028
Presión saturación	*Medidor de presión:* Incertidumbre de calibración (sensor e indicador)	6	Pa	50	-8.702E-05	-0.0005
	Estabilidad a largo plazo (sensor e indicador)	112.4	Pa	50	-8.702E-05	-0.0098
	Resolución y especificaciones o linealidad (indicador)	1	Pa	50	-8.702E-05	-0.0001
	Diferencias de presión en el saturador	100	Pa	50	-8.702E-05	-0.0087
	Estabilidad de presión	60	Pa	30	-8.702E-05	-0.0052
	Efectos de los tubos entre el saturador y el medidor	10	Pa	50	-8.702E-05	-0.0009
Presión del gas a la salida del generador	*Medidor de presión:* Incertidumbre de calibración (sensor e indicador)	6	Pa	50	1.588E-04	0.0010
	Estabilidad a largo plazo (sensor e indicador)	90.8	Pa	50	1.588E-04	0.0144
	Resolución (indicador)	0.6	Pa	50	1.588E-04	0.0001
	Estabilidad de presión	20	Pa	30	1.588E-04	0.0032
	Efectos de los tubos entre el saturador y el medidor	6	Pa	50	1.588E-04	0.0009
Incertidumbres debidas a fórmulas / cálculos	Saturation vapour pressure formula(es)	5.000E-05		50	16.055	0.0008
	Water vapour enhancement formula(fs)	1.122E-04		50	16.136	0.0018
	Saturation vapour pressure formula(ed)	5.000E-05		50	-16.136	-0.0008
	Water vapour enhancement formula(fd)	6.858E-05		50	-16.136	-0.0011
Otras	Caídas de presión en líneas de muestro	5.77	Pa	50	1.588E-04	0.0009
Incertidumbre combinada						0.0240
Grados efectivos de libertad				226		
Incertidumbre expandida				2.01		**0.048**

Tabla **4.4.1.6**: Ejemplo de cálculo de incertidumbre para un valor de temperatura de punto de rocío de 20 ºC.

3.5. Comparación clave internacional de temperatura de punto de rocío en el margen de 30 ºC a 95 ºC (CCT-K8)

En virtud del Acuerdo de Reconocimiento Mutuo (MRA), la equivalencia metrológica de los patrones nacionales de medida se determinará mediante un conjunto de comparaciones clave elegidas y organizadas por los Comités Consultivos del CIPM en estrecha colaboración con las Organizaciones Regionales de Metrología. El patrón nacional de humedad alta del INTA, validado en este trabajo, ha sido empleado para organizar una comparación clave mundial entre los principales laboratorios nacionales e Institutos Designados. La comparación ha sido organizada teniendo en cuenta todos los aspectos desarrollados en los apartados anteriores.

3.5.1. Protocolo

Se ha desarrollado un protocolo que define todos los aspectos técnicos relacionados con las medidas y la evaluación de los resultados para determinar el valor de referencia de la comparación clave (KCRV en sus siglas en inglés), así como los aspectos organizativos. El protocolo de la comparación ha sido sometido a una revisión por pares de dos pasos: primero por los miembros del CCT-WG.Hu (humedad) y del CCT-WG.KC (comparaciones clave). El protocolo aprobado está publicado en [13].

Para poder realizar la comparación en periodo de tiempo razonable, se ha configurado en dos lazos usando un patrón de transferencia en cada uno (véase la figura **4.5.1.1**). Se ha realizado la caracterización completa en INTA Esta comparación es coordinada y pilotada por el INTA, con el National Institute of Standards and Technology (NIST) como co-piloto en el margen de su patrón. Se ha organizado además que ambos lazos coincidan en BEV/E+E para la realización de un control de deriva intermedio antes de partir para Rusia y Japón.

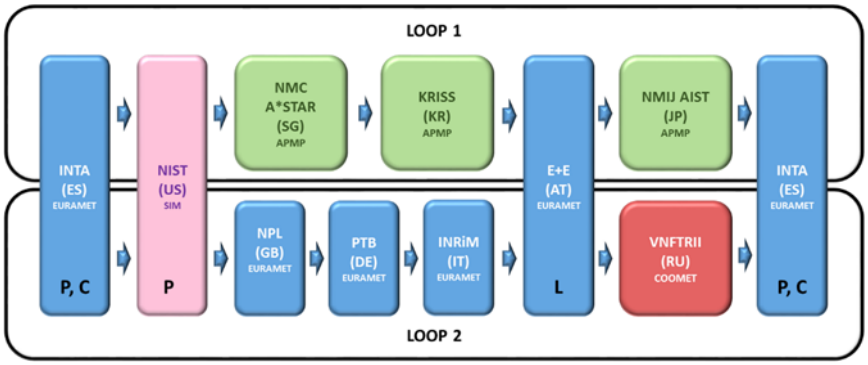

Fig. **4.5.1.1** Esquema de circulación de los patrones viajeros

En octubre de 2016 se completaron las medidas finales de referencia en el INTA y los dos instrumentos fueron medidos en el NIST de acuerdo con lo indicado en la planificación indicada en la figura **4.5.1.2**.

La comparación se ha desarrollada de acuerdo con la planificación y debido a que no se observaron en algunos países las formalidades de los cuadernos ATA, se decidió traer los instrumentos de vuelta a España para regularizar los cuadernos ATA y la reimportación en la U.E. y de paso hacer otra serie de medidas adicionales al detectarse una posible pequeña deriva en el instrumento de uno de los lazos. Los equipos llegaron al INTA a finales de abril y está prevista su entrega en los siguientes laboratorios antes de final de mayo de 2017 para completar las rondas de medidas.

Year		2016				2017											
Month		O	N	D	J	F	M	A	M	J	J	A	S	O	N	D	
Spain	ES	■	X														
United States of America	US		■	■	X												
Singapore	SG			■	■	■	X										
Republic of Korea	KR					■	■	X									
Austria	AT							■	■	X							
Japan	JP								■	■	X						
Spain	ES										■	■					

Comparison scheme of loop 1 (One column corresponds to two weeks; ■ = measurement, X = measurement / transportation).

Year		2016				2017											
Month		O	N	D	J	F	M	A	M	J	J	A	S	O	N	D	
Spain	ES	■	X														
United States of America	US		■	■	X												
United Kingdom	GB			■	■	X											
Germany	DE				■	■	X										
Italy	IT					■	■	X									
Austria	AT							■	■	X							
Russian Federation	RU								■	■	X						
Spain	ES										■	■					

Comparison scheme of loop 2 (One column corresponds to two weeks; ■ = measurement, X = measurement / transportation).

Fig. **4.5.1.2** Planificación incluida en el protocolo.

Se han aplicado todas las facetas desarrolladas en este trabajo, desde la caracterización y selección de los TRP antes de su integración en el espejo, como la evaluación de los factores de influencia, etc. En especial, dada la importancia demostrada de definir correctamente el caudal volumétrico, se decidió además diseñar y construir dos trampas de vapor y sus accesorios para determinar el caudal y hacer la medida de presión para determinar correctamente las caídas de presión. La figura **4.5.1.3** muestra el esquema indicado en el protocolo con los elementos facilitados. Las fotos están disponibles en [13].

Se fabricó además una toma de presión para medir la presión diferencial entre la cabeza de medida y la toma de presión exterior. Esta toma tiene las características dimensionales del endoscopio y se inserta en su lugar en la medida de presión diferencial.

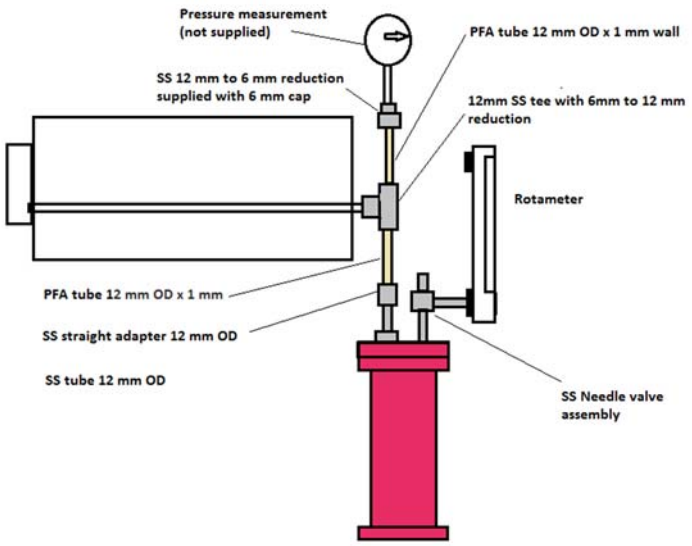

Fig. **4.5.1.3** Esquema de conexión de trampa de vapor y toma de medida de presión.

3.5.2. Resultados preliminares

De acuerdo con la normativa establecida por el BIPM sobre las comparaciones clave [7] no está permitido facilitar los resultados de la comparación hasta la aceptación del borrador A por parte de todos los participantes. No obstante, como soporte al trabajo realizado en aplicación de los criterios y técnicas desarrolladas y optimizadas en estos trabajos, se presentan a continuación y analizan de forma diferencial, las magnitudes de las diferencias entre el piloto (INTA), co-piloto (NIST) y laboratorio lazo (BEV/E+E).

La Figura **4.5.2.1** Muestra las diferencias del NIST y BEV/E+E relativas al valor inicial del INTA para el patrón de transferencia del lazo 1. Las barras de error son las CMC de dichos los laboratorios. Las líneas punteadas son una regresión lineal a los valores a efectos de evaluar la diferencia entre estos laboratorios. En todo el margen de solape, los valores están dentro de ± 10 mK. Esto es un resultado muy satisfactorio e indica que este instrumento no tiene una deriva apreciable, en base al histórico de medidas con el higrómetro monitor comparado entre el INTA y BEV/E+E en el marco del proyecto EURAMET [9] que fue informado en apartados anteriores.

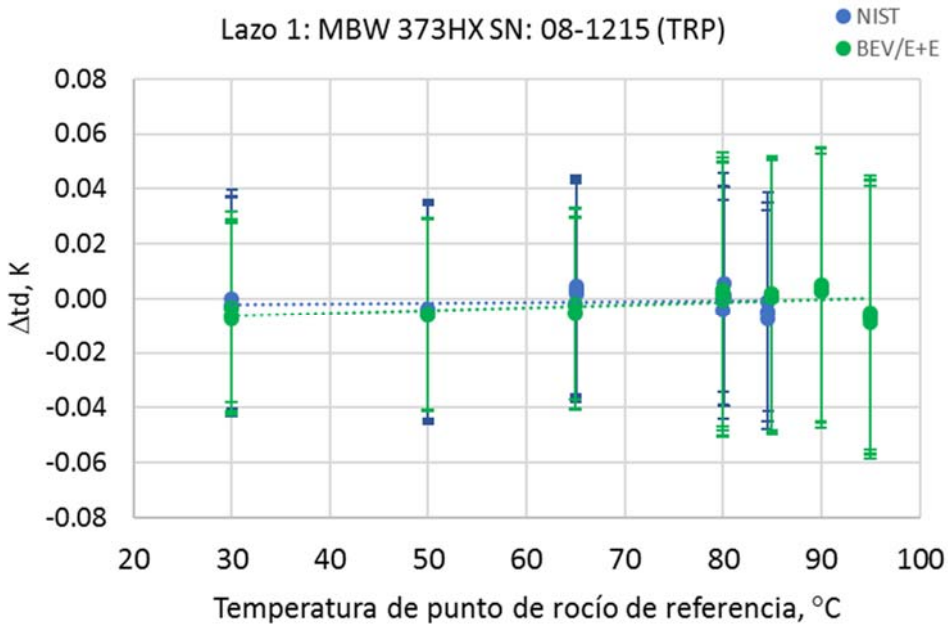

Fig. **4.5.2.1** Resultados de las diferencias de corrección relativa al INTA de NIST y BEV/E+E para el lazo 1

El mismo análisis se realiza para el patrón de transferencia del lazo 2 (véase la figura **4.5.2.2**). En este instrumento todo el margen de solape, los valores están dentro de ±15 mK con respecto al INTA y entre los participantes. Esto es un resultado, aun siendo muy satisfactorio, podría ser señal de que este instrumento tiene una deriva del orden de 11 mK.

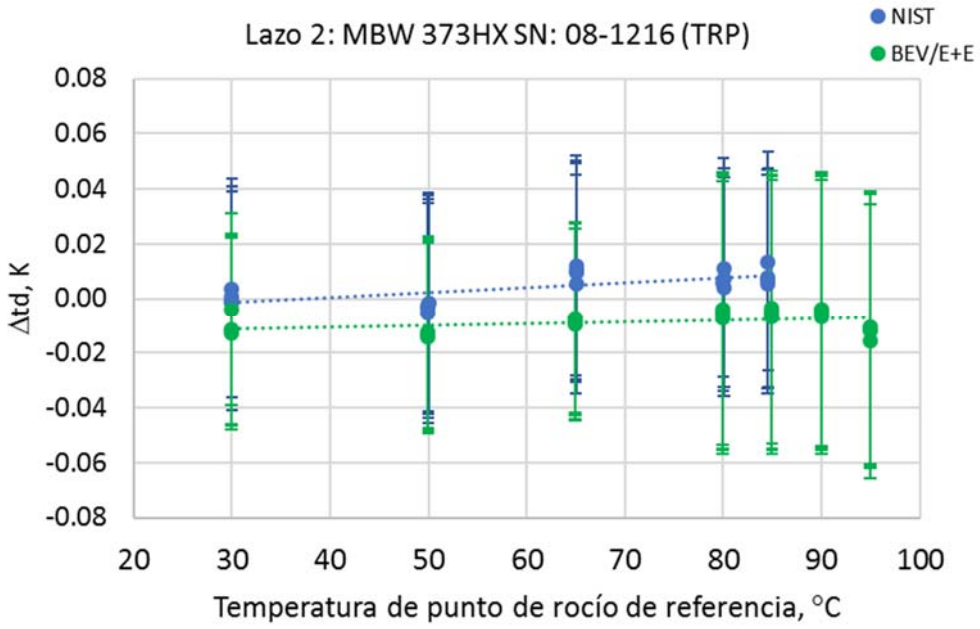

Fig. **4.5.2.2** Resultados de las diferencias de corrección relativa al INTA de NIST y BEV/E+E para el lazo 2

Para interpretar este resultado, se presenta en la figura **4.5.2.3** la diferencia entre la diferencia valores de resistencia medidos entre los dos instrumentos en cada laboratorio, relativo al INTA. Es decir:

$$\Delta R_{td} = [\, R_{td}(08\text{-}1216) - R_{td}(08\text{-}1215)\,]_{LAB} - [\, R_{td}(08\text{-}1216) - R_{td}(08\text{-}1215)\,]_{INTA} \quad (1)$$

Donde R_{td} es la resistencia en Ohmios, a la temperatura de rocío nominal t_d. La ordenada equivale a ± 20 mK, con una división de escala de 5 mK.

Esta medida es independiente de la trazabilidad, al ser solo función de la habilidad en fijar bien los caudales y establecer una diferencia de presión constante entre los dos instrumentos. Es un buen indicador de consistencia y además permite determinar la deriva relativa de los instrumentos.

Este parámetro tiene una incertidumbre asociada muy baja y se tiene previsto utilizar esto de forma novedosa para hacer el *linkage* entre los lazos de esta comparación y entre la comparación CCT-K8 y la EUROMET-T.K8, ya que el INTA y BEV/E+E participaron en ambas y midieron los dos lazos. Se prevé que esto reduzca sensiblemente la incertidumbre en la determinación de los grados de equivalencia entre laboratorios.

En la figura, las barras de error representan dos desviaciones típicas de las cuatro determinaciones de diferencia de resistencia, [R_{td}(08-1216) - R_{td}(08-1215)], de cada participante.

Si se miran los valores del NIST, que se realizaron tan solo dos meses después de los valores del INTA, se ve que las barras de error se solapan y que se observa una peor reproducibilidad en el valor del extremo del margen de su generador, pero no se puede apreciar deriva relativa.
Sin embargo, si observamos los valores de BEV/E+E vemos que son muy reproducibles y existe una diferencia sistemática media de 6 mK con una desviación típica de 1,7 mK. Este valor es coherente con la posible deriva del instrumento del lazo 2 que se observa en los resultados de BEV/E+E, transcurridos 6 meses desde los valores del INTA.

Todo lo anterior solo se podrá corroborar con las segundas medidas del piloto (INTA) en curso.

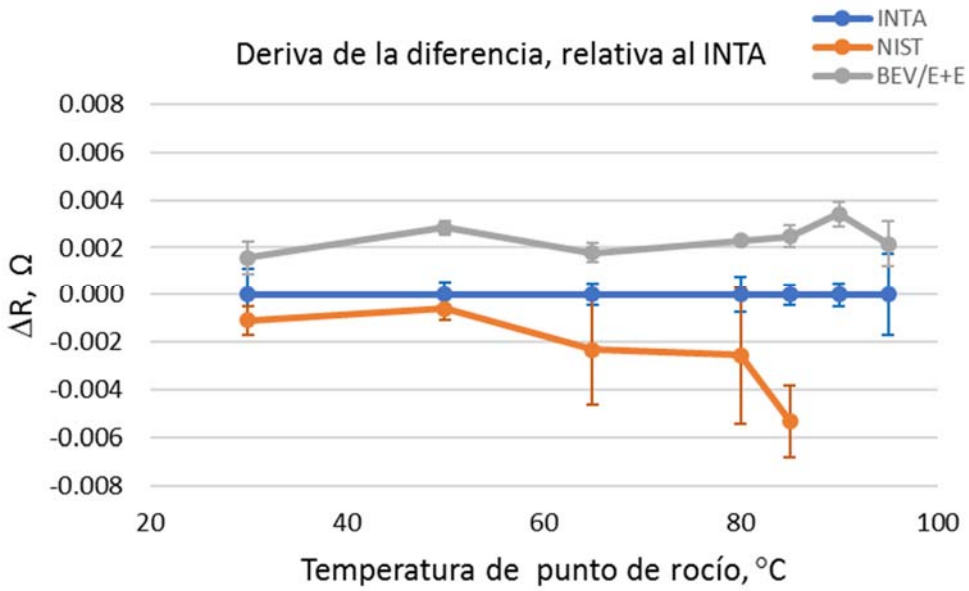

Fig. **4.5.2.3** Diferencia local entre las correcciones de los instrumentos de lazos 1 y 2

4. CONCLUSIONES

Los objetivos alcanzados en esta tesis nos permiten presentar las siguientes conclusiones:

Se ha ampliado y mejorado la capacidad de medida y calibración. La incertidumbre típica de medida de la temperatura de punto de rocío (para k=2) en el margen de interés de esta Tesis, ha pasado de ser de entre 0,10 °C y 0,15 °C de 50 °C a 75 °C, as ser de 0,050 °C en todo el margen, ampliado hasta 95 °C. Esto sitúa a España en el grupo de cabeza de países cuyos laboratorios nacionales e institutos designados con CMC en la magnitud de temperatura de punto de rocío.

Se ha realizado un estudio de magnitudes de influencia (repetibilidad, reproducibilidad y cociente de temperatura), mediante el análisis exhaustivo de calibraciones de distintos tipos de instrumentos para poder acometer con rigor la validación del nuevo generador y demostrar en el ámbito internacional su capacidad de medida y calibración.

Se ha desarrollado y perfeccionado una sistemática para asegurar la reproducibilidad de las condiciones de caudal de gas de muestreo de los patrones de transferencia para minimizar la contribución de incertidumbre debido a la influencia de la caída de presión resultante entre el punto de materialización de la unidad en el saturador del patrón y el punto de medida (espejo) del patrón de transferencia. Esta técnica ha sido incluida en los protocolos de comparaciones internacionales tanto del CCT y de organismos metrológicos regionales como EURAMET y APMP.

Se han determinado las contribuciones debido a los gradientes en el espejo de los DPM y la mejora de la estabilidad a largo plazo de los DPM mediante la caracterización, estabilización y selección previa de los TRP antes de su integración en los espejos de los patrones de transferencia. Esto es la primera vez que se publica un trabajo de este tipo y se determina la relación entre la trazabilidad metrológica vía termometría de contacto y la realización primaria de temperatura de punto de rocío

Se han publicado en el KDCB las nuevas capacidades de medida y calibración de higrómetros de punto de rocío con el patrón nacional de humedad en el margen de temperatura de punto de rocío de -10 ºC a 95 ºC, con la incertidumbre expandida de 0,050 ºC, que ahora disponen de las evidencias de su justificación con el trabajo desarrollado en esta Tesis.

A partir de esta nueva capacidad ya se puede dar trazabilidad a los ensayos climáticos en condiciones de 85 ºC / 85 %hr que demandaban los laboratorios de ensayos y que no tenían más remedio que acudir a otros países para obtener la trazabilidad metrológica. Además, la incertidumbre asignada es suficiente para asegurar el cumplimiento de especificaciones de los instrumentos más modernos usados en la industria nacional.

Los estudios de magnitudes de influencia y comportamiento de higrómetros de punto de rocío patrón y de uso industrial, han permitido determinar el alcance de calibración necesario para asegurar la trazabilidad metrológica en las condiciones de uso. Esto contribuye a determinar un alcance de calibración adecuado a las necesidades de los laboratorios y sostenible económicamente.

Por todo lo anterior se concluye que el laboratorio de temperatura y humedad del INTA está capacitado para dar los valores de referencia para una comparación clave del CCT en este margen de temperatura de punto de rocío.

La prueba final del alineamiento con el estado del arte en la medida de temperatura de punto de rocío en el margen de interés para la realización de la comparación internacional de temperatura de punto de rocío CCT-K8, vendrá de la aplicación del protocolo desarrollado en base a los conocimientos adquiridos en esta Tesis. Se ha iniciado una comparación clave, CCT-K8, y los resultados preliminares informados en esta Tesis, comparativa con el NIST y BEV/E+E, son coherentes con los objetivos perseguidos.

5. REFERENCIAS

[1] Benyon R, Mitter H, "*The new INTA high-range standard humidity generator and its comparison with the Austrian national humidity standard maintained at BEV/E+E*". Int. Journal of Thermophysics (2008), Vol. 29, Number 5, 1623-1631.

[2] Benyon R, Vicente T, Hernandez P, De Rivas L and Conde F. "Evaluation of the Long-Term Stability and Temperature Coefficient of Dew-Point Hygrometers". Int. Journal of Thermophysics (2012). Vol. 33, Issue 8-9, pp 1758-1770.

[3] Mitter H, Böse N, Benyon R and T. Vicente, "Pressure drop considerations in the characterization of dew-point transfer standards at high temperatures". Int. Journal of Thermophysics (2012), Vol. 33, Issue 8-9, pp 1726-1740.

[4] Benyon R, Böse N, Mitter H, Mutter D, Vicente T "An Investigation of the Relation Between Contact Thermometry and Dew-Point Temperature Realization". Int. Journal of Thermophysics (2012), Vol. 33, Issue 8-9, pp 1741-1757.

[5] Benyon R and Vicente T "Consistency of the national realization of dew-point temperature using standard humidity generators". Int. Journal of Thermophysics, (2012) Volume 33, Issue 8-9, pp 1550-1558.

[6] JCGM 100:2008. Evaluation of measurement data - Guide to the expression of uncertainty in measurement. BIPM. First edition September 2008. http://www.bipm.org .

[7] CIPM MRA-D-05. Measurement comparisons in the CIPM MRA. Version 1.6. March 2016. http://www.bipm.org/en/cipm-mra/cipm-mra-documents/

[8] IEC 60751:2008 Industrial platinum resistance thermometers and platinum temperature sensors.

[9] EURAMET P 1032 High-range dew-point temperature realization using two-pressure generators. http://www.euramet.org/technical-committees/search-tc-projects/.

[10] "The BIPM key comparison database". The current Calibration and Measurement Capabilities for INTA are available on http://kcdb.bipm.org/AppendixC/. Last update: February 2010.

[11] ENAC Accreditation number 16/LC10.007, Technical Annex Rev. 8 (2016). The current scope of accreditation is available on http://www.enac.es.

[12] M. Heinonen, "Report to the CCT on Key Comparison EUROMET.T-K6 (EUROMET Project no. 621): Comparison of the realisations of local dew/frost-point temperature scales in the range -50 °C to +20 °C", Draft B. Final Version. (2009).

[13] CCT-K8 Comparison of realizations of local scales of dew-point temperature of humid gas. Technical protocol (Approved CCT-WG.KC). 22/02/2017. Available on http://kcdb.bipm.org/appendixB/appbresults/CCT-K8/CCT-K8_Technical_Protocol.pdf..

[14] R. Benyon, J. De Lucas, A.Moratilla, Humidity calibration in the modern accredited laboratory, in Papers and Abstracts from the Third International Symposium on Humidity and Moisture, vol. 1 (National Physical Laboratory, Teddington, 1998), pp. 206–213.

[15] P. Mackrodt, R. Benyon, G. Scholz, State-of-the-art calibration of high-range chilled-mirrror hygrometers and their use in the intercomparison of humidity standard generators, in Papers and Abstracts from the Third International Symposium on Humidity and Moisture, vol. 1 (National Physical Laboratory, Teddington, 1998), pp. 159–166.

[16] R. Benyon, P. Huang, “A comparison of INTA and NIST humidity standard generators,” in Papers and Abstracts from the Third International Symposium on Humidity and Moisture, vol. 1 (National Physical Laboratory, Teddington, 1998), pp. 28–36.

[17] V.P. Petukhov, Meas. Tech. 25, 845 (1982).

[18] M. Lidbeck, J. Ivarsson, E. András, J.E. Holmen, T. Weckström, F. Andersen, Int. J. Thermophys. 29, 414 (2008).

[19] V.C. Fernicola, L. Iacomini, Int. J. Thermophys. 29, 1817 (2008).

[20] M. Heinonen, Metrologia 47, Tech. Suppl. 03003 (2010).

[21] EURAMET TC Project P-717, Progress report available on http://www.euramet.org. Accessed 01 March 2010.

[22] H. Mitter, The BEV/E+E elektronik standard humidity generator, in Proceedings of the 5th International Symposium on Humidity and Moisture, INMETRO, Brazil, 2006.

[23] G. Scholz, Bulletin OIML No. 97 (December 1984), pp. 18–27.

[24] P. Mackrodt, F. Fernandez, in Proceedings of TEMPMEKO 2001, 8th International Symposium on Temperature and Thermal Measurements in Industry and Science, ed. by B. Fellmuth, J. Seidel, G. Scholz (VDE, Berlin, 2002), pp. 589–596.

[25] ENAC Accreditation Number 16/LC150T, Technical AnnexRev. 7 (2008). The current scope of accreditation is available on http://www.enac.es . Accessed 01 March 2010.

[26]. E. Tegeler, D. Heyer, B.R.L. Siebert, Int. J. Thermophys. 29, 1174 (2008) 123.

[27] EURAMET-T.K8 Comparison in humidity (dew-point temperature high range), Technical protocol (Draft 20081212).

[28] CIPM Mutual Recognition Arrangement (CIPM-MRA): Mutual recognition of national measurement standards and of calibration and measurement certificates issued by nationalmetrology institutes, Paris, October 1999, Technical Supplement revised in October 2003. http://www.bipm.org/en/cipm-mra/ .

[29] Current scopes of accreditation of the INTA Metrology and Calibration Centre (Laboratory No. 16) in the fields of electricity, flow, pressure and temperature. http://www.enac.es .

[30] The ILAC Mutual Recognition Arrangement (ILAC-MRA). http://www.ilac.org/.

[31] TH/PRC/7234/106/INTA Ed. 02, Calibration of dew-point hygrometers using standard humidity generators.

[32] J.W. Lovell-Smith, Metrologia 43, 556 (2006).

[33] J.W. Lovell-Smith, Metrologia 44, L49 (2007).

[34] J.W. Lovell-Smith, Metrologia 46, 607 (2009).

[35] ISO/IEC 17025:2005, General requirements for the competence of testing and calibration laboratories.

[36] M. Heinonen, Report to the CCT on key comparison EUROMET.T-K6 (EUROMET Project No. 621): comparison of the realisations of local dew/frost-point temperature scales in the range−50 °C to+20 °C (Draft B, final version, 2009)

[37] L.P. Harrison, in Humidity and Moisture Fundamentals and Standards, vol. 3, ed. by A. Wexler, W.A. Wildhack (Reinhold Publishing, New York, 1965), pp. 3–69

[38] D. Sonntag, Z. Meteorol. 70, 340 (1990)

[39] L. Greenspan, J. Res. Nat. Bur. Stand. (U.S.) Phys. Chem. 80A, 41 (1976)

[40] B. Hardy, ITS-90 formulations for vapour pressure, frostpoint temperature, dewpoint temperature and enhancement factors in the range −100 to 100 ◦C, in Proceedings of Third International Symposium on Humidity and Moisture (National Physical Laboratory, London, 1998), pp. 214–221

[41] P717 EURAMET Comparison in humidity (dew-point temperature high range), http://www.euramet.org/index.php?id=tc-t-projects&no_cache=1&ctcp_projects[cmd]=details&ctcp_projects[uid]=596

6. SÍMBOLOS Y ABREVIATURAS

Pa	Unidad de presión. pascal
K	Unidad de temperatura. kelvin
U	Incertidumbre expandida
u	Incertidumbre típica
ν	Grados efectivos de libertad
APMP	Asia Pacific Metrology Program
BIPM	Bureau International des Poids et Mesures – Bureau Internacional de Pesas y Medidas
CCT	Comité consultatif de thermométrie – Comité Consultivo de Temperatura
CEM	Centro Español de Metrología
CIPM	Comité Internationale des Poids et Mesures - Comité Internacional de Pesas y Medidas
CMC	Capacidades de Medida y Calibración
CSM	Consejo Superior de Metrología
DPM	Dew Point Mirror (Higrómetro de punto de Rocio de espejo enfriado)
E+E	BEV/E+E Elektronik
EURAMET	Entidad Legal de la Metrología Europea para la Cooperación entre los Institutos Nacionales de Metrología Europeos y la Comisión Europea.
KC	Comparaciones clave
KCDB	Key Comparison Data Base
INM	Instituto Nacional de Metrología
INTA	Instituto Nacional de Técnica Aeroespacial
KCRV	Key Comparison Reference Value
MBW	MBW Calibration AG
MRA	Mutual Recognition Arrangement. Acuerdo de Reconocimiento Mutuo (ARM).
NIST	National Institute of Standards and Technology
NPL	National Physical Laboratory
OMR	Organización Metrológica Regional
PTB	Physikalishe-Technische Bundesanstalt
TRP	Termómetro de resistencia de platino

7. ANEXOS

- Benyon R, Vicente T, Hernandez P, De Rivas L and Conde F. “Evaluation of the Long-Term Stability and Temperature Coefficient of Dew-Point Hygrometers”. Int. Journal of Thermophysics (2012). Vol. 33, Issue 8-9, pp 1758-1770.
- Mitter H, Böse N, Benyon R and T. Vicente, “Pressure drop considerations in the characterization of dew-point transfer standards at high temperatures”. Int. Journal of Thermophysics (2012), Vol. 33, Issue 8-9, pp 1726-1740.
- Benyon R, Böse N, Mitter H, Mutter D, Vicente T “An Investigation of the Relation Between Contact Thermometry and Dew-Point Temperature Realization”. Int. Journal of Thermophysics (2012), Vol. 33, Issue 8-9, pp 1741-1757.
- Benyon R and Vicente T “Consistency of the national realization of dew-point temperature using standard humidity generators”. Int. Journal of Thermophysics, (2012) Volume 33, Issue 8-9, pp 1550-1558.
- CCT-K8 Comparison of realizations of local scales of dew-point temperature of humid gas. Technical protocol (Approved CCT-WG.KC). 22/02/2017.

Int J Thermophys
DOI 10.1007/s10765-012-1346-2

Evaluation of the Long-Term Stability and Temperature Coefficient of Dew-Point Hygrometers

R. Benyon · T. Vicente · P. Hernández · L. De Rivas · F. Conde

Received: 29 April 2010 / Accepted: 11 October 2012

Abstract The continuous quest for improved specifications of optical dew-point hygrometers has raised customer expectations on the performance of these devices. In the absence of a long calibration history, users with a limited prior experience in the measurement of humidity, place reliance on manufacturer specifications to estimate long-term stability. While this might be reasonable in the case of measurement of electrical quantities, in humidity it can lead to optimistic estimations of uncertainty. This article reports a study of the long-term stability of some hygrometers and the analysis of their performance as monitored through regular calibration. The results of the investigations provide some typical, realistic uncertainties associated with the long-term stability of instruments used in calibration and testing laboratories. Together, these uncertainties can help in establishing initial contributions in uncertainty budgets, as well as in setting the minimum calibration requirements, based on the evaluation of dominant influence quantities.

Keywords Calibration · Dew-point temperature · Drift · Humidity · Hygrometer · Traceability

1 Introduction

In the absence of a long calibration history, laboratory managers often rely solely on manufacturer specifications when estimating the components of uncertainty due to the long-term stability of the instruments and the effects of influence quantities such as the temperature dependence of the dew-point temperature reading. This leads in many cases to rather optimistic estimations of uncertainty and is particularly problematic

R. Benyon (✉) · T. Vicente · P. Hernández · L. De Rivas · F. Conde
Instituto Nacional de Técnica Aeroespacial, Torrejón de Ardoz, Madrid, Spain
e-mail: benyonpr@inta.es

Published online: 27 October 2012

in the assessment of new calibration laboratories seeking accreditation according to ISO/IEC 17025 [1]. Often, laboratories have significant difficulties in justifying some of the contributions in their uncertainty budgets, and in particular, the long-term stability in the actual conditions of use. This leads often to inevitable surprises in the first surveillance visit.

Instituto Nacional de Técnica Aeroespacial (INTA) is the Spanish designated institute for the field of humidity, and as such, performs the calibration of chilled-mirror hygrometers using standard humidity generators for realization of the dew-point temperature, in accordance with the calibration and measurement capabilities (CMCs) included in Appendix C of the CIPM-MRA [2,3]. Subsequent dissemination is carried out under accreditation by the Spanish National Accreditation Body (ENAC) [4] under the ILAC-MRA [5]. During this activity, the Laboratory has accumulated a wealth of data on its own and customer instruments used in diverse levels of demanding applications such as, for example, the research and testing laboratories within INTA. From this data, we report here the evaluation of the long-term performance of typical instruments under a range of conditions.

2 Measurements

2.1 Devices and Measurement Conditions

The chilled-mirror hygrometers investigated are listed in Table 1. These measure the condensation temperature of the water vapour in a sample of gas in a continuous flow configuration. Condensation on the mirror as the temperature is reduced from a value above the dew-point temperature produces a reduction in the reflectance signal detected by an optical sensor, compared to the higher signal corresponding to a clean mirror. This signal acts on a control loop that adjusts the current passing through thermoelectric coolers to obtain a constant thickness of condensate. The temperature of the mirror is determined using an industrial platinum resistance thermometer (IPRT) embedded below the surface of the mirror and is measured using an incorporated temperature indicator. In addition, in precision laboratory transfer standards, a second IPRT can be made available for direct measurement using external precision resistance measuring devices. For instruments with only one IPRT in the mirror, measurement of the sensor using an external resistance measuring device is also possible provided the incorporated temperature indicator is not left in open circuit.

The measurements reported here have been extracted from records of calibrations performed at INTA using standard humidity generators (for lowest uncertainty) [6–8] or by comparison with precision dew-point temperature hygrometers calibrated against the primary standards [9]. Unless otherwise specified, calibrations are performed with (a) a constant volumetric flow rate of $0.5\,\mathrm{L}\cdot\mathrm{min}^{-1}$ at the mirror, (b) a head temperature and pre-cooler temperature (where applicable) maintained approximately 30 °C above the measured dew-point temperature, (c) reformation of condensate before each measurement, (d) measurements taken at increasing levels of humidity, (e) absolute pressure at the mirror of approximately 101.3 kPa, and (f) ambient temperature at (23 ± 1) °C and ambient relative humidity kept less than 70 % rh.

Table 1 Details of instruments used in the work reported, showing the year of manufacture and calibration history

Type	ID	Make	Model	Year of manufacture	Calibration
Cal	A92a	MBW	DP3-D-BCS-I	1992	2003–2009
Cal	A92b	MBW	DP3-D-SH-I	1992	2000–2005
Cal	A92c	MBW	DP3-D-SH-III	1992	1997–2010
Cal	A92d	MBW	DP3-D-SH-III	1992	2001–2010
Cal	A92e	MBW	DP3-D-BCS-I	1992	2004–2010
Cal	B99	MICHELL	DEWMET-TDH	1999	1999–2002
Cal	A01	MBW	DP30-BCS-K2	2001	2001–2009
Cal	A06	MBW	373HX	2006	2009–2010
Test	C99	GENERAL EASTERN	M2 (Sensor 1211H-XR)	1999	1999–2007
Test	D99	EDGETECH	2002	1999	2004–2010
Test	D04	EDGETECH	DEWPRIME II (Sensor S)	2004	2004–2006
Test	B05	MICHELL	OPTIDEW (Sensor ST1)	2005	2005
Test	D05	EDGETECH	DEWPRIME II (Sensor S)	2005	2005–2009
Test	A07	MBW	473	2007	2007–2010
Test	B08a	MICHELL	OPTIDEW (Sensor ST2)	2008	2008–2010
Test	C08	GENERAL EASTERN	OPTISONDE (Sensor 1211H-SR)	2008	2008–2010
Test	B08b	MICHELL	OPTIDEW (Sensor ST1)	2008	2008–2010

The identification (ID) is a short designator for the make, composed of a letter followed by two digits representing the year of manufacture, and a letter where applicable to distinguish between instruments of the same make and year. The first column indicates whether the instrument is used in a calibration or a testing laboratory

2.2 Uncertainty of Measurement

In the figures included in this article all the error bars represent the expanded uncertainty of measurement (using a coverage factor $k = 2$ for a 95 % level of confidence), assigned at the time of calibration, and may appear large with respect to the dispersion of the data points. The assigned measurement uncertainty includes contributions arising from the reference standards (calibration, drift, influence quantities, saturation vapour-pressure reference equations), the method (pressure drops, chamber temperature uniformity where applicable, etc.), and the instrument itself (resolution, repeatability, stability during the calibration).

For calibration laboratory precision transfer standards, the dominant contributions to the uncertainty budget arise from the type B uncertainties associated with the reference standards and the method. For test laboratory standards, the dominant contributions are generally those attributable to the instruments themselves.

2.3 Temperature Coefficient

The temperature differential between the measurement head and the mirror, Δt, is a potential source of uncertainty, as the inevitable heat flux will lead to gradients within

the mirror. In instruments where it cannot be kept constant, there can be a variation of the measured dew-point temperature as a function of head temperature, and hence, Δt. For the purposes of this article, we have defined this as the temperature coefficient, in $°C \cdot °C^{-1}$ (the slope of the variation of the indicated dew-point temperature per °C change in head temperature).

3 Results and Discussion

3.1 Calibration Laboratory Transfer Standards

The results for the calibration of precision transfer standards, used in calibration laboratories and of less expensive chilled-mirror hygrometers used in testing laboratories for environmental testing and other applications, are presented and discussed in the following sections. In each case, the characterization of the dominating influence quantities and the long-term stability are addressed. To draw attention to the technology, rather than the manufacturer, reference to the instruments is made via a short identification (ID) composed of a capital letter (A–D) followed by two digits representing the year of manufacture and a lower case letter, where applicable, to distinguish between instruments of the same make and year. A summary of the results is presented in Table 2.

3.1.1 Influence Quantities

One of the influence quantities that affects the measurement of the dew-point temperature is the head-to-mirror temperature differential. For units where there is no pre-cooling of the head (i.e., its temperature cannot be controlled below ambient temperature), depending on the instrument construction, there can be a significant dependence of the gradients when the head heating is activated for measurements of the dew-point temperature close to the ambient temperature. One of the early INTA high-range transfer standards, A92a, is a clear example of this. Figure 1a shows the correction of the instrument in the dew-point temperature range of −10 °C to 70 °C based on the conversion of the measured PRT resistance to temperature using the international standard IEC 60751:2008. The circles represent measurements with the head heater off and the triangles those with the heater on. In both the cases, the incoming gas temperature is conditioned to 30 °C above the nominal dew-point temperature, with a lower limit of 30 °C. The lines are a linear least-squares fit to the data in both the cases. The excellent reproducibility of the instrument can be seen from the repeated measurements at 10 °C, 30 °C, and 60 °C. The offset at 20 °C is less than 20 mK. Figure 1b shows the results obtained on the modern version of the instrument, A06, where there is a continuous linear function over the range of −10 °C to 75 °C without any offset. Again, excellent reproducibility can be seen at −10 °C, 50 °C, and 65 °C. This offset has been seen also on another four instruments of the same construction and similar age. The most probable cause of the offset has to do with the head construction and, in particular, the connection of the embedded IPRT. To minimize stem conduction, the mirror has a short section with only two platinum wires in a high-gradient zone

Table 2 Summary of results of the investigation of drift and temperature coefficients for the instruments given in Table 1, ordered by calibration and test standards

Type	ID	Dew-point temperature (°C)	Head temperature (°C)	PRT/display	Long-term stability ($mK \cdot year^{-1}$)	Temperature coefficient ($mK \cdot K^{-1}$)
Cal	A92a	−10 to 75	$t_d + 30$	PRT	−2.1	Not evaluated
Cal	A92b	1 to 15	$t_d + 30$	PRT	2.3	Not evaluated
				Disp	14.4	
Cal	A92c	−50 to 20	$t_d + 30$	PRT	0.0	Not evaluated
Cal	A92d	−50 to −10	$t_d + 30$	PRT	1.5 to 1.9	Not evaluated
Cal	A92e	1 to 30	$t_d + 30$	Disp.	37.2 to 49.5	Not evaluated
Cal	A01	−30 to 60	$t_d + 30$	PRT	0.2 to 9.2	Not evaluated
				Disp	1.3 to 5.8	
Cal	A06	−10 to 50	$t_d + 30$	PRT	0.0 to 6.0	Not evaluated
Test	B99	1 to 37	23 to 40	Disp	57 to 141	−1.0 to −3.0
Test	C99	−10 to 58	23 to 60	Disp	1.4 to 35.3	+5.6
Test	D99	−10 to 65	5 to 67	Disp	15.6	−3.2
Test	D04	−10 to 40	15 to 45	Disp	32.4 to 66.7	+2.5
Test	B05	−10 to 49	10 to 50	Disp	Not evaluated	−10.2
Test	D05	−10 to 49	10 to 50	Disp	2.2 to 77	−10.0
Test	A07	−10 to 60	20 to 62	Disp	5.6 to 14.6	+0.2
Test	B08a	−10 to 75	11 to 78	Disp	20.0	+31 to +32
Test	C08	−10 to 58	23 to 60	Disp	10.3 to 44.8	+0.4
Test	B08b	−10 to 58	23 to 60	Disp	26.4 to 30	−3.6

The temperature coefficient has not been evaluated for instruments with integral head heater control

that is not accounted for with the four-wire resistance measurement. The offset is kept constant with the fixed head-to-mirror temperature differential. More information on influence quantities is given in [10].

3.1.2 Long-Term Stability

The long-term stability can be obtained from repeated calibrations of the instrument. However, very different results can be obtained if the unit is calibrated in terms of the instrument display or in terms of the direct measurement of the same PRT using an external resistance bridge. Figure 2 shows the long-term stability of A92b, an instrument designed for measurements up to 60 °C, that has a medium mirror and a single-stage thermoelectric cooler. The figure shows the drift observed at a dew-point temperature of 5 °C relative to the correction obtained in the first calibration in 2000, for a PRT resistance measured with an external bridge and the corresponding measurements of the analog output ($10\,mV \cdot K^{-1}$), represented by squares and circles, respectively. The expanded uncertainty of measurement ($k = 2$) is 0.10 K. The lines represent linear least-squares fits to the data, whose slope yields a drift of $2.3\,mK \cdot year^{-1}$ and $14.4\,mK \cdot year^{-1}$ for the PRT and analog outputs, respectively.

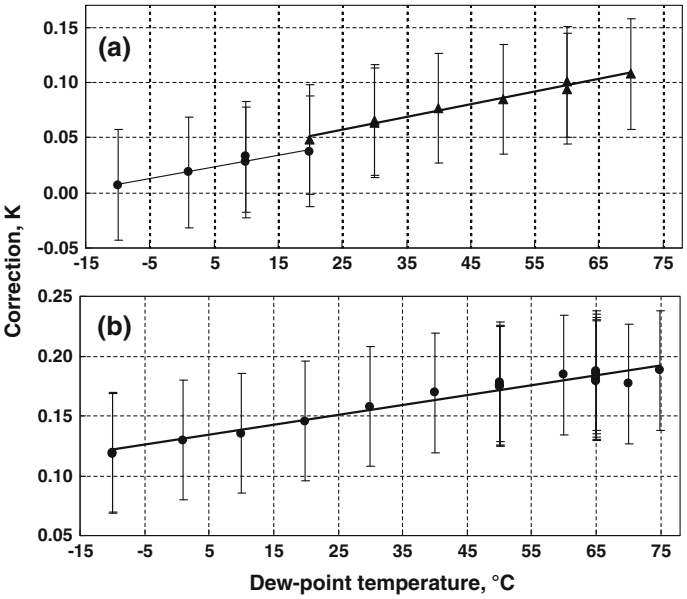

Fig. 1 Corrections measured for (a) A92a, an older instrument with large mirror and integrated head heating on (*triangles*) and off (*circles*) and (b) A06, a more modern instrument with medium-sized mirror and head heating on over the range (see text for details). In all figures, the *error bars* represent the expanded uncertainty of measurement ($k = 2$)

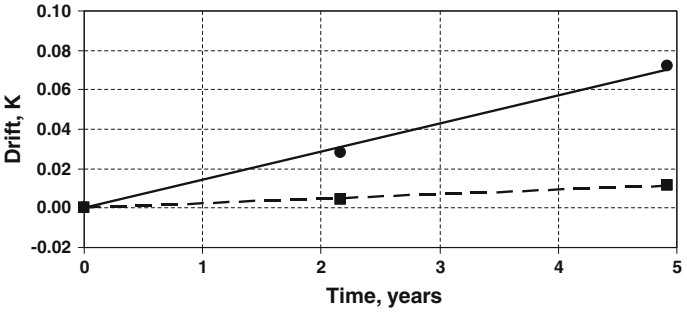

Fig. 2 Long-term stability of A92b, an instrument with a medium-sized mirror and single-stage thermoelectric cooler. Drift in dew point relative to calibration in 2000 measured using external bridge (*solid squares*) and analog output (*solid circles*) with scaling at $10\,\mathrm{mV} \cdot \mathrm{K}^{-1}$

The situation with a more modern instrument, A01, with a medium mirror and two independent PRTs installed in the mirror can be seen in Fig. 3a and b for the resistance and analog output, respectively. In the case of the analog output, the maximum drift in 6 years is between 1 mK at −30 °C and 55 mK at 60 °C and between 8 mK at −30 °C and 35 mK at 60 °C for the resistance measurement. For this unit, the improved electronics have reduced the difference significantly, although there is not sufficient data to claim this in general. The main advantage of measuring the PRT directly is the lack of risk of losing historical information if the electronics has to be repaired. With more

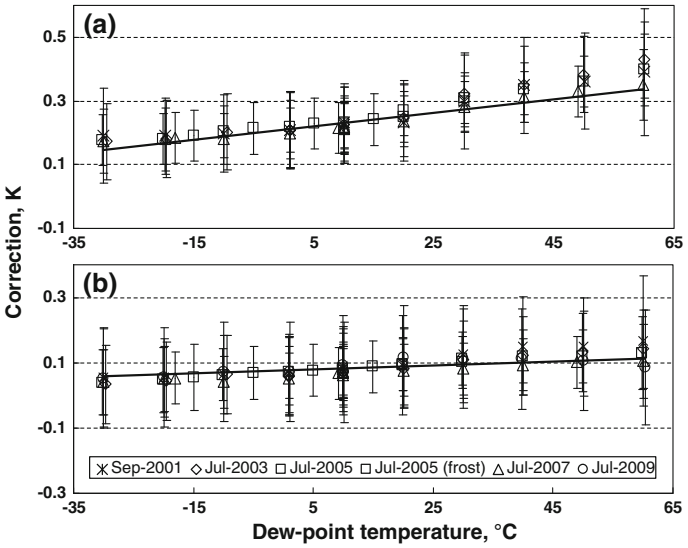

Fig. 3 Long-term stability of A01, an instrument with a medium-sized mirror and two-stage thermoelectric cooler measured using (a) external bridge and (b) analog output ($10\ \mathrm{mV} \cdot \mathrm{K}^{-1}$)

modern completely digital units, such as A06, where a prior selection of the PRTs inserted has been made after thermal annealing and cycling, even better results for drift can be obtained [10,11].

Figure 4 shows the long-term stability of the first two transfer standards acquired by the Laboratory that have been used as monitors of the standard humidity generators. The low-range unit, A92c has a pre-cooler refrigeration unit, a small mirror, a three-stage thermoelectric cooler, and a head for a maximum temperature of 60 °C. Its long-term stability is shown: (a) at −50 °C and (b) at −20 °C. The long-term stability of the high-range unit, A92b, with a large mirror and a single thermoelectric cooler is shown in Fig. 4c at 50 °C. As can be seen, no drift can be detected in the low-range unit over 12 years and for the high-range unit, the drift over 8 years is less than 20 mK. The graphs also show the excellent level of combined reproducibility of the hygrometers and generators over a decade. The observed stability can be justified, considering the IPRTs embedded in the mirror are of a ceramic encapsulated design and thus highly annealed at elevated temperatures inherent in the fabrication process, and are then only used over a very narrow temperature range and upper temperature limit.

3.2 Test Laboratory Standards

3.2.1 Influence Quantities

The cases studied in the previous section were for precision laboratory transfer standards with integral head heating that were operated at constant conditions of temperature differential between the head and the mirror temperature. It has been shown that

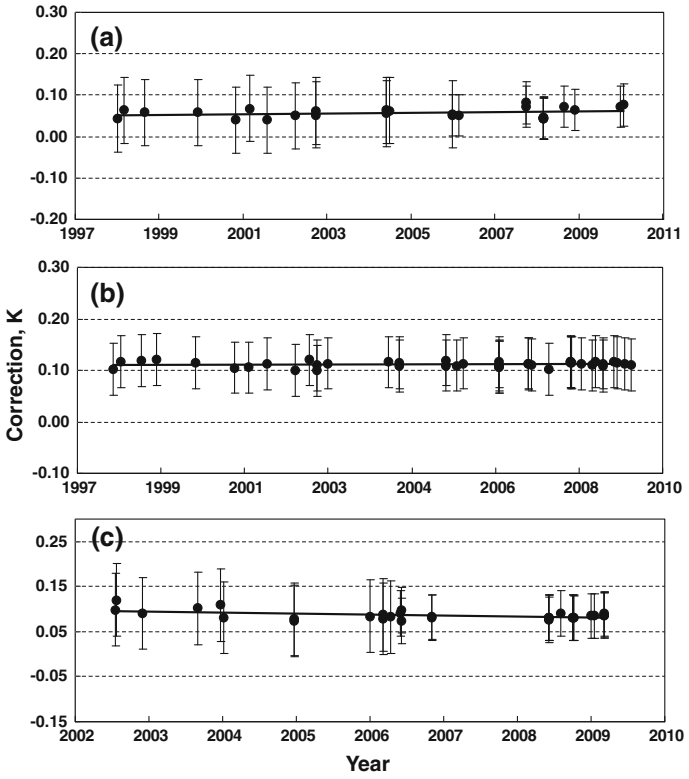

Fig. 4 Long-term stability of A92c, an instrument with small mirror, three-stage thermoelectric cooler, and pre-cooler at: (a) −50 °C and (b) −20 °C. Long-term stability of A92b (see Fig. 2) at +50 °C is shown in (c)

under these conditions, the most well-defined calibration results are obtained. However, in general industrial applications and climatic and other testing laboratories, instruments with a lower demand for accuracy, but with more importance placed on robustness and cost, are employed. Usually these instruments have a remote head that is connected to a display and control unit. The head, unlike the calibration laboratory transfer standards, does not have integral head heating and is placed directly in the test chamber or in an external heated enclosure, together with the sampling system. To obtain the lowest uncertainties of use with these instruments, it is necessary to perform their calibration with the sensor head at temperatures commensurate with the conditions of use. If this is not possibly due to the varied nature of the application, then calibration needs to be performed with the sensor head at several representative temperatures. Measurements need to be performed over the dew-point temperature range that the temperature depression of the thermoelectric coolers permits, with overlaps at each temperature. Figure 5a and b shows examples of the calibration of the analog outputs of B05 and B08a—two instruments with remote sensors. In Fig. 5a, the calibration has been performed at three head temperatures: 10 °C, 23 °C, and 50 °C with the indicator and control unit kept at 23 °C ± 1 °C. As can be seen, the instrument response

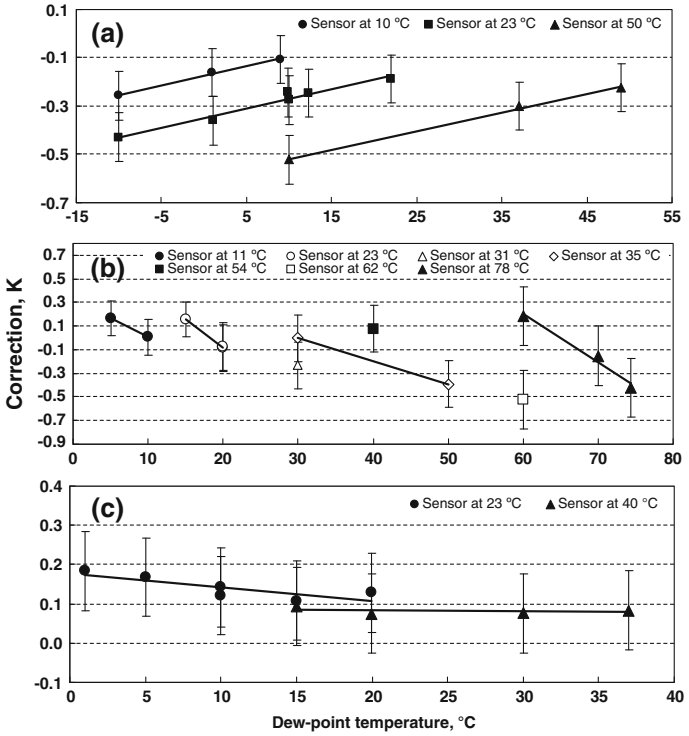

Fig. 5 Temperature coefficient studies of (a) B05, (b) B08a, and (c) B99, which are test laboratory instruments with remote sensors

is linear at a given temperature, but the whole characteristic shifts as the temperature is changed, that is, the slope and linearity of the dew-point temperature correction curve are maintained. Figure 5b shows the response of B08a, which has the same model indicator and control unit as B05, but has a head designed for higher temperatures. Here, the instrument was calibrated with the head at seven different temperatures. The temperature coefficient is of the opposite sign of that found in the previous case and much larger in magnitude, yielding values of $+0.031\,\mathrm{K}\cdot\mathrm{K}^{-1}$ and $+0.032\,\mathrm{K}\cdot\mathrm{K}^{-1}$ for dew-point temperatures of 10 °C and 60 °C, respectively. In Fig. 5c, the temperature coefficients for B99, which is an older instrument from the manufacturer of B05 and B08a are obtained for dew-point temperatures of 15 °C and 20 °C for head temperatures between 23 °C and 40 °C are negligible ($-0.001\,\mathrm{K}\cdot\mathrm{K}^{-1}$ and $-0.003\,\mathrm{K}\cdot\mathrm{K}^{-1}$, respectively). However, the slope of the dew-point temperature correction changes. The three instruments in Fig. 5 have the same claimed specification, but although the manufacturer reports not having made any relevant design changes, it had changed the supplier of some of the components used in the remote sensor. What can be seen from the data is that the magnitude of the correction increases as the mirror depression increases, that is, the greater is the driving current through the thermoelectric coolers. Clearly, the instrument should be calibrated over a head-to-mirror depression, Δt, as close as possible to the conditions of use. It must be noted that the extent of

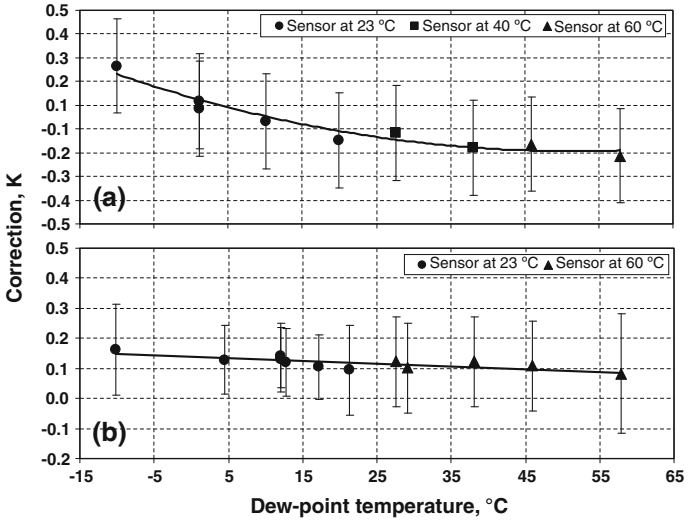

Fig. 6 Temperature coefficient studies of two instruments with different remote sensors: (a) C99, an older instrument giving analog output and (b) C08, a more modern instrument with digital display

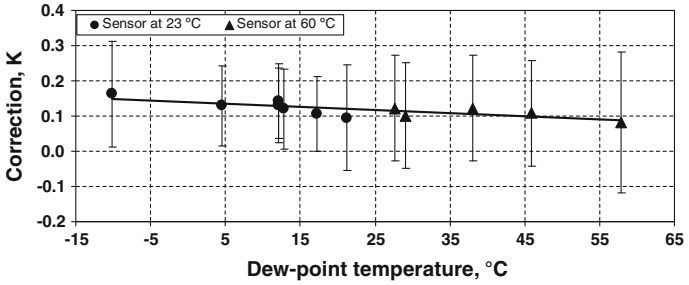

Fig. 7 Temperature coefficient studies of D04, an instrument with two-stage thermoelectric cooler and digital display, for sensor temperatures of 10 °C, 23 °C, and 60 °C. The temperature coefficient is also negligible

evaluation is quite different for the third unit, so the comparative performance cannot be established conclusively.

Figure 6 shows the results of two industrial instruments with different remote sensors with single-stage thermoelectric coolers: (a) C99 and (b) C08. In both the cases, no significant temperature coefficient can be detected and the dew-point correction can be represented adequately by a single function in each case: quadratic and linear, respectively, with residuals of the order of the instrument repeatability. Note, however, that for the same dew-point temperature range the correction spans 0.3 K in the first case, and only 0.1 K in the second. Figure 7 shows the calibration of instrument D04, which has a two-stage thermoelectric cooler, in terms of the digital display at three sensor temperatures (10 °C, 23 °C, and 60 °C). The temperature coefficient is clearly negligible and the correction can be represented by a linear function with a span in the correction of only 0.06 K. Finally, Fig. 8 shows the calibration of a digital instrument, A07 with a remote sensor with a two-stage thermoelectric cooler, in terms of the analog

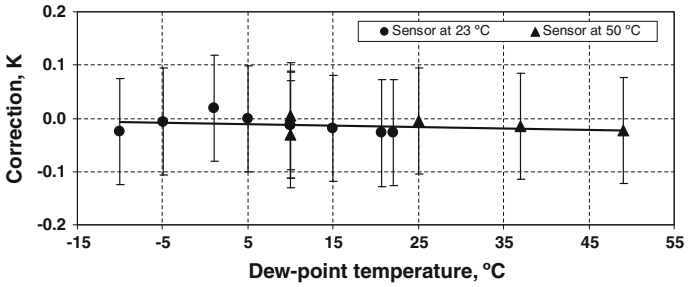

Fig. 8 Temperature coefficient studies of A07, a modern digital instrument with remote sensor, two-stage thermoelectric cooler, and analog output, for sensor temperatures of 23 °C and 50 °C. The temperature coefficient is also negligible

output. The temperature coefficient in the range of 23 °C to 50 °C is also negligible as can be seen at the 10 °C point, measured at both the temperatures and spans less than 0.05 K. The resulting correction can be represented by a linear function with residuals less than 0.02 K.

3.2.2 Long-Term Stability

As in the case of the calibration laboratory transfer standards, the long-term stability is obtained from repeated calibrations of the instrument. However, due to the possibility of significant temperature coefficients, the initial calibrations necessary to establish the temperature dependence of the correction need to be more comprehensive than the subsequent calibrations that are intended to estimate the long-term stability. Figure 9 shows three cases of instruments whose temperature coefficient was reported in the previous section. Figure 9a corresponds to instrument B05 where the temperature dependence of two calibrations is almost identical, as evidenced by the linear fit to the 2008 and 2010 data with a dashed and solid line, respectively. Figure 9b shows the calibration history of instrument D05 from 2005 to 2009, where no significant drift can be attributed within the instrument reproducibility and repeatability. Figure 9c shows the case of a modern digital instrument, A07, from 2007 to 2010. As in the previous two cases, no significant drift can be attributed within the instrument reproducibility and repeatability.

3.3 Recommendations on Calibration Extent and Interval

In general, the calibration of dew-point hygrometers is a costly exercise and a balance between the technical requirements and cost needs to be maintained. In general terms, an initial calibration has to be much more exhaustive to determine the main characteristics of the instrument over the operating range. For instruments with integral head-temperature control, the best advice is to keep the head temperature at a fixed temperature above the nominal measured dew-point temperature. The first calibration can then cover the range at nominal dew-point temperatures at 10 °C intervals, and must include the lower and upper limit required. Subsequent calibrations can then be performed at the limits and at 20 °C intervals, for example. Once the calibration drift

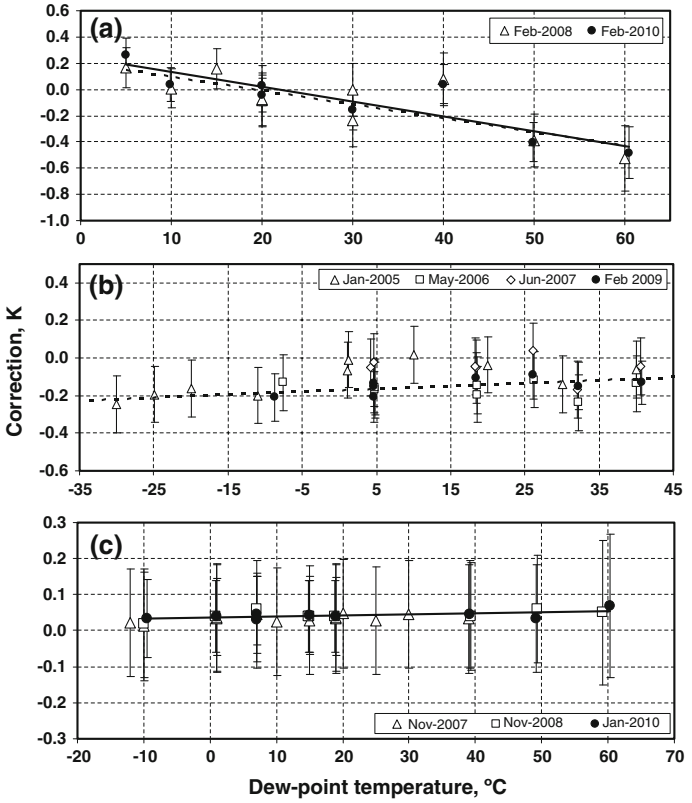

Fig. 9 Long-term stability of instruments: (a) B08a, (b) D04, and (c) A07

has been confirmed, then the interval can be progressively extended up to 3 years, provided the user has a means of performing checks between calibrations. For example, we have shown that the drift of the internal PRT (measured with an external resistance measurement device) can be much lower than that for the combined PRT and indicator or analogue output. So, for example, if checks can be performed on the indicator via electrical simulation, then confidence can be maintained and the larger calibration interval is justified.

For instruments that do not have integral head control, the authors recommend an initial calibration carried out at several probe temperatures over the operating range (the minimum number will depend on the mirror depression capability), with at least three nominal dew-point temperatures at each probe temperature and with overlapping points, to determine the temperature coefficient. Subsequent calibrations to determine drift can be performed at a reduced number of points covering the range. It is not sufficient to just order a calibration specifying the nominal dew-point temperatures.

In any case, for confidence in establishing the calibration interval, the existence of a prior calibration history in real conditions of use, together with the ability to perform checks between calibrations that are effective within the estimated drift allowance, is fundamental.

4 Conclusion

A study of the long-term stability and temperature coefficients of a representative sample of hygrometers and the analysis of their performance over the lifespan of the instruments through regular calibration using the INTA humidity calibration facilities has been presented and discussed. The need to evaluate the possible temperature coefficients, especially in the case of units with remote sensors or without integral head-temperature control, has been addressed. The results of the investigations show that with an adequate calibration history and careful use, chilled-mirror dew-point hygrometers can be sufficiently stable to establish relatively large calibration intervals if adequate checks between calibrations are performed. In the case of precision laboratory transfer standards, the advantages of direct measurement of the PRT with an external resistance bridge has been emphasized to reduce the risk of loss of calibration history in the case of repair to the instrument display electronics, particularly important in interlaboratory comparisons. This has also been shown to be useful in minimizing the effects of drift not attributable to the sensor element, important in the case of older instruments, where usually analogue outputs are measured due to the limited resolution of the industrial display. The examples demonstrate the achievable levels of measurement uncertainty associated with the sensor temperature (and, hence, the dew-point depression) and drift (long-term stability) for a range of chilled-mirror hygrometers.

References

1. ISO/IEC 17025:2005, General requirements for the competence of testing and calibration laboratories
2. CIPM Mutual Recognition Arrangement (CIPM-MRA), "Mutual recognition of national measurement standards and of calibration and measurement certificates issued by national metrology institutes" (Paris, 14 October 1999), Technical Supplement revised in October 2003. http://www.bipm.org/en/cipm-mra/
3. "The BIPM key comparison database," Current Calibration and Measurement Capabilities for INTA are available on http://kcdb.bipm.org/AppendixC/. Accessed February 2010
4. ENAC Accreditation Number 16/LC150H, Technical Annex Rev. 7 (2008), Current scope of accreditation is available on http://www.enac.es. Accessed February 2010
5. The ILAC Mutual Recognition Arrangement (ILAC-MRA), http://www.ilac.org/
6. P. Mackrodt, R. Benyon, G. Scholz, State-of-the-art calibration of high-range chilled-mirrror hygrometers and their use in the intercomparison of humidity standard generators, in *Proceedings of Third International Symposium on Humidity and Moisture* (National Physical Laboratory, UK, 1998), pp. 159–166
7. R. Benyon, P. Huang, "A comparison of INTA and NIST humidity standard generators," in *Proceedings of Third International Symposium on Humidity and Moisture* (National Physical Laboratory, UK, 1998), pp. 28–36
8. R. Benyon, H. Mitter, Int. J. Thermophys. **29**, 1623 (2008)
9. R. Benyon, J. De Lucas, A. Moratilla, Humidity calibration in the modern accredited laboratory, in *Proceedings of Third International Symposium on Humidity and Moisture* (National Physical Laboratory, UK, 1998), pp. 206–213
10. R. Benyon, N. Böse, H. Mitter, D. Mutter, T. Vicente, Int. J. Thermophys. doi:10.1007/s10765-012-1343-5
11. M. Heinonen, Report to the CCT on key comparison EUROMET.T-K6 (EUROMET Project No. 621): comparison of the realisations of local dew/frost-point temperature scales in the range −50°C to +20°C (Draft B, final version, 2009)

Int J Thermophys
DOI 10.1007/s10765-012-1345-3

Pressure-Drop Considerations in the Characterization of Dew-Point Transfer Standards at High Temperatures

H. Mitter · N. Böse · R. Benyon · T. Vicente

Received: 29 March 2010 / Accepted: 11 October 2012

Abstract During calibration of precision optical dew-point hygrometers (DPHs), it is usually necessary to take into account the pressure drop induced by the gas flow between the "point of reference" and the "point of use" (mirror or measuring head of the DPH) either as a correction of the reference dew-point temperature or as part of the uncertainty estimation. At dew-point temperatures in the range of ambient temperature and below, it is sufficient to determine the pressure drop for the required gas flow, and to keep the volumetric flow constant during the measurements. In this case, it is feasible to keep the dry-gas flow into the dew-point generator constant or to measure the flow downstream the DPH at ambient temperature. In normal operation, at least one DPH in addition to the monitoring DPH are used, and this operation has to be applied to each instrument. The situation is different at high dew-point temperatures up to 95 °C, the currently achievable upper limit reported in this paper. With increasing dew-point temperatures, the reference gas contains increasing amounts of water vapour and a constant dry-gas flow will lead to a significant enhanced volume flow at the conditions at the point of use, and therefore, to a significantly varying pressure drop depending on the applied dew-point temperature. At dew-point temperatures above ambient temperature, it is also necessary to heat the reference gas and the mirror head of the DPH sufficiently to avoid

H. Mitter (✉)
E+E Elektronik Ges.m.b.H. (BEV/E+E), Engerwitzdorf, Austria
e-mail: helmut.mitter@epluse.at

N. Böse
Physikalisch-Technische Bundesanstalt (PTB),
Braunschweig, Germany

R. Benyon · T. Vicente
Instituto Nacional de Técnica Aeroespacial (INTA),
Torrejón de Ardoz, Madrid, Spain

Published online: 27 October 2012

condensation which will additionally increase the volume flow and the pressure drop. In this paper, a method is provided to calculate the dry-gas flow rate needed to maintain a known wet-gas flow rate through a chilled mirror for a range of temperature and pressures.

Keywords Calibration · Generator · Humidity · Dew-point temperature · Pressure drop · Standards

List of Symbols

d_a	Density of dry-air component of humid air
$e_w(t)$	Saturation vapour pressure above water at temperature t in pure phase
$e'_w(p,t)$	Saturation vapour pressure of a mixture of vapour and CO_2 free air and N_2, respectively
$f_w(p,t)$	Enhancement factor
M_a	Molar mass of dry air
n	Total numbers of moles at output SHG
n'	Total numbers of moles at output condensation trap
n_a	Numbers of moles of dry air
n_v	Numbers of moles of vapour at output SHG
n'_v	Numbers of moles of vapour at the output of the condensation trap
p	Pressure
p_a	Ambient pressure
p_h	Pressure at the point of use (i.e., at the chilled-mirror sensor)
p_{ref}	Gas pressure at point of reference
q	Humid-gas volume flow at the point of use (mirror head)
$q_{m.a}$	Dry-gas mass flow at the DPH-branch (connection lines, point of use, condensation trap)
q_{in}	Dry-gas volume flow into the generator
$q_{m.in}$	Dry-gas mass flow into the generator
q_{out}	Volume flow coming out of the condensation trap
R	Universal gas constant
T	Absolute temperature
T_0	Absolute temperature at 0 °C
t_a	Ambient temperature
t_d	Dew-point temperature at point of reference
$t_{d.h}$	Dew-point temperature at point of use
t_h	Gas temperature at point of use
t_v	Temperature of connection line to the generator
V	Volume
x_v	Water-vapour mole fraction generated with SHG
x'_v	Water-vapour mole fraction after condensation trap
Δp	Pressure drop between point of use and point of reference
Δt_d	Pressure-drop effect on dew-point temperature

1 Introduction

The development of precision optical dew-point hygrometers (DPHs) has experienced a very significant improvement in the last decade, with instruments now able to achieve levels of reproducibility better than ±20 mK over a wide-temperature range. These instruments are commonly used as transfer standards for the comparison of standard humidity generators (SHGs). The current levels of calibration and measurement capability (CMC) claimed by the national metrology institutes (NMIs) and their designated institutes (DIs) require strict measurement protocols to reduce the impact of the dominating influence quantities on the comparison results. These include, for example, the minimization of variation in (a) mirror gradients through fixing the head-to-mirror temperature differential; (b) thermal loading effects by fixing the gas flow and preconditioning the gas temperature; and (c) mirror temperature measurements through use of a precision resistance bridge to monitor the platinum resistance thermometer (PRT) embedded in the mirror.

Until very recently, the EURAMET and CCT key and supplementary comparisons have not covered the range above 20 °C (e.g., CCT-K6, EURAMET.T-K6, and APMP.T-K6 in the range from −50 °C to +20 °C). However, the onset of EURAMET.T-K8, APMP.T-K8, and CCT-K8, covering the range from 30 °C to 95 °C, have required further considerations in defining the reproducible measurement conditions adequate for the different sampling configurations required by the various types of SHGs used in the national realizations of the dew-point temperature.

This paper addresses the methodology developed for the measurement protocols of the high-range comparisons and the method validation in the range from 30 °C to 95 °C, consistent with the specifications of the available state-of-the-art transfer standards with the focus on the pressure drop between the "point of use" and the "point of reference" and the correct adjustment of gas flow in order to establish a constant pressure drop for dew-point temperatures up to 95 °C. However, it is also applicable to calibration laboratories that want to improve calibration uncertainties in the high humidity range and to DPH users who want to make accurate dew-point temperature measurements at dew points above ambient temperature.

2 Gas Flow Relations

2.1 Measurement Configuration

When calibrating a DPH, a device (SHG) is used to generate humid gas with a defined mole fraction, x_v, and thus, to pressurize the sensor in the mirror head of the DPH with a previously defined gas flow. The important point is that the mole fraction between the SHG output and the mirror of the DPH must not change, e.g., due to condensation and absorption effects in the connection lines. This is ensured primarily at dew-point temperatures above room temperature via adequate heating of the connection lines and the DPH gas feed, and by selecting suitable materials.

The reference dew point, t_d, is determined by measuring the pressure p_{ref}, at the reference point and according to Harrison [1], this produces the following relationship

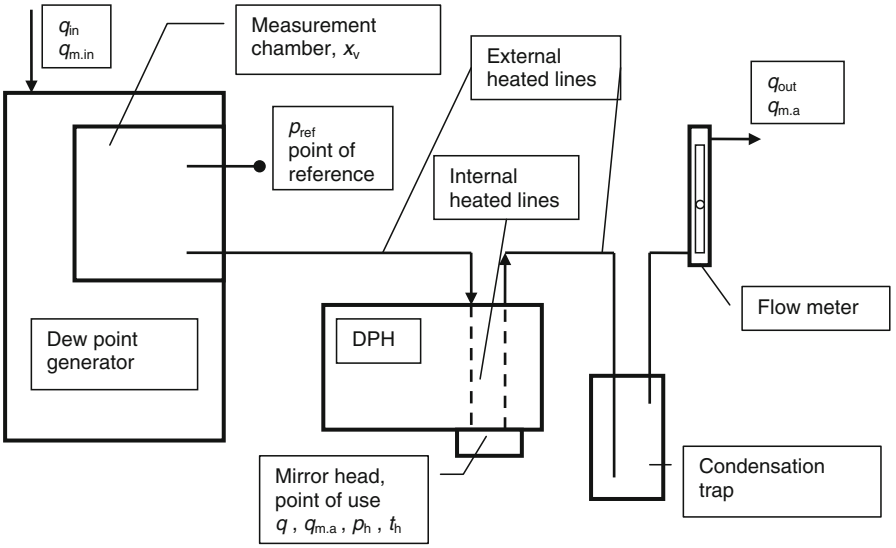

Fig. 1 Setup for calibration of a chilled-mirror hygrometer using temperature-conditioned air sampled from the test chamber of a two-pressure generator. Pressure at the chilled-mirror sensor is estimated from pressure measured in the chamber upstream of the hygrometer by taking into account the pressure drop between the point of reference (test chamber) and the point of use (mirror head of the hygrometer)

for the dew-point temperature at the reference point (for formula symbols, see List of Symbols)

$$x_v = \frac{n_v}{n} = \frac{n_v}{n_a + n_v} \tag{1}$$

$$e'_w\left(p_{ref}, t_d\right) = x_v p_{ref} \tag{2}$$

using the formula for the saturation vapour pressure in the pure phase according to Sonntag [2] and the enhancement factors according to Greenspan [3] and Hardy [4]

$$e'_w\left(p, t\right) = e_w\left(t\right) f_w\left(p, t\right). \tag{3}$$

Figures 1 and 2 depict schematically the typical configurations of measuring equipment as used when calibrating a DPH using as SHG, when sampling from a chamber and from a single-pressurized line, respectively. Independent of the type of humidity generator or dew-point hygrometer used, the relevant difference is the location of the position of the pressure measurement for the reference point. These configurations are representative of those used in experimental testing of the gas flow models.

The dew-point temperature is measured at the mirror of the DPH, and then the gas is taken from the DPH to a condensation trap, where the water vapour contained in the humid gas that exceeds a dew-point temperature equivalent to the ambient temperature (or lower if it is cooled), will be removed. The dried gas is led through a needle valve and flow-meter assembly to check the sampled gas flow, q_{out}. An alternative to

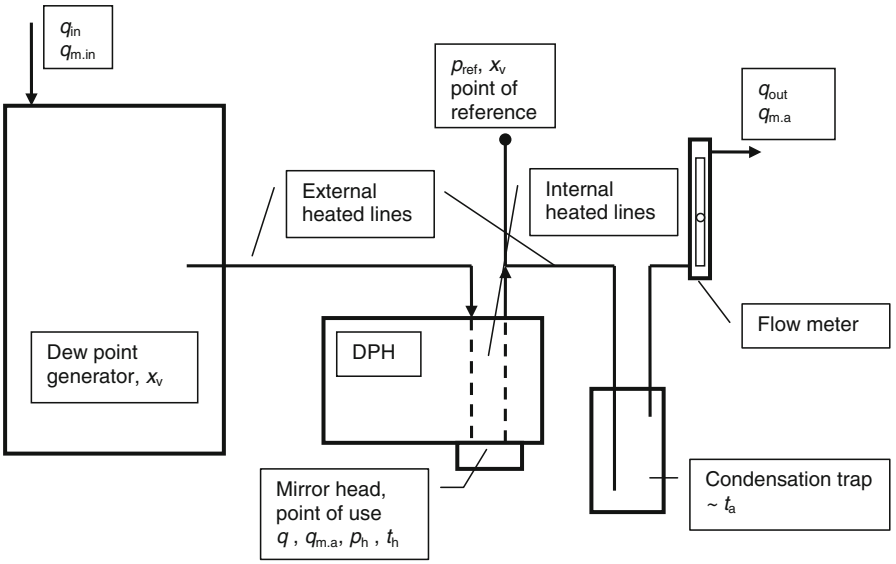

Fig. 2 Setup for calibration of a chilled-mirror hygrometer using temperature-conditioned air from a single-pass dew-point generator (two pressure or single pressure). Pressure at the chilled-mirror sensor is estimated from the pressure measured downstream of the hygrometer by taking into account the pressure drop between the point of reference (outlet hygrometer) and the point of use (mirror head of the hygrometer)

checking the gas flow after the condensation trap is to check the dry-gas volume flow supplied to the generator q_{in}. Usually, both flows are at ambient temperature, and for q_{in}, only the different gas pressures have to be taken into account. Another possibility is to measure mass flows of the dry gas $q_{m.in}$ or $q_{m.a}$.

Ideally, the reference pressure, p_{ref}, would need to be measured directly in the mirror head for the DPH mirror. However, this results in technical difficulties as it cannot be ensured that the dew-point measurement is not being affected by the pressure measurement via condensation effects or blind-hole effects. For this reason, the pressure measurement is arranged at a non-critical point of the sample gas path. As a consequence, the pressure p_h at the point of use (DPH mirror head) is different from the reference pressure, p_{ref}, due to the volume flow between the two points. This pressure difference causes a difference in dew-point temperature and must be corrected or taken into account in the measurement uncertainty estimate. Depending on the measurement setup, the reference pressure is either measured directly in the measurement chamber of the generator (see Fig. 1) or immediately after the DPH outlet (Fig. 2). At a volume gas flow of $0.5\,\mathrm{L}\cdot\mathrm{min}^{-1}$, the pressure loss between the point of reference and the point of use is around 1 hPa (Fig. 2) or around 0.2 hPa (Fig. 2) when using a standard stainless-steel tube with a 4 mm internal diameter in the commonly used length. The resultant dew-point correction is approximately 2 mK to 14 mK.

As it is difficult to measure the volume flow of a hot and very humid gas directly, the gas flow is measured after the condensation trap at ambient temperature. This measured volume gas flow, q_{out}, after the condensation trap is used to determine and to set a constant volume gas flow, q, through the DPH mirror head to keep the pressure

drop constant between "the point of reference" and "the point of use," independent of the applied dew-point temperature.

Typical values for the mirror head conditions are

- volume flow, $q = 0.5\,\mathrm{L} \cdot \mathrm{min}^{-1}$,
- pressure, $p_\mathrm{h} > p_\mathrm{a}$, usually several hPa above p_a to maintain a sufficient gas flow through the DPH,
- temperature of mirror head and internal heated line: $t_\mathrm{v} = t_\mathrm{h} = t_\mathrm{d} + 30\,^\circ\mathrm{C}$.
- It should be noted that a commercial DPH usually has an upper temperature limit for the head temperature and the internal tube temperature which has to be accordingly considered at the gas flow calculations.

For a case of "point of reference" in the measuring chamber (Fig. 1), the temperature of the heated external line from the generator to the DPH t_v must be equal to t_h.

2.2 Gas Flow Model

A relationship is calculated between the volume flow under measuring head conditions and the volume flow after the condensation trap. By setting a volume flow after the condensation trap, q_out, as a function of the reference dew-point temperature, a constant volume flow, q, can be maintained in the measuring head under measuring head conditions. At the same time, this means that the pressure loss, Δp, between the point of use and the point of reference is not dependent on the dew-point temperature and the loading of the carrier gas with water vapour.

The assumption below is that the humid gas is ideal, i.e., state changes can be described sufficiently well by the general gas equation. The effect of the pressure loss between the point of reference and the point of use is also assumed to be small. In other words, the pressure loss does result in a measurable change in the dew-point temperature, but for calculating the volume flow ratios, the pressures $p_\mathrm{ref} \approx p_\mathrm{h}$ can be set to the same as the pressure in the condensation trap. The error occurring here is equivalent to the ratio of pressure loss to the absolute pressure p_h in the DPH measuring head and is therefore, normally far below 1 % of the volume flow. Similarly, in this approximation, the dew point at the point of reference t_d and the dew point at the point of use $t_\mathrm{d.h}$ are approximately equalized. A further assumption is that the gas temperature corresponds sufficiently accurately to the temperatures in the connection lines, measuring head, and condensation trap.

Under these assumptions, the same relationships are obtained at the point of use as for the reference dew point (Eqs. 1, 2):

$$x_\mathrm{v} = \frac{n_\mathrm{v}}{n} = \frac{n_\mathrm{v}}{n_\mathrm{a} + n_\mathrm{v}} \tag{4}$$

$$x_\mathrm{v} p_\mathrm{h} = e'_\mathrm{w}\left(p_\mathrm{h}, t_\mathrm{d.h}\right) \approx e'_\mathrm{w}\left(p_\mathrm{ref}, t_\mathrm{d}\right) = x_\mathrm{v} p_\mathrm{ref}. \tag{5}$$

In the condensation trap, the water vapour where the dew point exceeds the ambient temperature t_a is removed and the following is obtained after the condensation trap:

$$x'_{\mathrm{v}} = \frac{n'_{\mathrm{v}}}{n'} = \frac{n'_{\mathrm{v}}}{n_{\mathrm{a}} + n'_{\mathrm{v}}} \tag{6}$$

$$e'_{\mathrm{w}}\left(p_{\mathrm{ref}}, t_{\mathrm{a}}\right) = x'_{\mathrm{v}} p_{\mathrm{ref}}. \tag{7}$$

The dry-gas fraction, and thus, n_{a} do not change in this process and Eqs. 4 and 6 can be compared via n_{a}

$$n_{\mathrm{v}}\left(\frac{1}{x_{\mathrm{v}}} - 1\right) = n'_{\mathrm{v}}\left(\frac{1}{x'_{\mathrm{v}}} - 1\right) \tag{8}$$

and from Eq. 8 with $n_{\mathrm{v}} = x_{\mathrm{v}} n$ and $n'_{\mathrm{v}} = x'_{\mathrm{v}} n'$, we get

$$n\left(1 - x_{\mathrm{v}}\right) = n'\left(1 - x'_{\mathrm{v}}\right). \tag{9}$$

The general gas equation implies directly that volumes, and thus, volume flows are proportional to the number of moles and the absolute temperature,

$$V = \frac{R}{p} n T. \tag{10}$$

and the ratio of the volume flows at the point of use, q, and after the condensation trap, q_{out}, is obtained directly with the respective temperatures, t_{h} and t_{a},

$$\frac{q}{q_{\mathrm{out}}} = \frac{1 - x'_{\mathrm{v}}}{1 - x_{\mathrm{v}}} \frac{T_0 + t_{\mathrm{h}}}{T_0 + t_{\mathrm{a}}}. \tag{11}$$

The dry-gas mass flow can be calculated directly from the density of the gas. At mirror-head conditions ($t_{\mathrm{d.h}} \sim t_{\mathrm{d}}$, $p_{\mathrm{h}} \sim p_{\mathrm{ref}}$, q, t_{h}, $e'_{\mathrm{w}}\left(p_{\mathrm{ref}}, t_{\mathrm{d}}\right)$), the density of the dry-air component of humid air, d_{a}, can be calculated using the general gas equation:

$$d_{\mathrm{a}} = \frac{M_{\mathrm{a}}}{R} \frac{\left(p_{\mathrm{ref}} - e'_{\mathrm{w}}\left(p_{\mathrm{ref}}, t_{\mathrm{d}}\right)\right)}{T_0 + t_{\mathrm{h}}} \tag{12}$$

and the mass flow of dry air, $q_{\mathrm{m.a}}$, is given by

$$q_{\mathrm{m.a}} = q d_{\mathrm{a}} = q \frac{M_{\mathrm{a}}}{R} \frac{\left(p_{\mathrm{ref}} - e'_{\mathrm{w}}\left(p_{\mathrm{ref}}, t_{\mathrm{d}}\right)\right)}{T_0 + t_{\mathrm{h}}}. \tag{13}$$

The mass flow rate of dry air remains unchanged throughout the whole gas flow path to each DPH under test.

2.3 Constant Dry-Gas Flow, q_{out}

Using the gas-flow model (Sect. 2.2), the influence on the pressure loss between the point of reference and point of use, and thus, on the deviation of the dew-point

measurement via a DPH from the dew-point representation at the point of reference is shown, calculated with operation at a constant dry-gas flow.

To achieve this, an SHG in accordance with Fig. 1 is assumed, where the mole fraction x_v is generated in a measuring chamber, and by measuring the pressure p_{ref}, a reference dew point t_d is displayed (Eq. 2). The DPH is operated using a gas flow of $0.5\,L \cdot min^{-1}$; the pressure loss Δp between the point of reference and the point of use has been determined at a dew-point temperature of $t_d < t_a$ with 1 hPa.

The dew-point temperature is thus increased in increments from 0 °C to 95 °C. During the calibration process, the volume flow that is measured after the condensation-trap needle valve using a flow meter is kept constant with $q_{out} = 0.5\,L \cdot min^{-1}$. The connection line between the measuring chamber and DPH and the internal heaters (measuring head and internal measuring gas lines) on the DPH, are each set to 30 °C above the dew-point temperature, whereby the maximum temperature is limited to 115 °C.

The volume flow at the point of use and in the connection line to the SHG is described by Eq. 11 for an ambient temperature of $t_a = 23\,°C$, $t_v = t_h = t_d + 30\,°C$ (limitation at 115 °C). The ambient temperature of 23 °C results in a mole fraction $x'_v = 0.0277$ on the condensation trap outlet. The system pressure $p_{ref} \sim p_h$ is the normal pressure of 1013.25 hPa. The resultant pressure loss q between the point of reference and the point of use with the volume flow Δp is calculated via Eq. 14. It is assumed here that the pressure loss of a volume flow is the same within the measurement uncertainty in the area of interest for humid and dry air. This assumption is also confirmed via experimental testing of the model in Sect. 3.2 and Fig. 5.

At dew points below 20 °C, the pressure loss is sufficiently stable and can be corrected with sufficient accuracy using the known value of $\Delta p = 1$ hPa, i.e., the measured volume flow q_{out} is a good approximation for the humid-gas flow at the point of use. Above $t_d = 50\,°C$, however, the volume flow q, and thus, the pressure loss starts to rise significantly due to the ever increasing loading of the dry air with water vapour. At $t_d = 95\,°C$, the pressure loss reaches a value of approximately 14 hPa with a corresponding effect on the dew point of $\Delta t_d \sim 0.4\,°C$ (see Table 1).

2.4 Constant Volume Flow, q

To maintain a constant volume flow, q, under DPH conditions, the volume flow after the condensation trap q_{out} is set according to Eq. 11 with $q = \text{const}$. This sets a pressure loss between the point of reference and the point of use that is independent of the corresponding dew point, that can be corrected accordingly. For calculating the required gas flow after the condensation trap, the same parameters are used as in Sect. 2.3:

$t_v = t_h = t_d + 30\,°C$ (limit at 115 °C); $t_a = 23\,°C$; $p_{ref} = 1013.25\,hPa$

The volume flow, q, in the measuring head of the DPH is defined at $0.5\,L \cdot min^{-1}$. Table 2 lists values for the volume flow, q_{out}, being set and the dry-gas mass flow, $q_{m.a}$, via the DPH and the condensation trap. Measuring points for the EURAMET.T-K8 comparison (P717) [5] are printed in bold.

Table 1 Calculated effects on pressure drop and dew-point temperature at point of use under constant dry-gas flow conditions $q_{out} = 0.5\ \mathrm{L \cdot min^{-1}}$ (See Sect. 2.3 for details, List of Symbols for listed parameters)

t_d (°C)	$e'_w(p_{ref}, t_d)$ (hPa)	x_v	t_h (°C)	q ($\mathrm{L \cdot min^{-1}}$)	$\Delta p = p_{ref} - p_h$ (hPa)	$e'_w(p_{ref}, t_d) \frac{p_h}{p_{ref}}$ (hPa)	$t_{d.h}$ (°C)	Δt_d (K)
0	6.136	0.006	30	0.50	1.00	6.130	−0.014	−0.014
10	12.329	0.012	40	0.52	1.05	12.316	9.985	−0.015
20	23.486	0.023	50	0.54	1.10	23.460	19.983	−0.017
30	42.651	0.042	60	0.57	1.16	42.602	29.980	−0.020
40	74.199	0.073	70	0.61	1.25	74.107	39.977	−0.023
50	124.171	0.123	80	0.66	1.37	124.003	49.973	−0.027
60	200.621	0.198	90	0.74	1.57	200.309	59.966	−0.034
65	251.917	0.249	95	0.80	1.72	251.488	64.962	−0.038
70	313.909	0.310	100	0.89	1.94	313.309	69.956	−0.044
75	388.282	0.383	105	1.01	2.25	387.418	74.947	−0.053
80	476.869	0.471	110	1.19	2.76	475.568	79.932	−0.068
85	581.641	0.574	115	1.50	3.70	579.519	84.906	−0.094
90	704.680	0.695	115	2.09	5.76	700.675	89.849	−0.151
95	848.139	0.837	115	3.91	14.12	836.317	94.615	−0.385

Table 2 Calculated values of the volume flow rate, q_{out}, after the condensation trap at ambient temperature and system pressure $p = 1013.25$ hPa for a constant volume flow of $0.5\ \mathrm{L \cdot min^{-1}}$ under DPH conditions

t_d (°C)	$e'_w(p_{ref}, t_d)$ (hPa)	x_v	t_h (°C)	q_{out} ($\mathrm{L \cdot min^{-1}}$)	$q_{m.a}$ ($\mathrm{g \cdot s^{-1}}$)
0	6.136	0.006	30	0.50	0.0096
10	12.329	0.012	40	0.48	0.0093
20	23.486	0.023	50	0.46	0.0089
30	**42.651**	**0.042**	**60**	**0.44**	0.0085
40	74.199	0.073	70	0.41	0.0079
50	**124.171**	**0.123**	**80**	**0.38**	0.0073
60	200.621	0.198	90	0.34	0.0065
65	**251.917**	**0.249**	**95**	**0.31**	0.0060
70	313.909	0.310	100	0.28	0.0054
75	388.282	0.383	105	0.25	0.0048
80	**476.869**	**0.471**	**110**	**0.21**	0.0041
85	**581.641**	**0.574**	**115**	**0.17**	0.0032
90	**704.680**	**0.695**	**115**	**0.12**	0.0023
95	**848.139**	**0.837**	**115**	**0.06**	0.0012

Values for the requested dry-gas mass flow, $q_{m.a}$, are also given. (See Sect. 2.4 for details, List of Symbols for listed parameters)

Figure 3 shows the volume flow, q_{out}, to be set corresponding to the dew-point temperature t_d for a constant volume flow, $q = 0.5\ \mathrm{L \cdot min^{-1}}$, under DPH conditions for various system pressures $p_h \sim p_{ref}$. The specified values for the EURAMET.T-K8 comparison [5] are shown as circles.

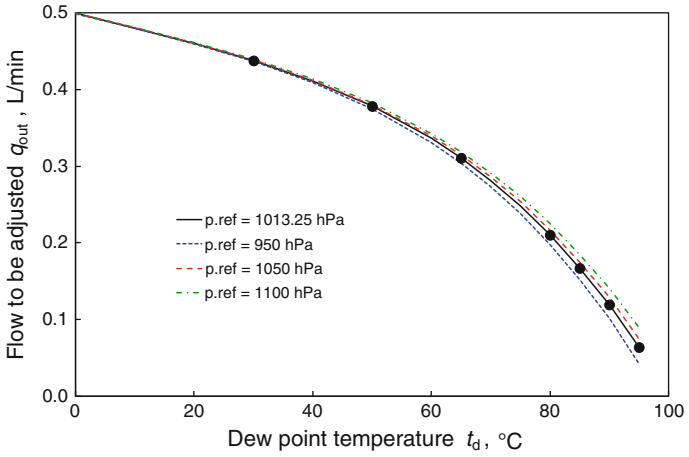

Fig. 3 Flow rate of gas exiting the condensation trap, that is required to ensure a constant volume flow of $0.5\,\mathrm{L}\cdot\mathrm{min}^{-1}$ through the DPH for different system pressures p_{ref}. *Circles* indicate the EURAMET P717 measurement points (see text for details)

3 Measurements

3.1 Pressure Drop Depending on Volume Flow

The pressure drop has been measured based on the volume flow of dry air between the input and output of a DPH (MBW 373-LHX). This device type permits the internal temperature of the gas line t_{h} to be set in a wide range from $\sim t_{\mathrm{a}}$ to 115 °C. With the DPH currently used, this is a special design with no internal gas pump, whereby the gas feed is symmetrical between the input and output relating to the measuring head and also produces a symmetrical pressure drop for this DPH. The special design without an internal gas pump has therefore been chosen because the gas pump causes additional interference in the gas flow which results in poorly reproducible and increased pressure drops in the area of the gas pump. The symmetry of the pressure drop has also been tested via a direct pressure measurement in the measuring head and comparison with the pressure at the input and output for different volume flows.

The volume flow, q, under measuring head conditions has been varied in two different ways:

$q_{\mathrm{out}} = 0.5\,\mathrm{L}\cdot\mathrm{min}^{-1} = \mathrm{const}$, variation of the internal temperature of the gas line from ambient temperature up to 115 °C and variation of $q = q_{\mathrm{out}}$ in the range of $0\,\mathrm{L}\cdot\mathrm{min}^{-1}$ to $3\,\mathrm{L}\cdot\mathrm{min}^{-1}$ at a constant internal temperature $t_{\mathrm{h}} \sim t_{\mathrm{a}}$.

Depending on the measuring conditions, an internal volume flow, q, is set that results in a corresponding pressure difference, Δp, between the input and output of the DPH. For a volume flow of $q = 0.5\,\mathrm{L}\cdot\mathrm{min}^{-1}$, a pressure drop of approximately 0.4 hPa is set between the input and output of the DPH; correspondingly, between the measuring head and output, there is a pressure drop of ∼0.2 hPa.

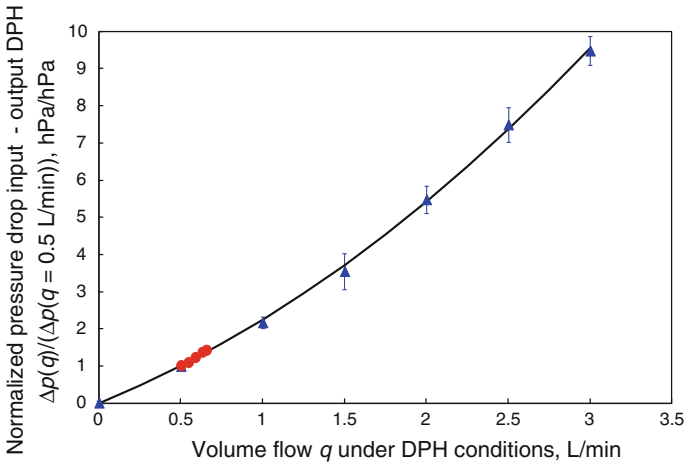

Fig. 4 Variation in the normalized pressure drop from inlet to outlet of a MBW373 LHX, resulting from varying the internal flow rate directly at ambient temperature (*blue triangles*) or indirectly by varying the DPH internal temperature (*red circles*). The least-squares fit to the points (*black line*) is given in the text as Eq. 14. The uncertainty *bars* indicates the combined uncertainty of pressure difference measurements and the uncertainty of flow adjustment with a coverage factor of $k = 2$

The pressure difference measurements for the volume flows given above have been normalized to the measurement at $q = 0.5\,\mathrm{L} \cdot \mathrm{min}^{-1}$ and represented in Fig. 4. The normalized pressure difference depending on the volume flow q can be described via a second-order polynomial. With $q = 0$, the pressure drop is equal to 0 in line with the definition,

$$\frac{\Delta p(q)}{\Delta p_{q=0.5\,\mathrm{L}\cdot\mathrm{min}^{-1}}} = 1.764\,\mathrm{min}\cdot\mathrm{L}^{-1} q + 0.473\,\mathrm{min}^2\cdot\mathrm{L}^{-2}\, q^2. \tag{14}$$

The empirical formula (Eq. 14) is used to estimate pressure drops depending on the volume flow at a known pressure drop with $q = 0.5\ \mathrm{L} \cdot \mathrm{min}^{-1}$.

3.2 Pressure Drop Under Humid-Air Conditions

The pressure drop was measured between the input and output of a MBW 373 LHX without an internal gas pump as described in Sect. 3.1 under actual humid conditions. The differential pressure measurements were obtained using two Paroscientific 6000-200A absolute pressure transducers with a changeover switch to gain access of transducer 1 to the input and transducer 2 to the output and *vice versa*. The differential pressure was calculated from the values of the transducers at both switch configurations to eliminate the zero-point offsets. Both pressure transducers were stabilized at 35 °C; the access to the gas sample was sufficiently heated to avoid condensation effects. In between the transducer access and the transducer itself, a condensation trap was arranged to avoid condensation at the transducers. The dew point was applied

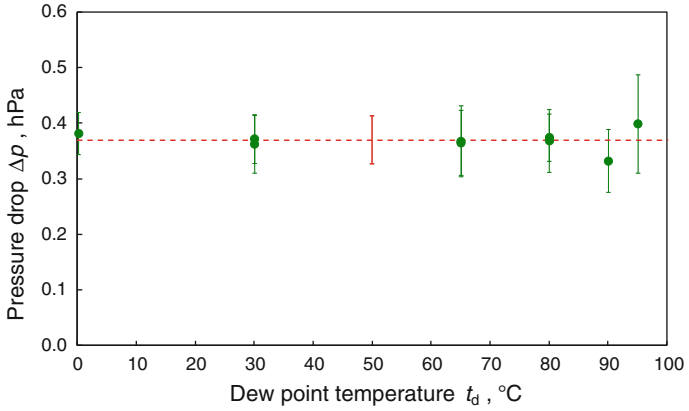

Fig. 5 Pressure drop under humid-air conditions between the input and output of a MBW373 LHX without an internal gas pump to avoid additional effects by the pump. The volume flow q under DPH conditions has been adjusted accordingly, Table 2 and Fig. 3. The uncertainty *bars* indicate the combined uncertainty of pressure difference measurements and the uncertainty of flow adjustment with a coverage factor of $k = 2$. *Dashed line* indicates the average of all measurements with an expanded uncertainty *bar* ($k = 2$) drawn at $t_d = 50\,°C$

using a single-pass dew-point generator in a single-pressure configuration [6], and the volume flow of the reference gas was adjusted according to Fig. 3 and Table 2 in order to maintain a constant volume flow, $q = 0.5\ \mathrm{L} \cdot \mathrm{min}^{-1}$, under DPH conditions.

The results obtained are depicted in Fig. 5. They confirm a correct adjustment of the volume flow using the method described. This ensures a constant pressure drop, within the uncertainty of the measurement, over the entire range of applied dew-point temperatures.

3.3 Comparison of Different Sampling Configurations

As part of commissioning and validating a new SHG, at rising dew-point temperatures, increasing deviations from the existing system have been determined, although the same references have been used for pressure and temperature. At dew-point temperatures above approximately 50 °C, the deviations became significant, and at $t_d = 75\,°C$, they reached values that were far in excess of that expected for the estimated measurement uncertainty.

An analysis of the operating mode of both generators delivered the following result:

The existing SHG is a commercial system that has been upgraded and optimized in terms of the measuring equipment [7]. The gas feed corresponds precisely to the setup shown in Fig. 1 with the point of reference in the SHG measuring chamber and a reference gas removal via a 2 m long heated line. Therefore, the point of reference is positioned upward of the flow to the point of use in the measuring head of the transfer DPH, in accordance with Fig. 1. With the first comparative measurements, this generator was operated at a constant dry-gas flow, whereby with a rising dew point and thus essentially an exponentially rising loading of the dry gas with water vapour, a

rising volume flow was set in the connection line and in the DPH in accordance with Table 1.

The generator being validated was the INTA high-range humidity generator [8] with a gas flow path in accordance with Fig. 2 and a point of reference positioned downstream after the transfer DPH. This generator was operated in accordance with Sect. 2.4 using a constant volume flow under DPH conditions.

As a transfer DPH, a MBW 373 HX was used where the internal gas pump had been removed and replaced with a stainless-steel tube to avoid the additional undesired pressure effects described previously. This gave the device a slightly longer gas feed after the mirror and not the symmetrical pressure drop as described in Sect. 3.1.

At the start of the measurements for both SHGs, the pressure difference between the point of reference and the point of use was measured above the endoscope connection of the DPH using a 10 hPa differential pressure transmitter and operation with sufficiently dry gas with a dew point of approximately 1 °C and a volume flow rate of $0.5\,\mathrm{L}\cdot\mathrm{min}^{-1}$ specified for the transfer DPH. At rising dew points, however, the operation of the first generator with a constant dry-gas flow resulted in a significant increase in the volume flow, and thus, in an increase in the actual pressure drop between the point of reference and the point of use, whereby the correction was no longer valid with the measured pressure drop and resulted in the monitored deviation when comparing both generators.

By shifting the operation of both generators to a constant volume flow q under DPH conditions in line with Sect. 2.4 and Table 2, the differences between the two generators disappear. Figure 6 shows the differences between the calibration results in the overlapping range of both generators after switching to constant volume flow under DPH conditions. The error bars correspond to twice the combined standard deviation of the measurements at each nominal value. It can be seen clearly that the values obtained are entirely consistent with the ±20 mK currently assigned by the Laboratory as the

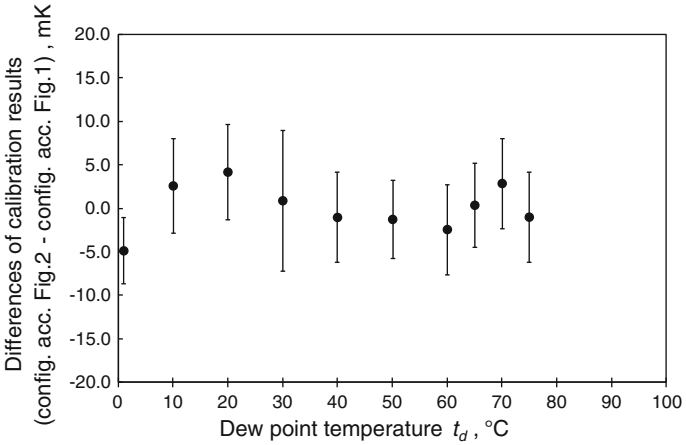

Fig. 6 Difference between calibration results of MBW373-HX (SN: 06-1112) according to the configurations in Figs. 1 and 2 (high-range generator) in the overlapping range of both generators (see Sect. 3.3 for details)

combined reproducibility of the DPH and SHG, based on long-term repeated measurements over several years with negligible drift, within this semi-interval. This value includes contributions due to the effects of contamination, hysteresis, and pressure-drop determination, representing the current achievable limit with a state-of-the-art DPH.

4 Discussion

The influences of gas flow on the pressure drop and on the dew-point calibration in the high dew-point range up to 95 °C have been shown. A method has been described and applied, which shows that a constant volume flow at the conditions of measurement of the dew-point hygrometer ensures an independent pressure drop as a function of the dew-point temperature.

Typical values for the pressure drop between the point of use and point of reference are, depending on the measuring configuration, of the order of 0.2 hPa to 1 hPa at a volume flow rate of $0.5\,\mathrm{L}\cdot\mathrm{min}^{-1}$. This pressure drop requires corrections in the reference dew point of approximately 2 mK to 14 mK.

In Sect. 2.3, a model calculation demonstrates that with operation of a DPH with a constant dry-gas flow of $0.5\,\mathrm{L}\cdot\mathrm{min}^{-1}$, the actual volume flow rises sharply under measurement conditions with rising dew-point temperatures, and thus, increasing loading of the carrier gas with water vapour, and ultimately at a dew point of 95 °C, reaching a value of approximately $3.9\,\mathrm{L}\cdot\mathrm{min}^{-1}$. Accordingly, the pressure drop rises from 1 hPa to 14.1 hPa, for example, with the necessary corrections to the reference dew point of approximately 0.4 °C.

However, if the dry-gas flow is set so that there is a constant volume flow under measurement conditions (Table 2, Fig. 3), a constant pressure drop is set simultaneously between the point of reference and the point of use, and the required dew-point correction due to the pressure drop is independent of the reference dew-point temperature. Section 2.2 presents a corresponding model for the gas volume flows.

The critical factor is the experimental testing of the pressure drop in Sect. 3.2 under humid-air conditions up to a dew point of 95 °C. With the correct setting of the dry-gas flow in line with Table 2, a constant pressure drop is produced, and thus, a dew-point-independent correction of the reference dew point (Fig. 5).

The recommended method has been used to compare two SHGs via a transfer DPH (Sect. 3.3, Fig. 6). The results reported confirm that the method described is independent of the point of reference in the case of two-pressure generators, within the combined limits of reproducibility of the generators and transfer standards used. The method described is of special applicability to the protocols for key and supplementary comparisons, where the contributions to the uncertainty in the key comparison reference values, due to the transfer standards, need to be minimized.

There is a high probability that the actual volume flow through the measuring chamber of the DPH also has an effect on the temperature gradients via the mirror surface and between the mirror surface and the embedded PRT of the DPH. It is therefore to be expected that, with the described method of constant volume flow under measuring head conditions, significant improvements could also be achieved in terms of repro-

ducibility and stability with different measuring equipment. However, these effects do not form part of the content of this study and are reserved for future investigations.

References

1. L.P. Harrison, in *Humidity and Moisture Fundamentals and Standards*, vol. 3, ed. by A. Wexler, W.A. Wildhack (Reinhold Publishing, New York, 1965), pp. 3–69
2. D. Sonntag, Z. Meteorol. **70**, 340 (1990)
3. L. Greenspan, J. Res. Nat. Bur. Stand. (U.S.) Phys. Chem. **80A**, 41 (1976)
4. B. Hardy, ITS-90 formulations for vapour pressure, frostpoint temperature, dewpoint temperature and enhancement factors in the range −100 to 100 °C, in *Proceedings of Third International Symposium on Humidity and Moisture* (National Physical Laboratory, London, 1998), pp. 214–221
5. P717 EURAMET Comparison in humidity (dew-point temperature high range), http://www.euramet.org/index.php?id=tc-t-projects&no_cache=1&ctcp_projects[cmd]=details&ctcp_projects[uid]=596
6. H. Mitter, The BEV/E+E Elektronik standard humidity generator, in *Proceedings of 5th International Symposium on Humidity and Moisture*, Brazil, 2006
7. P. Mackrodt, R. Benyon, G. Scholz, State-of-the-art calibration of high-range chilled-mirror hygrometers and their use in the intercomparison of humidity standard generators, in *Proceedings of Third International Symposium on Humidity and Moisture* (National Physical Laboratory, London, 1998), pp. 159–166
8. R. Benyon, H. Mitter, Int. J. Thermophys. **29**, 1623 (2008)

Int J Thermophys
DOI 10.1007/s10765-012-1343-5

An Investigation of the Relation Between Contact Thermometry and Dew-Point Temperature Realization

R. Benyon · N. Böse · H. Mitter · D. Mutter · T. Vicente

Received: 29 April 2010 / Accepted: 8 October 2012

Abstract Precision optical dew-point hygrometers are the most commonly used transfer standards for the comparison of dew-point temperature realizations at National Metrology Institutes (NMIs) and for disseminating traceability to calibration laboratories. These instruments have been shown to be highly reproducible when properly used. In order to obtain the best performance, the resistance of the platinum resistance thermometer (PRT) embedded in the mirror is usually measured with an external, traceable resistance bridge or digital multimeter. The relation between the conventional calibration of miniature PRTs, prior to their assembly in the mirrors of state-of-the-art optical dew-point hygrometers and their subsequent calibration as dew-point temperature measurement devices, has been investigated. Standard humidity generators of three NMIs were used to calibrate hygrometers of different designs, covering the dew-point temperature range from −75 °C to +95 °C. The results span more than a decade, during which time successive improvements and modifications were implemented by the manufacturer. The findings are presented and discussed in the context of enabling the optimum use of these transfer standards and as a basis for determining contributions to the uncertainty in their calibration.

R. Benyon (✉) · T. Vicente
Instituto Nacional de Técnica Aeroespacial (INTA), Torrejón de Ardoz, Spain
e-mail: benyonpr@inta.es

N. Böse
Physikalisch-Technische Bundesanstalt (PTB), Braunschweig, Germany

H. Mitter
E+E Elektronik Ges.m.b.H. (BEV/E+E), Engerwitzdorf, Austria

D. Mutter
MBW Calibration, Ltd. (MBW), Wettingen, Switzerland

Published online: 30 October 2012

Keywords Calibration · Dew-point temperature · Humidity · Hygrometer · Platinum resistance thermometer · Transfer standard

1 Introduction

A precision chilled-mirror hygrometer (CMH) is an essential complement to a standard humidity generator, where, as a monitor, it can provide the necessary quality assurance of the generated dew point of conditioned gas supplied to the instrument under calibration. There are many potential sources of error within generators and associated sampling systems (small leaks, contamination, incorrect pressure readings, etc.) that without such monitoring could go undetected and lead to large systematic errors. Such optical dew-point hygrometers are also used by many National Metrology Institutes (NMIs) and designated institutes (DIs) as secondary standards to provide traceability to a primary dew-point realization in another country. They are also used by calibration laboratories to obtain traceability from the NMI or DI [1]. In well defined and carefully implemented measurement configurations, these transfer standards can be used with a reproducibility better than ±20 mK in the range of −50 °C to +95 °C [2–5].

A CMH generally comprises a gold- or rhodium-plated copper mirror mounted on a thermoelectric cooler with a miniature platinum resistance thermometer (PRT) embedded below the mirror surface in contact with the moist gas. There have been many claims by instrument manufacturers as to the "fundamental" nature of CMHs, and the potential to rely on temperature calibration instead of humidity calibration [6]. However, the main influence quantities that affect the performance of the temperature sensors incorporated into the hygrometer are the considerable heat flux and the conduction effects within an assembly with reduced dimensions and compact construction. It is not the intention of the authors to propose temperature calibration as a substitute for humidity calibration, but to use the information obtained in the assessment of the influence quantities.

Temperature metrologists are well aware of the difficulties associated with the measurement of surface temperature, even in carefully designed systems configured specifically for this purpose [7], without having taken into account the humidity-related constraints (suitability of materials, desorption, etc.). Instrument manufacturers, aware of the problems involved, take these factors into consideration in an attempt to reduce their effects by careful design and selection of materials. For example, to minimize the heat flow between the condensation surface area and the remaining components, and also to reduce the thermal load on the thermoelectric coolers used to control the temperature of the condensation surface, materials of comparatively low specific thermal conductivity are employed in the surrounding area. This limits heat dissipation to connections, terminals, and/or the device housing. The low specific thermal conductivity of the area around the temperature-controlled mirror surface leads to significant temperature gradients, so its temperature needs to be controlled so that condensation only occurs in the vicinity of the mirror surface, but not on the surrounding surface areas. On the other hand, materials with a high thermal conductivity are required in order to deliver the thermal energy required to the condensation surface with a temperature

gradient as low as possible, normally using a heat-conducting paste layer. A key issue in keeping the mirror gradients to a minimum is the temperature preconditioning of the gas prior to its contact with the mirror. Successful reproducible operation requires all these parameters to be controlled.

The continuous quest for improved calibration and measurement capabilities (CMCs) commensurate with the instrument manufacturers' specifications for precision condensation hygrometers has led NMIs to develop and implement better humidity standards, followed by the need for more precise key comparisons (KCs) to support their CMC claims included in Appendix C of the CIPM-MRA. The details of the standard humidity generators and CMCs applicable to this study are summarized in Table 1 for a confidence level of approximately 95 %. It is not the purpose of this study to show differences between different laboratories that are signatories of the CIPM-MRA, but to use these capabilities to investigate the relation between the temperature and dew-point calibrations within the limits imposed by their respective CMCs.

The uncertainty associated with the materialization of the dew-point temperature of the gas applied to the hygrometers and the difficulty in separating the contributions due to the generator and hygrometer impose practical limits to the quantification of the influence quantities due to temperature gradients, but at least enable an upper limit to be established.

In the following sections, the calibration results of carefully selected PRTs calibrated by comparison in liquid baths are compared with those obtained in terms of the dew-point temperature after their integration into the CMH.

Table 1 Details of standard humidity generators and CMCs used in this study

Laboratory	Generator	Dew/frost-point range	CMC[a] (mK)
BEV/E+E	Single/two-pressure generator (1P/2P) with saturation over ice	−75 °C to <−55 °C	200–50[a]
		−55 °C to −25 °C	50
	Single/two-pressure generator with saturation over water	−25 °C to 65 °C	35
		>65 °C to 95 °C	50
INTA	Two-pressure generator with saturation over ice (TSC 4500)	−75 °C to <−70 °C	150
		−70 °C to <−60 °C	100
		−60 °C to <−10 °C	50
	Two-pressure generator with saturation over water (TSC 9000)	−10 °C to 60 °C	50
		>60 °C to 70 °C	100
		>70 °C to 75 °C	150
	Two-pressure generator with saturation over water (E+E)	0 °C to 95 °C	50
PTB	Two-pressure generator with saturation over water (2P-HRHG)	−25 °C to 60 °C	35
		>60 °C to 80 °C	45[a]
	Coulometric generator with water electrolysis (CTHG)	−90 °C to <−85 °C	100[a]
		−85 °C to <−75 °C	90[a]
		−75 °C to <−65 °C	80[a]
		−65 °C to <−55 °C	70[a]
		−55 °C to <−25 °C	60[a]

[a] These uncertainties have been calculated by the laboratory but have not been submitted for evaluation and inclusion in Appendix C of the CIPM-MRA. They have been included in the table due to their relevance in the discussions of the results of this investigation

Table 2 Details of hygrometers used in the investigation and the traceability of the PRTs calibrated prior to integration in the measuring heads

Model	Serial no.	Dew-point temperature	Mirror diam. (mm)	PRT cal. range	PRT Cal	Date
DP30-SHSXIII	97-1220	−75 °C to 20 °C	5	−80 °C to 60 °C	TH400665	08/05/1998
DP30-BCS-K2	99-1128	−10 °C to 90 °C	10	−80 °C to 100 °C	TH401796	21/01/2000
373LX	01-0428	−60 °C to 1 °C	5	−98 °C to 23 °C	TH403169	31/07/2001
373 L	02-0920	−50 °C to 20 °C	5	−60 °C to 60 °C	TH404636	08/03/2003
373 L	02-0921	−50 °C to 20 °C	5	−60 °C to 60 °C	TH404642	07/03/2003
373 L	02-0922	−50 °C to 20 °C	5	−60 °C to 60 °C	TH404643	07/03/2003
373 L	02-0923	−50 °C to 20 °C	5	−60 °C to 60 °C	TH404647	12/03/2003
373 L	02-0924	−50 °C to 20 °C	5	−60 °C to 60 °C	TH404644	07/03/2003
373 L	02-0925	−50 °C to 20 °C	5	−60 °C to 60 °C	TH404637	08/03/2003
373LHX	03-1110	−60 °C to 95 °C	5	−80 °C to 100 °C	MBW040921	21/09/2004
373HX	06-1112	−10 °C to 95 °C	10	−10 °C to 105 °C	TH408346E	15/03/2007

2 Transfer Standards

The transfer standards studied in this work are listed in Table 2. They comprise two generations of instruments that were manufactured between 1998 and 2007. The first two digits of the serial numbers correspond to the year in which the construction of the hygrometer was initiated, completion being shortly after the integration of the PRTs in the mirror after the calibration date given in the last column. The units have rhodium-plated copper mirrors of either 5 mm or 10 mm diameter at the visible surface in contact with the gas (see Fig. 1). Two miniature glass-encapsulated PRTs of 5 mm length and 1.5 mm diameter (see Fig. 2) are inserted radially along the diameter of the enlarged area of the mirror parallel to the mirror surface. The mirror and PRTs are integrated in the head module, that in the latest generation of hygrometers is detachable, as shown in Fig. 3 for the most modern version of the digital instrument covering the full range.

3 Characterization and Selection of Sensor Elements

Prior to calibration, the miniature PRT sensor elements were assembled into a re-sealable miniature copper block, designed to house the elements and thermally anchor the fine leads which are then led to the connector via a thin-walled stainless-steel sheath. Initially, assemblies with five PRTs were produced. More recently, sensors have been mounted individually in a format more compatible with the triple-point-of-water cells, and calibration by comparison with standard platinum resistance thermometers (SPRT) in a liquid calibration bath with conventional copper blocks.

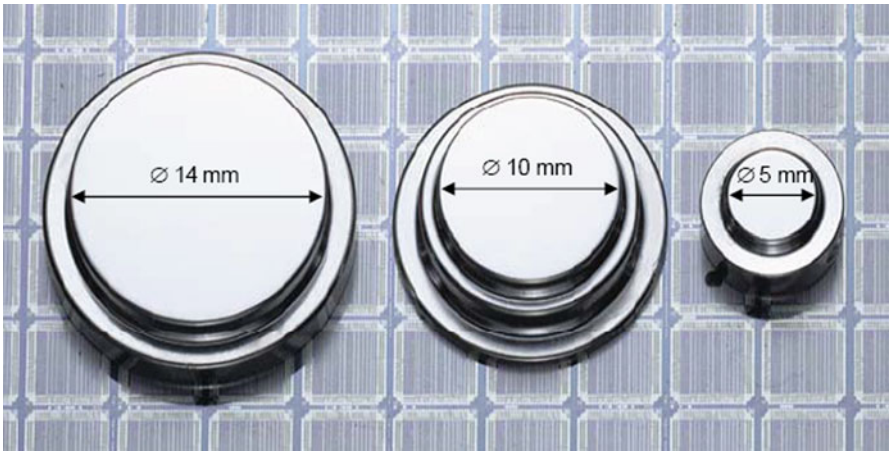

Fig. 1 Details of the three mirror sizes used in the instruments used in this study

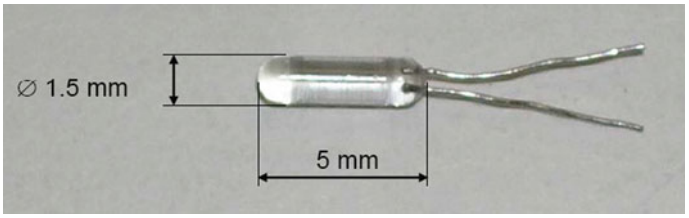

Fig. 2 Details of the Netsushin Co. Ltd., Model MG-1505 glass-encapsulated PRT

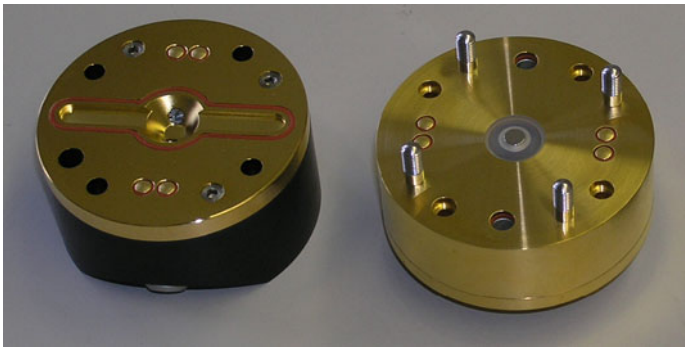

Fig. 3 Details of the detachable measuring head modules of the 373L(HX)

Once assembled, the PRTs were subjected to temperature cycling between the extremes of the intended calibration range until stabilization was observed or the sensors were rejected. After each temperature, the resistance was measured at a value close to the middle of the range, which in the cases reported was the triple point of water. Following this cycling, the PRTs were calibrated by comparison with SPRTs after the first ten points (see Table 1 for equipment list); Fig. 4 shows the stability at

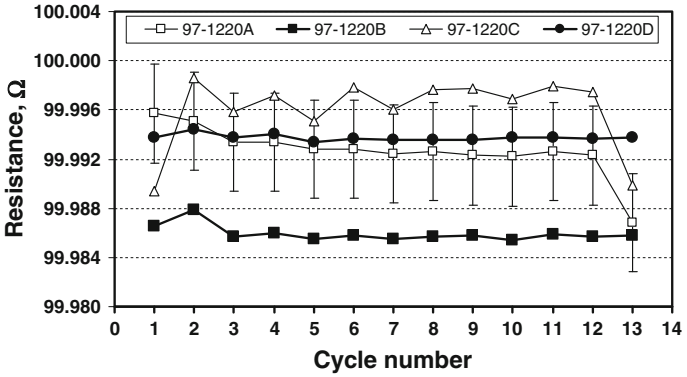

Fig. 4 Stability at the triple point of water for a batch of PRTs upon cycling from −80 °C to +60 °C, for 97-1220, calibration reference TH400665 (INTA). Points 11 and 13 are before and after the calibration from −80 °C to +60 °C

Table 3 Results of determination of the hysteresis of the PRTs for SN: 97-1220 from cycles from −80 °C to +60 °C, measured at the triple point of water

Temperature (°C)	Hysteresis (mK) 97-1220A	97-1220B	97-1220C	97-1220D
0.01	1.5	0.8	3.6	0.8

Table 4 Results of determination of self-heating at 1 mA and 75 Hz for PRTs evaluated for SN: 97-1220

Temperature (°C)	Self-heating (mK) 97-1220A	97-1220B	97-1220C	97-1220D
0.01	19	16	18	18
−69.6	17	12	20	21
59.7	17	20	–	31

the triple point of water for a batch of four PRTs upon cycling from −80 °C to +60 °C for instrument 97-1220. The solid symbols correspond to the two PRTs that were selected for the instrument. The last three points correspond to the initial, mid, and final triple points during the calibration. The vertical scale corresponds to 10 mK per division. Values of hysteresis, defined as the half-width of the interval encompassing the measurements once stabilization is observed, are summarized in Table 3. For the PRTs selected for the transfer standard (with suffixes B and D), the value is below 1 mK.

The self-heating of the sensors was measured at the extremes of the range and at the triple point of water. The results obtained are presented in Table 4. For the two sensors selected, the self-heating produced by a measurement current of 1 mA was of the order of 20 mK in the range the instrument is subsequently used. The standards and equipment used in the calibration of the PRTs are listed in Table 5.

Table 5 Details of standards and equipment used in the calibration of the PRTs

Description	Make	Model
Standard platinum resistance thermometers	Rosemount	162CE
AC resistance bridge	ASL	F700A
AC/DC standard resistor in oil bath	Tinsley	5685A
Temperature calibration baths	Rosemount	915

4 Data Analysis

4.1 Choice of Reference Function

The Callendar–Van Dusen (CVD) equation expressing the relationship between resistance and temperature is

$$R_{\mathrm{t}} = R_0 \left[1 + At + Bt^2 + C\,(t - 100)\,t^3\right], \tag{1}$$

where t is the temperature (ITS-90) (in °C), R_t is the resistance at temperature t, and R_0 is the nominal resistance of 100 Ω at 0 °C. The industrial PRT reference function given in Ref. [8] has parameters $A = 3.9083 \times 10^{-3}\,^{\circ}\mathrm{C}^{-1}$, $B = -5.775 \times 10^{-7}\,^{\circ}\mathrm{C}^{-2}$, and $C = -4.183 \times 10^{-12}\,^{\circ}\mathrm{C}^{-4}$ for $t < 0\,^{\circ}\mathrm{C}$, and $C = 0$ for $t > 0\,^{\circ}\mathrm{C}$. Equation 1, together with these parameters, will be called here as the reference function or CVD reference function. Note that, following calibration, the parameters A, B, and C for each PRT selected for incorporation into a CMH were determined by a least-squares fitting process (as in Sect. 4.2).

Several studies have shown that systematic differences exist between the ITS-90 temperature (t_{90}) and the temperature calculated using a CVD function fitted to experimental data. It has been shown that with good industrial PRTs, the use of the ITS-90-based deviation functions provide a better fit and it has been suggested that the ITS-90 deviation functions be applied to a broad spectrum of industrial and laboratory applications [9]. However, for the narrow temperature range and large number of calibration points in the current investigation, use of the CVD reference function is sufficient to provide a common baseline, enabling presentation of results as differences from the reference function. Such use is consistent with the methodology applied in recent KCs [10,11]. Note that, in practice, the temperature at the PRT sensor is calculated from the measured resistance R by solving the fitted CVD function and the CVD reference function for t.

4.2 Contact Thermometry

The calibration of each PRT was carried out in a temperature-controlled bath and for each PRT, a new set of CVD coefficients R_0, A, B, and C were obtained by

least-squares fitting Eq. 1 to the resultant set of reference temperature values and corresponding four-wire resistance values measured with an excitation current of 1 mA.

The residual error in the fit is defined such that the error associated with the ith point $e_i = R_{\mathrm{fit},i} - R_i$, where R_i and $R_{\mathrm{fit},i}$ are the measured resistance and the resistance calculated using the fitted CVD function, respectively, for a given reference temperature t_i. The "residuals" allow the quality of the fit and the appropriateness of the CVD function to describe the resistance temperature behavior to be assessed. Note that the residuals may also be expressed in terms of temperature in which case we have $e_{t,i} = t_{\mathrm{fit},i} - t_i$, where $t_{\mathrm{fit},i}$ is the temperature calculated using the fitted CVD function for a given measured resistance R_i.

4.3 Dew-Point Temperature Realization

The transfer standards with the pre-calibrated PRTs were calibrated for the dew-point temperature using the Austrian [12], German [13,14], and Spanish [3,6,4] national humidity standards. The inclusion of measurements performed by several laboratories is intended to show that the results are not just valid for a specific measurement configuration, and can be compared within the limits of the expanded uncertainty of each laboratory.

The reproducibility of the transfer standards was optimized by ensuring each laboratory followed a measurement protocol specifying: (a) constant volumetric flow rate of the gas at the conditions of the mirror at $0.5\,\mathrm{L}\cdot\mathrm{min}^{-1}$ [5]; (b) the pre-cooler and head temperature to be set to 30 °C above the measured dew-point temperature; (c) evaporation and re-formation of condensate prior to each measurement; and (d) measurements to be taken at increasing levels of humidity.

At each nominal dew-point temperature, the generated dew-point temperatures t_{H}, and the resistance R of the mirror PRT are measured. In order to compare the contact thermometry and dew-point temperature realizations, we may use either the CVD reference function or the particular fitted CVD function for that PRT to calculate the temperature t_{T} at the PRT sensor. We then calculate the difference, $\Delta t_{\mathrm{HT}} = t_{\mathrm{H}} - t_{\mathrm{T}}$.

Note that, if the effect of temperature gradients and other factors associated with the particular construction and use of some transfer standards is not considered, the relationship between R and t_{H} may not be well fitted by a CVD equation. Thus, the residuals to the fits of Eq. 1 to the dew-point calibration data allow assessment of the quality of the data.

5 Results

In Sect. 5.1, we discuss the quality of the data as reflected in the temperature and dew-point temperature residuals, and in Sect. 5.2, we compare the pre-insertion temperature calibration measurements and the subsequent dew-point temperature measurements using the reference CVD function as the baseline. The instruments investigated (see Table 2) can be divided into two different generations, in terms of design and specifications, namely, the older units with digital display and analog electronics, and the newer generation that is completely digital. The first two in the table are low- and

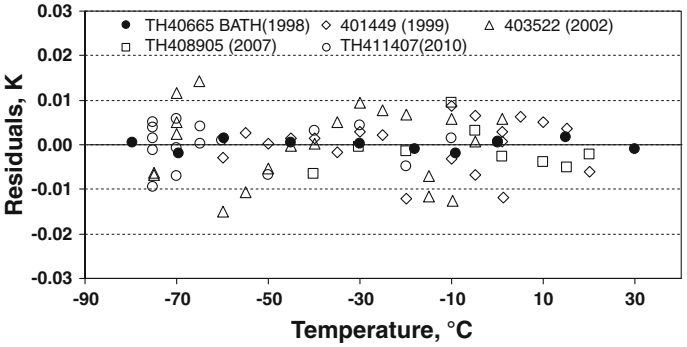

Fig. 5 Residuals of least-squares fit to EN 60751:2008 reference function for calibration by comparison in temperature baths, for SN: 97-1220 (TH40665) and three dew-point temperature calibrations from 2005 to 2010. Values above and below −10 °C are from different generators (INTA)

high-range units with different head designs and mirror sizes. The other nine cover four different configurations, of which six units belong to a set used in a regional KC.

5.1 Quality of Data

The expanded uncertainty ($k = 2$) associated with the pre-insertion calibration of the PRTs carried out at INTA and at MBW is estimated to be between 10 mK and 20 mK [15] for 95 % uncertainty intervals. The temperature residuals associated with the fitted CVD functions are presented as solid symbols in Figs. 5, 6, and 7 depicting the residuals for instruments SN: 97-1220 (−75 °C to 20 °C), SN: 03-1110 (−60 °C to 95 °C), and SN: 06-1112 (−10 °C to 95 °C). The corresponding standard errors of the residuals are 1.4 mK, 7.2 mK, and 1.3 mK, respectively. The larger value for instrument 03-1110 is consistent with the calibration uncertainty assigned by MBW and is dominated by measurements made at −60 °C and −70 °C.

The hollow symbols in Figs. 5, 6, and 7 correspond to residuals to CVD functions fitted to the dew-point temperature calibrations. Clearly, the residual error for these calibrations is greater than that shown for the temperature calibrations; however, the CVD functions still, for the most part, seem well suited to the data. The dew-point temperature residuals are discussed in detail in Sects. 5.1.1–5.1.3.

5.1.1 Low Range (Analog Technology)

Figure 5 shows the residuals of three humidity calibrations in the dew-point temperature range from −75 °C to 20 °C from 2005 to 2010 (hollow symbols) performed at INTA on instrument SN: 97-1220. This instrument has a three-stage thermoelectric cooler and integrated refrigeration. The values of the residuals all lie within ±15 mK, a factor of three greater than the temperature calibration uncertainty (solid symbols). This result is satisfactory, given that in the worst case this only represents one-fifth of the CMCs associated with the individual calibration points and is consistent with the acceptance criterion of ±20 mK established in the calibration procedure.

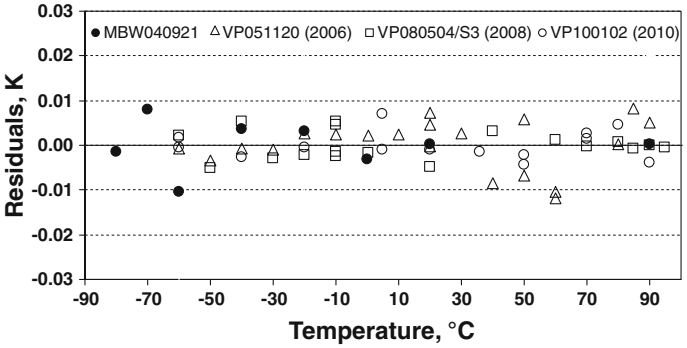

Fig. 6 Residuals of least-squares fit to EN 60751:2008 reference function for calibration by comparison in temperature baths, for SN: 03-1110 (MBW040921) and dew-point temperature calibrations from 2006-01 to 2010-01 (BEV/E+E)

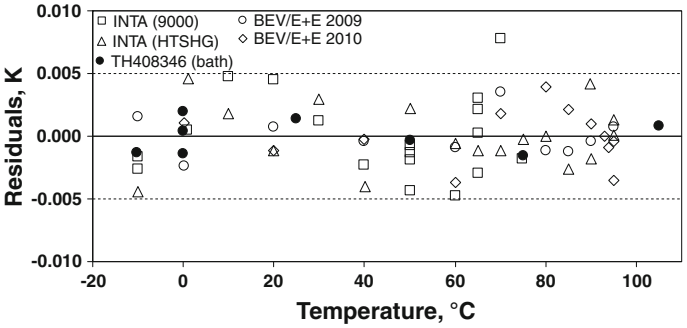

Fig. 7 Residuals of least-squares fit to EN 60751:2008 reference function for calibration by comparison of PRT (TH408346E) in temperature baths (*solid symbols*) and for dew-point temperature calibrations at INTA (both high-range generators) and BEV/E+E , for SN: 06-112

5.1.2 Extended Range (Digital Technology)

Figure 6 shows the results obtained at BEV/E+E for SN: 03-1110 in the range of −60 °C to 95 °C from 2006 to 2010 with similar results to those reported for the analog low-range unit. This instrument also has a three-stage thermoelectric cooler but has a different design of measuring head appropriate for high-temperature operation.

5.1.3 High Range (Digital Technology)

Figure 7 shows the results obtained by the BEV/E+E (1P) and INTA (2P using both high-range generators) over the range from −10 °C to 95 °C on SN: 06-1112. This instrument has a 10 mm diameter mirror, a single-stage thermoelectric cooler, and does not have in-built refrigeration. The results obtained at both laboratories show excellent agreement between the results in terms of the dew-point temperature and the calibration in baths, with residuals within ±5 mK, of the same order as the temperature calibration.

5.2 Comparison Between PRT Temperature and Dew-Point Temperature Calibrations

The difference obtained between the calibrations performed with standard humidity generators and calibrations of the PRTs in temperature baths are presented and discussed for each case.

5.2.1 Analogue Technology

Two units have been studied that have different measuring heads, and mirror sizes that jointly cover the dew-point temperature range from −75 °C to 90 °C. These were the first instruments of each type to have the prior PRT characterization and selection procedure implemented.

Figure 8 shows the difference between the generated dew-point temperature (INTA) and the corresponding PRT bath calibration, Δt_{HT}, for SN: 97-1220 from 1999 to 2010. The PRT is 97-1220D (see Fig. 4). It should be noted that values above and below −10 °C are from different generators, with an overlap from −10 °C to 1 °C (INTA). In order to put this result into context, it must be noted that in the range from −60 °C to +20 °C where the CMC is 50 mK, the mean value of Δt_{HT} is approximately −50 mK, with a dispersion that is consistent with the results of these calibrations depicted in Fig. 5 and the established acceptance criterion for the measurements (±20 mK). The magnitude of Δt_{HT} decreases gradually by 50 mK as the dew-point temperature approaches the lower limit of −75 °C. This cannot be necessarily attributed to temperature gradients caused by the increased heat flux as the three thermoelectric coolers are driven harder, because the assigned CMC in this range is between two and three times that in the preceding range. This effect has also been observed in a digital instrument by BEV/E+E, using a generator with a lower estimated uncertainty in the low range, as shown in Fig. 13. In both cases, the total interval over which the differences span is approximately 60 mK and the heads are of a different design and construction. The only thing in common between both units is that they have three-stage thermoelectric coolers.

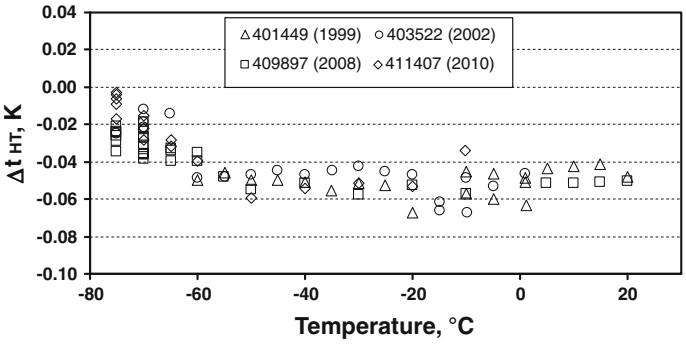

Fig. 8 Difference between generated dew-point temperature (INTA) and PRT bath calibration, Δt_{HT}, for 97-1220

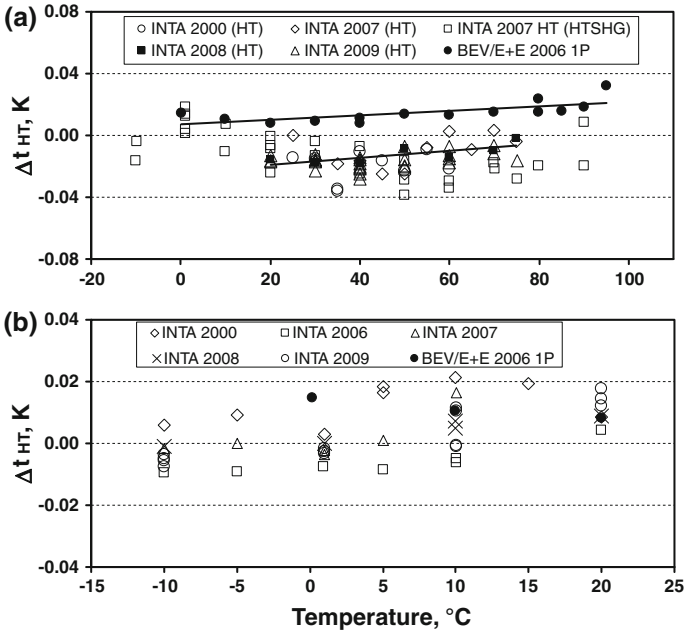

Fig. 9 Difference between generated dew-point temperature (BEV/E+E and INTA) and PRT bath calibration, Δt_{HT}, for 99-1128 (a) with head heater on and (b) with head heater off

A high-range instrument with a larger mirror, SN: 99-1128, was calibrated using both high-range generators at INTA in the two-pressure mode and the generator at BEV/E+E, operated in the single-pressure mode. The differences obtained are depicted in Fig. 9a, b for measurements performed with the head heater on for all the range and with it switched off for measurements below the ambient temperature of the laboratory. This instrument exhibits a characteristic typical of this series and its predecessors. The value of Δt_{HT} at a nominal dew-point temperature of 20 °C with the head at 23 °C or 50 °C is approximately 20 mK. The differences obtained with the head heater on are (0 ± 40) mK if the data from both laboratories are taken into consideration. This also incorporates the systematic difference between the INTA 9000 generator operated in the two-pressure mode and the BEV/E+E generator operated in the single-pressure mode (represented by solid symbols with linear regression). If the values without the head heater are considered, then they are in good agreement, and the difference obtained varies smoothly from −10 mK at −10 °C to +20 mK at 20 °C. In any case, the differences observed between the dew-point temperature and PRT calibration are all within the humidity CMC of both laboratories.

5.2.2 Digital Technology

The first of the digital series with a PRT characterized prior to integration was a low-range instrument (small mirror, three-stage coolers, and in-built refrigeration) with serial number 01-0428. Figure 10 shows the first calibration of the unit performed

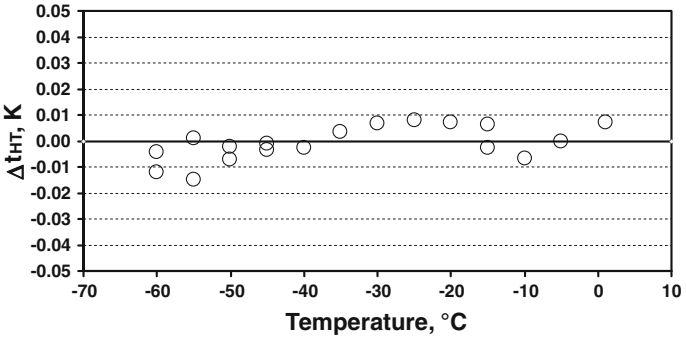

Fig. 10 Difference between generated dew-point temperature (INTA) and PRT bath calibration, Δt_{HT}, for 01-0428 in 2002

in 2002. The difference between the generated dew-point temperature and the PRT bath calibration, Δt_{HT}, is within ± 10 mK down to -50 °C, and within ± 15 mK down to -60 °C. Writing $\Delta t_{\mathrm{HT}} = t_{\mathrm{H}} - t_{\mathrm{T}}$, then $|\Delta t_{\mathrm{HT}}| \leq 10$ mK for $t \geq -50$ °C, and $|\Delta t_{\mathrm{HT}}| \leq 15$ mK for $-60\,^{\circ}\mathrm{C} \leq t < -50\,^{\circ}\mathrm{C}$.

The next batch of PRTs characterized at INTA were destined for use in a key comparison in the dew-point temperature range from -50 °C to 20 °C [10]. Of all the PRTs studied, 12 were selected by the pilot and installed in the units by the manufacturer. The identification of the PRTs installed in each unit was not made available until the publication of Draft B of the comparison. The results for the three pairs of instruments, with the values for PTB, BEV/E+E, and INTA, and the difference between these and the temperature calibration performed at INTA are presented, as in the previous cases. Figure 11a shows the values of PTB for instruments 03-0920 and 03-0921 (Loop 1). Figure 11b shows the values of PTB and INTA for 03-0922 and 03-0323 (Loop 2). Figure 11c shows the values of BEV/E+E and INTA for 03-0924 and 03-0325 (Loop 3). The solid and dashed lines are the linear fits to the data for the first and second instruments in each set, respectively, for the non-INTA calibrations. In all cases, the dependence of the difference as a function of the applied dew-point temperature follows linear relationships with observed maximum departures from linearity of ± 10 mK. For a given instrument, the reported differences fall within an interval of 50 mK over the full range investigated. Finally, in Fig. 12, the values obtained by INTA for the four instruments measured (Loops 2 and 3) are presented together. In this case, the differences obtained between the dew-point and temperature calibrations are all within (0 ± 30) mK. This closer agreement can be expected, because, in the absence of significant drift, the highest correlation between bath calibration and dew-point temperature exists for the INTA results, as all the sources of traceability and instruments employed for temperature measurement in the generators and used in the calibration in the baths are common. The result of the key comparison [10] concluded that no drift or tendency could be identified in any loop corroborating this result.

Figure 13 shows the results obtained for a digital instrument, serial number 03-1110, which covers the full range of the work reported in just one instrument. The difference corresponds to the measurements performed by BEV/E+E from 2006 to 2010, compared to the PRT bath calibration of MBW (Ref: MBW040921). In the

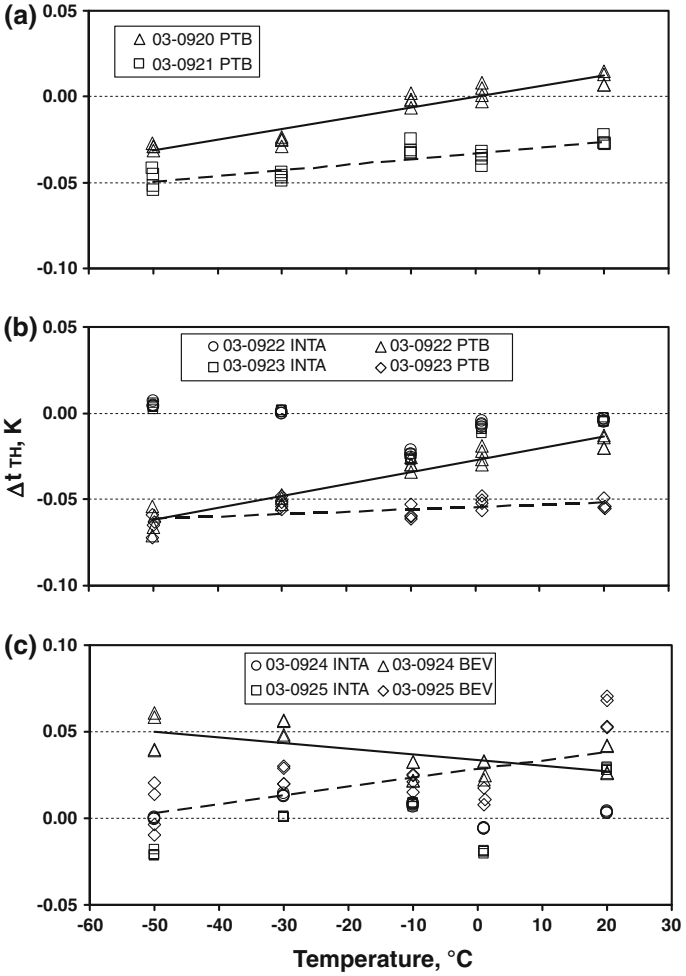

Fig. 11 Difference between generated dew-point temperature and PRT bath calibration, Δt_{HT}, for (a) 03-0920 and 03-0921 (PTB); (b) 03-0922 and 03-0323 (PTB and INTA), and (c) 03-0924 and 03-0325 (BEV/E+E and INTA)

high range, from −10 °C to 95 °C, all the values are within ±20 mK. However, as the temperature is reduced to −60 °C, a similar effect to that observed with the analogue unit in this range (see Fig. 8) was found.

The last instrument characterized was a high-range digital unit without refrigeration, serial number 06-1112, used as the monitoring transfer standard for the INTA high-range humidity generator. This instrument is also used for the collaboration with BEV/E+E in the framework of EURAMET Project P-1032 [16], covering the implementation of a high-range standard humidity generator at INTA, its subsequent validation, and the optimization of CMCs. Figure 14 shows the difference between the generated dew-point temperature and PRT bath calibration for the measurements at BEV/E+E in 2009 and 2010, and the INTA measurement performed with both generators in the interim in 2009. The drift of the instrument is negligible up to 80 °C,

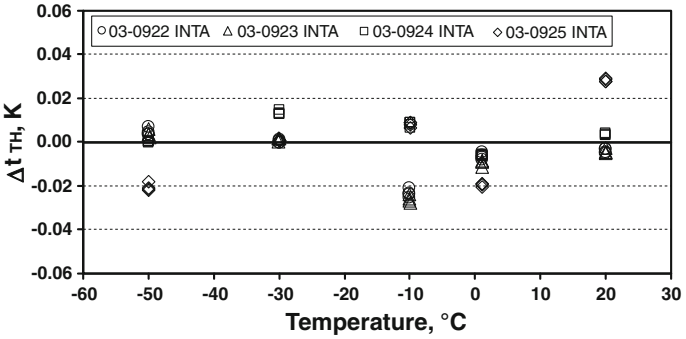

Fig. 12 Difference between generated dew-point temperature and PRT bath calibration, Δt_{HT}, for 03-0922, 03-0923, 03-0924, and 03-0325 (INTA)

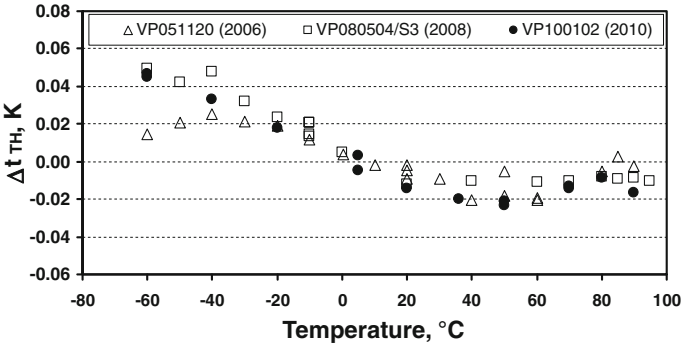

Fig. 13 Difference between generated dew-point temperature and PRT bath calibration, Δt_{HT} (MBW), for SN: 03-1110 (MBW040921) for three calibrations from 2006-01 to 2010-01 (BEV/E+E)

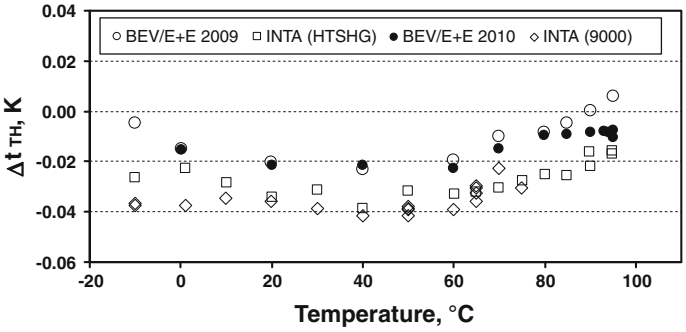

Fig. 14 Difference between generated dew-point temperature (BEV/E+E and INTA) and PRT bath calibration, Δt_{HT}, for 06-1112. BEV/E+E 2009 and 2010 and INTA with both generators in 2009

and is a maximum of 15 mK at 95 °C, well within the 50 mK expanded uncertainty assigned. The overall span of the data at one laboratory in 1 year is 20 mK, from −10 °C to 95 °C, with the BEV/E+E results closer to the nominal value produced by the PRT calibration. The difference between the BEV/E+E and INTA calibrations is

systematically different by 20 mK, and is maintained throughout the work performed. The possible causes for this have not yet been identified and are also a part of the collaborative project between both laboratories. In any case, taking into account all of the information available, the difference between dew-point temperature realization and PRT bath calibration is between −40 mK and +10 mK over the range.

5.3 Uncertainty

Although fit for purpose in view of the results obtained in terms of the published CMCs of the participating laboratories, the method employed in this investigation has a large relative uncertainty associated with the temperature difference. In order to directly measure the gradients in the mirror and separate this contribution from the combined effects of the dew-point temperature realization and contact thermometry, a complementary procedure using the reduction of uncertainty of paired temperature sensors, similar to that applied for heat meters in Ref. [17], should be considered. Furthermore, the simultaneous measurement of both PRTs fitted in the mirrors should be considered and this would allow the direct determination of the mirror gradients with minimum uncertainty.

6 Conclusion

The work reported covers the investigation, using standard humidity generators, of 11 precision chilled-mirror transfer standards of different designs that together cover the dew-point temperature range from −75 °C to +95 °C. The instrument mirrors were fitted with miniature PRTs embedded below the condensation surface. These sensors had been thermally cycled and calibrated by comparison in temperature baths prior to integration in the mirrors. The instruments were manufactured between 1997 and 2006 and represent the evolution of the state of the art for this type of instrument.

The results of the dew-point temperature and bath-temperature calibrations have been compared using reference functions for industrial PRTs based on the Callendar Van Dusen equation as a common baseline. There are slight differences in results for the different types of instruments (analog, digital, with and without temperature stabilized heads) and in the different dew-point ranges, but overall there is good agreement between the temperature calibration and dew-point calibration. The results obtained in all cases show agreement within 50 mK and to within 10 mK in certain parts of the range. Further work is needed to evaluate the performance below −50 °C where the maximum differences were observed.

The differences reported are likely related to mirror gradients and to particular instrument design factors. The results cannot be extrapolated to other designs of CMHs in general, but they do exemplify the current state of the art. Each instrument evaluated had its own peculiarities and limitations, and the methodology employed here can be applied subsequently to other instrument designs to establish the level of applicability in each case.

This study demonstrates that with care placed on the selection of temperature sensors prior to integration into the CMH, optimum values for long-term stability can

be obtained, an upper limit to the mirror gradient can be established, and the quality of the dew-point calibration of the hygrometer can be checked with respect to the contact thermometry calibration in terms of the residuals of the least-squares fit to the reference function.

References

1. R. Benyon, J. De Lucas, A. Moratilla, in *Papers and Abstracts from the Third International Symposium on Humidity and Moisture*, vol. 1 (National Physical Laboratory, Teddington, 1998), pp. 206–213
2. P. Mackrodt, R. Benyon, G. Scholz, in *Papers and Abstracts from the Third International Symposium on Humidity and Moisture*, vol. 1 (National Physical Laboratory, Teddington, 1998), pp. 159–166
3. R. Benyon, P. Huang, in *Papers and Abstracts from the Third International Symposium on Humidity and Moisture*, vol. 1 (National Physical Laboratory, Teddington, 1998), pp. 28–36
4. R. Benyon, H. Mitter, Int. J. Thermophys. **29**, 1623 (2008)
5. H. Mitter, N. Böse, R. Benyon, T. Vicente, Int. J. Thermophys. doi:10.1007/s10765-012-1345-3
6. V.P. Petukhov, Meas. Tech. **25**, 845 (1982)
7. M. Lidbeck, J. Ivarsson, E. András, J.E. Holmen, T. Weckström, F. Andersen, Int. J. Thermophys. **29**, 414 (2008)
8. IEC 60751:2008, Industrial platinum resistance thermometers and platinum temperature sensors
9. V.C. Fernicola, L. Iacomini, Int. J. Thermophys. **29**, 1817 (2008)
10. M. Heinonen, Metrologia 47, Tech. Suppl. 03003 (2010)
11. EURAMET TC Project P-717, Progress report available on http://www.euramet.org. Accessed 01 March 2010
12. H. Mitter, in *Proceedings of the 5th International Symposium on Humidity and Moisture*, INMETRO, Brazil, 2006
13. G. Scholz, Bulletin OIML No. 97 (December 1984), pp. 18–27
14. P. Mackrodt, F. Fernandez, in *Proceedings of TEMPMEKO 2001, 8th International Symposium on Temperature and Thermal Measurements in Industry and Science*, ed. by B. Fellmuth, J. Seidel, G. Scholz (VDE, Berlin, 2002), pp. 589–596
15. ENAC Accreditation Number 16/LC150T, Technical Annex Rev. 7 (2008). The current scope of accreditation is available on http://www.enac.es. Accessed 01 March 2010
16. EURAMET TC Project P-1032, progress report available on http://www.euramet.org. Accessed 01 March 2010
17. E. Tegeler, D. Heyer, B.R.L. Siebert, Int. J. Thermophys. **29**, 1174 (2008)

Int J Thermophys
DOI 10.1007/s10765-012-1342-6

Consistency of the National Realization of Dew-Point Temperature Using Standard Humidity Generators

R. Benyon · T. Vicente

Received: 4 May 2010 / Accepted: 8 October 2012

Abstract The comparison of two high-range standard humidity generators used by Instituto Nacional de Técnica Aeroespacial to realize dew-point temperature in the range from −10 °C to +95 °C has been performed using state-of-the art transfer standards and measurement procedures, over their overlapping range from −10 °C to +75 °C. The aim of this study is to investigate the level of agreement between the two generators, to determine any bias, and to quantify the level of consistency of the two realizations. The measurement procedures adopted to minimize the effect of the influence factors due to the transfer standards are described, and the results are discussed in the context of the declared calibration and measurement capabilities (CMCs).

Keywords Dew-point temperature · Humidity · Hygrometer · Standard humidity generator · Traceability

1 Introduction

The Spanish national humidity standards in the range of −10 °C to +95 ° are currently maintained using two standard humidity generators of completely different saturator designs, measurement configurations, and flow-rate capabilities. The two high-range generators overlap from −10 °C to +75 °C. The calibration and measurement capabilities (CMCs) ($k = 2$) are for the newer generator, 50 mK over the full range, and for the older generator, 50 mK from −10 °C to 50 °C, then increasing to 150 mK at 75 °C. Both the generators are based on the "two-pressure" principle, i.e., they rely on the saturation of a constant flow of air with respect to a plane surface of liquid water at elevated pressure and subsequent isothermal expansion. In the calculation of

R. Benyon (✉) · T. Vicente
Instituto Nacional de Técnica Aeroespacial, Torrejon de Ardoz, Spain
e-mail: benyonpr@inta.es

Published online: 27 October 2012

the reference dew-point temperature generated, a knowledge of the saturation vapor-pressure (SVP) formulation and enhancement factors is required. The new high-range standard humidity generator can also be operated in a single-pressure mode, eliminating the uncertainty introduced by these equations.

Although, in principle, the internal consistency of two-pressure generators can be checked by generating the same nominal values using different saturator temperature and pressure combinations [1], one of the most robust tests of saturator efficiency is to compare different saturator designs using the same nominal saturator temperature and pressure combinations (thus minimizing the influence of the SVP formulations and enhancement factors).

Precision optical dew-point hygrometers have been used to investigate the level of agreement between the two high-range generators in the overlapping dew-point temperature range from −10 °C to +75 °C to demonstrate the consistency of the two realizations that comprise the Spanish national humidity standard. The work reported demonstrates that the dew-point temperatures realized by both generators are consistent within the level of reproducibility of the transfer standards used to the point that customers obtaining traceability from either generator or who have subsequent calibrations using different generators will not observe any systematic difference due to the reference dew-point generator.

2 Measurements

2.1 Standard Humidity Generators

2.1.1 New High-Range Standard Humidity Generator (HTSHG)

This generator was constructed using key components supplied by BEV/E+E as part of a EURAMET project [2], and is operated in the range of −10 °C to +95 °C with pressures up to 1.0 MPa and flow rates up to $2\,\mathrm{L}\cdot\mathrm{min}^{-1}$. Saturator (low and high) and chamber pressure measurements are made with precision quartz absolute pressure gauges with full-scale values of 0.31 MPa, 2.0 MPa, and 0.15 MPa, respectively. Additionally, two pressure transducers with full-scale values of 1.0 MPa and 0.34 MPa, and kept in a thermally controlled enclosure, are connected in parallel with the other saturator and chamber absolute pressure gauges, respectively. Measurement of the saturator pressure is made at the saturator inlet, and the hygrometer pressure is measured at the instrument outlet in a heated tee arrangement. The saturator temperature is determined using two metal-sheathed 25 Ω standard platinum resistance thermometers (SPRT) meeting the requirements of ITS-90, and a precision AC resistance bridge with temperature-controlled 25 Ω and 100 Ω standard resistors. The SPRTs are immersed in the saturator bath in wells on the final saturator element.

2.1.2 Old High-Range Standard Humidity Generator (TSC9000)

The old high-range generator [3] is an optimized commercially available generator used in the dew-point temperature range from −10 °C to +75 °C. It has a maximum

saturator pressure of 2.0 MPa, and the saturator temperature range used is 4 °C to 78 °C. A chamber of internal dimensions (305 mm × 305 mm × 305 mm) is located in the bath above the saturator. The full generator flow passes from the saturator, through the expansion valve and into the chamber after passing though a heat exchanger in the bath, and exits the saturator through a motorized ball valve that is used to control the absolute pressure of the chamber. The chamber pressure measurement is made via a tube connected directly to the chamber, and the humid gas sample is taken from the top of the chamber to each of the hygrometers through one of four independently heated lines. The generator gas flow rate is in the range of $30\,\mathrm{L}\cdot\mathrm{min}^{-1}$ to $100\,\mathrm{L}\cdot\mathrm{min}^{-1}$. In the old generator, saturator temperature measurements are in the gas stream at the outlet of the second saturator element, in the bath close to the outlet of the first saturator element and at the outlet of the second element. The reference pressure sensors are connected in parallel with the original internal absolute pressure transducers which are only used for control purposes.

Modifications of the generator to optimize the original manufacturer configuration include relocation of condensate level sensors and introduction of a presaturator bypass so that the pressure-regulated dry gas can be used to back-purge both pressure measurement lines during temperature and pressure changes to avoid condensation of the humid gas within them that could damage the sensors and yield incorrect pressure readings through partially filling the measurement tubing with water.

In addition to this, gas sampling from the chamber to the hygrometers under test has been improved using four new stainless-steel, temperature-controlled sampling lines with a modified outer sleeve to permit immersion of the end of the heated lines into the bath without perturbing the bath homogeneity and to avoid any temperature drop due to bath fluid evaporation by the heated line at the high-temperature limit.

2.2 Transfer Standards

For comparison of the two high-range generators, three state-of-the-art MBW 373HX dew-point hygrometers were used. The hygrometers were fitted with endoscopes that permit condensate observation.

2.3 Measurement Protocol

Measurements of the transfer standards were performed in accordance with the protocol of the EURAMET-T.K8 comparison [4], and direct resistance measurements of the platinum resistance thermometer (PRT) in the hygrometer mirrors were analyzed with respect to the corrections with respect to the standard for an industrial PRT [5] as described in [6]. Measurements were performed under the following conditions: (a) the volumetric flow rate of the gas at the conditions of the mirror was kept constant at $0.5\,\mathrm{L}\cdot\mathrm{min}^{-1}$; (b) the head temperature was 30 °C, which is above the measured dew-point temperature; (c) condensate was evaporated and reformed prior to each measurement; (d) the nominal absolute pressure of the head was kept at 101.3 kPa; (e) ambient conditions were a temperature of (23 ± 1) °C and a relative humidity less than 70 %rh; and (f) measurements were taken at increasing levels of humidity.

Mirrors were cleaned frequently with isopropanol followed by deionized water, to reduce the effects of possible contamination. Pressure drops in the sampling lines were determined, and the volumetric flow was adjusted following the procedure detailed in [7].

Measurements were performed in three stages:

- The three transfer standards were calibrated using the old TSC9000 at dew-point temperatures from −10 °C to +60 °C every 10 °C and then every 5 °C up to 75 °C. Two reiterations were performed at each dew-point temperature, except at the points defined in [4], namely, 30 °C, 50 °C, and 65 °C, where at least four reiterations were made.
- The three transfer standards were calibrated using the new HTSHG at dew-point temperatures of −10 °C, 1 °C, 10 °C, 20 °C, 30 °C, 50 °C, and 65 °C with the same number of reiterations as with the TSC9000 and also at the remaining dew-point temperatures above the overlapping range up to 95 °C [4].
- Transfer standard 06-1112 was calibrated using the HTSHG at dew-point temperatures of 40 °C, 60 °C, 70 °C, and 75 °C at the remaining nominal values measured on the TSC9000.

In general, the saturator pressure was chosen to yield a generated dew-point temperature approximately 5 °C below the saturator temperature except for the dew-point temperature of 75 °C, where the bath was maintained at 78 °C, due to the limitations of the TSC9000. Throughout the measurements, the absolute pressure at the hygrometer point of reference was maintained at 101.3 kPa (approximately 5 kPa above atmospheric pressure). These are the generator conditions that have been used by INTA as commissioning the generator to be able to maintain pressure within the range of the low-range saturator transducer for optimum measurement and enhancement-factor uncertainty.

2.4 Traceability

Traceability of the defining temperature and pressure measurements in the two-pressure generators, as well as all the auxiliary parameters, is to *Centro Español de Metrologia* (CEM), the Spanish National Metrology Institute (NMI), and where this is not possible, to other NMIs that are signatories to the CIPM-MRA [8]. This is realized via the calibration services covered by the Entidad Nacional de Acreditación (ENAC) accreditations of the laboratories of the INTA Metrology and Calibration Centre [9] under the auspices of the ILAC-MRA [10].

3 Results and Discussion

The results obtained are depicted in Fig. 1. For each generated dew point the difference $\Delta T_{\mathrm{d}} = T_{\mathrm{TSC9000}} - T_{\mathrm{HTSHG}}$ between the transfer standard reading of the TSC9000 and the HTSHG was calculated and plotted as a function of the dew-point temperature. As can be seen, all differences are within ±2 mK except at 30 °C where the difference between the value obtained by transfer standard 08-0414 differs by 5 mK

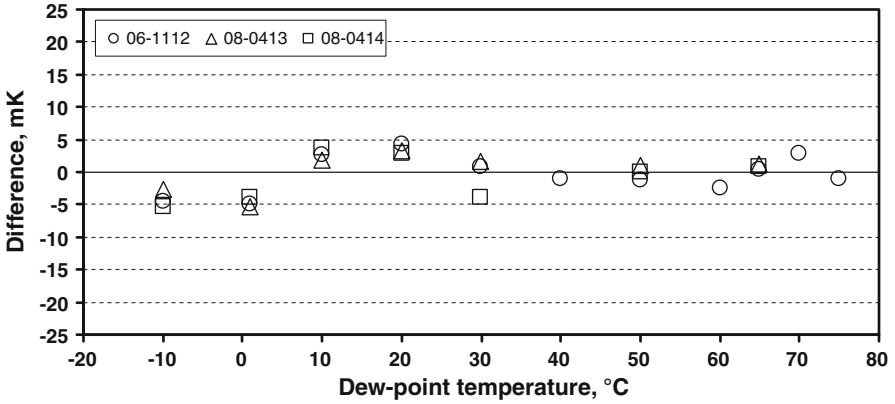

Fig. 1 Differences between high-range generators (TSC9000–HTSHG) from −10 °C to +75 °C, measured using three transfer standards simultaneously

Table 1 Mean values and standard deviations of the difference between the realized dew/frost-point temperatures of the old (TSC9000) and new (HTSHG) high-range generators [TSC9000-HTSHG]

	Difference $\Delta T_d = T_{TSC9000} - T_{HTSHG}$ (mK)			
Transfer standard	06-1112	08-0413	08-0414	All
Mean	−0.4	0.1	−0.8	−0.3
SD	2.9	3.0	3.6	3.0
n (TSC9000, HTSHG)	(19, 63)	(26, 61)	(26, 41)	(71, 165)

The number of total calibration points, *n*, measured using each hygrometer on each generator is indicated in the bottom row

from the other two. There is no evidence of a relevant systematic bias between the generators, and the differences are practically symmetrically distributed around zero. The arithmetic mean and standard deviation were considered suitable statistics for summarizing the data and the means and standard deviations obtained for each transfer standard individually and for the whole set are in good agreement, as presented in Table 1, showing a mean difference of −0.3 mK and a standard deviation of 3 mK over the complete data set. The claimed CMCs for these two generators are between 50 mK and 150 mK for the TSC9000 and 50 mK for the HTSHG [11] at a confidence level of approximately 95 %.

In order to show the contributions to the expanded measurement uncertainty assigned to the generated reference dew-point temperature, an example uncertainty budget for a dew-point temperature of 20 °C is presented in Table 2. The columns from left to right are the measurement quantity, the individual contribution to the uncertainty, the assigned typical uncertainty, the unit, the assigned degrees of freedom, the sensitivity coefficient, and the standard uncertainty contribution to the generated dew-point temperature. This budget is equally applicable for both generators at this value, as the same type of instrumentation, traceability, and acceptance criteria are applicable. Detailed uncertainty calculations are documented in [12], and take into consideration the aspects indicated in [13–15]. A negative sign in the sensitivity coefficient indicates

Table 2 Example uncertainty budget for a generated dew-point temperature of 20 °C

Q_i	Contribution	Uncert. $U_{(Q_i)}$	D.o.f. v_i	Sensitivity coefficient	Contrib. u_i (°C)
Saturation temperature	*Thermometer*				
	Calibration uncertainty (sensor and indicator unit)	0.002 °C	50	0.927	0.0019
	Long-term stability (sensor and indicator)	0.005 °C	50	0.927	0.0046
	Self-heating and residual heat fluxes (sensor)	0.001 °C	50	0.927	0.0009
	Resolution and accuracy or linearity (indicator unit)	0.001 °C	50	0.927	0.0009
	Saturator				
	Temperature homogeneity	0.012 °C	50	0.927	0.0107
	Temperature stability	0.003 °C	30	0.927	0.0028
Saturation pressure	*Pressure gauge*				
	Calibration uncertainty (sensor and indicator unit)	6 Pa	50	-8.702×10^{-5}	−0.0005
	Long-term stability (sensor and indicator)	112.4 Pa	50	-8.702×10^{-5}	−0.0098
	Resolution and accuracy or linearity (indicator unit)	1 Pa	50	-8.702×10^{-5}	−0.0001
	Pressure differences in the saturator	100 Pa	50	-8.702×10^{-5}	−0.0087
	Stability of pressure	60 Pa	30	-8.702×10^{-5}	−0.0052
	Effect of the tubing between the saturator and the pressure gauge	10 Pa	50	-8.702×10^{-5}	−0.0009
Gas pressure at the generator outlet	*Pressure gauge*				
	Calibration uncertainty (sensor and indicator unit)	6 Pa	50	1.588×10^{-4}	0.0010
	Long-term stability (sensor and indicator)	90.8 Pa	50	1.588×10^{-4}	0.0144
	Resolution (indicator unit)	0.6 Pa	50	1.588×10^{-4}	0.0001
	Stability of pressure	20 Pa	30	1.588×10^{-4}	0.0032
	Effect of the tubing between the saturator and the pressure gauge	6 Pa	50	1.588×10^{-4}	0.0009

Table 2 contined

Q_i	Contribution	Uncert. $U_{(Q_i)}$	D.o.f. ν_i	Sensitivity coefficient	Contrib. u_i (°C)
Uncertainty due to formulae/calculations	Saturation vapor-pressure formula (e_s)	5.000×10^{-5}	50	16.055	0.0008
	Water-vapor enhancement formula (f_s)	1.122×10^{-4}	50	16.136	0.0018
	Saturation vapor-pressure formula (e_d)	5.000×10^{-5}	50	−16.136	−0.0008
	Water-vapor enhancement formula (f_d)	6.858×10^{-5}	50	−16.136	−0.0011
Others	Pressure drop in sampling line	5.77 Pa	50	1.588×10^{-4}	0.0009
Combined uncertainty					0.0240
Effective degrees of freedom			226		
Expanded uncertainty			2.01		0.048

that an increasing value of the influence factor results in a decrease in the generated, dew-point temperature. However, in the investigation of the differences between the generators, there are many terms in both realizations that cancel out as they are highly correlated (e.g., same traceability in temperature and pressure measurements, and same models of instruments in both cases, same saturation vapor-pressure and enhancement factor uncertainties as well as the same pressure/temperature combinations were used).

The transfer standard drift is negligible as all measurements were performed in 8 weeks and thus the dominating contributions to uncertainty are those attributable directly to the transfer standards and the corrections due to pressure drops in both generators from the point-of-head pressure measurement to the reference point on the mirror. The pressure corrections are, in the case of the TSC9000, a 200 Pa drop in the heated line from the chamber to the mirror, and for the HTSHG, a pressure increase of approximately 20 Pa from the downstream pressure measurement. The contribution to the generated dew-point temperature of the uncertainty in their determination is within a semi-interval of 5 mK [7], leading to a standard uncertainty contribution of 3.0 mK. As far as the transfer standards are concerned, the combined generator and transfer standard reproducibility in this range is within the semi-interval of 10 mK, as taken from historical data for the monitoring transfer standard 06-1112 and confirmed by the reproducibility of the three transfer standards at each nominal dew-point temperature. The mean difference obtained between generators was −0.30 mK, and the standard deviation of this difference is 3.0 mK. Taking all these factors into account, the reference dew-point temperatures realized by the generators in their common dew-point temperature range of −10 °C to +75 °C can be considered equivalent to within 13 mK, for a coverage factor $k = 2$.

4 Conclusion

A comparison of the old and new high-range standard humidity generators used for the national realization of dew-point temperature at the Spanish designated institute, INTA, has shown their consistency in the overlapping range of −10 °C to +75 °C, within the repeatability of the transfer standards. For NMIs obtaining traceability from INTA in this range, the results ensure that the calibration history and, in particular, the record of the long-term stability of their transfer standards is maintained. Similarly, the integrity of the link to past and future comparisons is maintained even though a different humidity generator is used. At the same time, the two generators are complementary, offering different ranges of flow rates as required and as indicated in INTA's declared CMCs in the key and supplementary comparisons database (KCDB), a public website [11].

References

1. H. Mitter, The BEV/E+E elektronik standard humidity generator, in *Proceedings of the 5th International Symposium on Humidity and Moisture*, Brazil, 2006
2. R. Benyon, H. Mitter, Int. J. Thermophys. **29**, 1623 (2008)
3. P. Mackrodt, R. Benyon, G. Scholz, State-of-the-art calibration of high-range chilled-mirrror hygrometers and their use in the intercomparison of humidity standard generators, in *Proceedings of Third*

International Symposium on Humidity and Moisture, vol. 1 (National Physical Laboratory, 1998), pp. 159–166
4. EURAMET-T.K8 Comparison in humidity (dew-point temperature high range), Technical protocol (Draft 20081212)
5. IEC 60751:2008, Industrial platinum resistance thermometers and platinum temperature sensors
6. R. Benyon, N. Böse, H. Mitter, D. Mutter, T. Vicente, Int. J. Thermophys. doi:10.1007/s10765-012-1343-5
7. H. Mitter, N. Böse, R. Benyon, T. Vicente, Int. J. Thermophys. doi:10.1007/s10765-012-1345-3
8. CIPM Mutual Recognition Arrangement (CIPM-MRA): Mutual recognition of national measurement standards and of calibration and measurement certificates issued by national metrology institutes, Paris, October 1999, Technical Supplement revised in October 2003. http://www.bipm.org/en/cipm-mra/
9. Current scopes of accreditation of the INTA Metrology and Calibration Centre (Laboratory No. 16) in the fields of electricity, flow, pressure and temperature. http://www.enac.es
10. ILAC Mutual Recognition Arrangement (ILAC-MRA). http://www.ilac.org/
11. The BIPM key comparison database, The Current Calibration and Measurement Capabilities for INTA. http://kcdb.bipm.org/AppendixC/. Accessed February 2010
12. TH/PRC/7234/106/INTA Ed. 02, Calibration of dew-point hygrometers using standard humidity generators
13. J.W. Lovell-Smith, Metrologia **43**, 556 (2006)
14. J.W. Lovell-Smith, Metrologia **44**, L49 (2007)
15. J.W. Lovell-Smith, Metrologia **46**, 607 (2009)

CCT-K8 Comparison of realizations of local scales of dew-point temperature of humid gas

Dew-point Temperature: 30 °C to 95 °C

Technical protocol (Approved CCT WG.KC)

Contents

1. INTRODUCTION 2

2. ORGANIZATION 3
   - 2.1 Participants 3
   - 2.2 Method of comparison 3
   - 2.3 Handling of artefacts 5
   - 2.4 Transport of artefacts 5
   - 2.5. Costs 6

3. DESCRIPTION OF THE TRAVELLING STANDARDS 6
   - 3.1. Artefacts 6

4. MEASUREMENT INSTRUCTIONS 7
   - 4.1. Measurement process 7
   - 4.2. Data collection 12

5. REPORTING OF MEASUREMENT RESULTS 13

6. UNCERTAINTY OF MEASUREMENT 15

7. BILATERAL EQUIVALENCE 16

8. THE KEY COMPARISON REFERENCE VALUE (KCRV) 16

APPENDIX A. DETAILS OF PARTICIPATING INSTITUTES 19
APPENDIX B. PROVISIONAL TIME SCHEDULE FOR THE COMPARISON 21
APPENDIX C. PACKING / UNPACKING INSTRUCTIONS 22
APPENDIX D. FORM FOR REPORTING ON RECEIPT OF TRAVELLING STANDARDS 29
APPENDIX E. IEC 60751 RELATIONSHIP 32
APPENDIX F. TEMPLATE FOR SUBMISSION OF RESULTS 33
APPENDIX G. EXAMPLES OF FLOW-METER SETTINGS 34
APPENDIX H. GUIDE ON USE OF SWAGELOK FITTINGS 35
APPENDIX I. DOCUMENT REVISION HISTORY 37

1. INTRODUCTION

1.1 Under the Mutual Recognition Arrangement (MRA)[1] the metrological equivalence of national measurement standards will be determined by a set of key comparisons chosen and organized by the Consultative Committees of the CIPM working closely with the Regional Metrology Organizations (RMOs).

1.2 At the 24th Meeting of the CCT in May 2008, it was agreed to organise a CCT Comparison in dew-point temperature (high range) as a follow-up of the existing CCT-K6 dew-point temperature comparison, as proposed by CCT-WG6 (Now WG-Hu).

1.3 The completed registration form for the proposed CCT-Kx high range dew-point key comparison was submitted on 26/09/2008 and registered in the KCDB database on 29/09/2008

1.4 This technical protocol has been drawn up by the Coordinator in consultation with the nominated participants listed in Section 2. It is based on the protocol developed by CCT/WG6 and designed to encourage coherence between CCT-K8 and the corresponding RMO-K8s.

1.5 The procedure outlined in this document cover the technical operations to be followed during measurement of the travelling standards. The procedure, which follows the guidelines established by the BIPM[2,3] is based on current best practice in the use of dew/frost-point hygrometers and takes account of the experience gained from the CCT-K6, EURAMET.T-K6, EURAMET.T-K8 and APMP.T-K8.

1.6 This comparison is aimed at establishing the degree of equivalence between realisations of local scales of dew-point temperature of humid gas, in the range from 30 °C to 95 °C, among the participating national metrology institutes (NMI)[4].

---

[1] *MRA, Mutual Recognition Arrangement, BIPM, 1999.*

[2] *T.J. Quinn, "Guidelines for key comparisons carried out by Consultative Committees", Appendix F to the MRA, BIPM, Paris.*

[3] *CIPM MRA-D-05. "Measurement comparisons in the CIPM MRA"*

[4] *The term national metrology institute and acronym (NMI) also encompasses the designated institutes (DI) throughout the document.*

2. ORGANIZATION

2.1 Participants

2.1.1 A list of participants is given in table 1. Details of mailing and electronic addresses are given in **Appendix A.**

2.1.2 The participants are divided into two groups. Each group will form a comparison loop. To link the loops to each other, the loops have besides the two Pilots one common participant who measures also both travelling standards.

2.1.3 INTA is the Coordinator of the comparison and the Pilot for both loops, taking main responsibility for running the comparison. NIST is Assistant Pilot. The third, common participant is BEV/E+E who also covers the full range of the comparison, complementing the capability of NIST.

2.1.4 By their declared intention to participate in this key comparison, the laboratories accept the general instructions and the technical protocol written down in this document and commit themselves to follow strictly the procedures of this protocol as well as the version of the "Guidelines for Key Comparisons" in effect at the time of the initiation of the Key Comparison.

2.1.5 Once the protocol and list of participants have been approved, no change to the protocol or list of participants may be made without prior agreement of all participants.

2.1.6 All participants must submit an uncertainty budget of their humidity standards.

Table 1 List of participants (*C*=Coordinator, *P*=Pilot, *L*=Linking laboratory)

RMO	NMI	Country	Role	Loop
APMP	Korea Research Institute of Standards and Science (KRISS)	KR		1
	National Metrology Centre (NMC-A*STAR)	SG		1
	National Metrology Institute of Japan (NMIJ), AIST	JP		1
COOMET	VNIIFTRI East Siberian Branch (VNIIFTRI)	RU		1
EURAMET	Instituto Nacional de Técnica Aeroespacial (INTA)	ES	***C, P***	1, 2
	Istituto Nazionale di Ricerca Metrologica (INRiM)	IT		2
	National Physical Laboratory (NPL)	GB		2
	Physikalisch-Technische Bundesanstalt (PTB)	DE		2
	E+E Elektronik Ges.m.b.H. (BEV/E+E)	AT	***L***	1, 2
SIM	National Institute for Standards and Technology (NIST)	US	***P***	1, 2

2.2 Method of comparison

2.2.1 The comparison is of the realization of local scales of dew-point temperature at the participating NMIs.

2.2.2 The comparison will be made by calibration of travelling standards purchased by *Centro Español de Metrología* (CEM) and deposited at INTA as part of the

Spanish humidity national metrology infrastructure. The travelling standards will measure dew-point temperature of a sample of moist gas produced by a participant's standard generator.

2.2.3 The comparison is carried out in two parallel loops with separate travelling standards (See Fig. 2.2.1). Measurements will start in the Pilot and Assistant Pilot laboratories. The other participants in the loop will then perform comparison measurements at the dew-point temperatures required. The last participant will then return the travelling standard to the Pilot to carry out final measurements to monitor drift. The draft of a time schedule for this comparison can be found in **Appendix B**. Allowing between 4 and 6 weeks per set of measurements (including shipping), this comparison will have a duration of approximately 10 months.

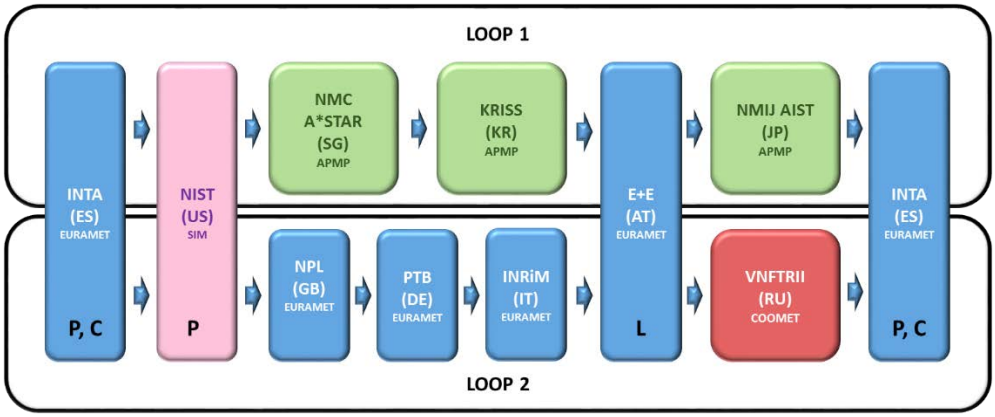

Fig. 2.2.1 Circulation scheme

2.2.4 All results are to be communicated directly to the Pilot (INTA) within three weeks after the completion of the measurements by a laboratory. If this time is seriously exceeded without coordination with the Pilot, the results of this laboratory may be excluded from the comparison. Exclusion of a participant's results from the report may occur if the results are not available in time to prepare the draft report.

2.2.5 Each participant must inform the Pilot within 24 hours of the arrival and despatch of the travelling standards, with copy to the Coordinator. If for some reason, the measurement facility is not ready or customs clearance takes too much time in a country, the participating laboratory must contact the Pilot immediately.

2.2.6 In case of serious difficulty with customs, or other delays which might over-run the time period of the ATA Carnet, the Pilot may request the instruments be returned to the holder of the ATA Carnet (INTA) or to the Assistant Pilot laboratory (NIST), or the sequence of participation may be changed to the most practical arrangement.

2.2.7 The Coordinator (INTA) must be informed about any delays in the schedule.

2.3 Handling of artefacts

2.3.1 The artefacts should be examined immediately upon receipt at the laboratory. All participants are expected to follow all instructions in the operator's manual provided by the instrument manufacturer. For proper unpacking, subsequent packing and shipping to the next participant, detailed instructions have been provided in **Appendix C** of this protocol. During packing and unpacking, all participants should check the contents with the packing list.

2.3.2 The travelling standards should only be handled by authorized persons and stored in such a way as to prevent damage.

2.3.3 During operation of the travelling standards, if there is any unusual occurrence, e.g., loss of heating control, large oscillations, etc. the Pilot laboratory should be notified immediately before proceeding.

2.4 Transport of artefacts

2.4.1 The transportation process begins when the artefact leaves the sending laboratory and does not end until it reaches the destination laboratory. All participants should follow the following general guidelines:

(1) Plan the shipment well in advance. The recipient should be aware of any customs issues in their country that could delay the testing schedule. The shipping laboratory must be aware of any national regulations covering the travelling standard to be exported.

(2) Mark the shipping container "**FRAGILE SCIENTIFIC INSTRUMENTS**" "**TO BE OPENED ONLY BY LABORATORY STAFF**" and with arrows showing "**THIS WAY UP**"; attach shock indicators and seal the container (e.g. with old calibration marks etc.).

(3) Determine the best way to ship the travelling standard to the next participant. In general ground transportation by truck with an approved courier must be preferred.

(4) Obtain the recipient's current shipping address. If possible, have it shipped directly to the laboratory. Note that the addresses in **Appendix A** may be outdated.

(5) Coordinate the shipping schedule with the recipient. The sending laboratory should provide the recipient with the details of the carrier, the tracking number (AWB or other reference), the exact travel mode, and the estimated time of arrival.

(6) Instruct the recipient to confirm receipt and condition upon arrival to the sender and the Pilot. A form for reporting on the receipt of the travelling standards is shown in **Appendix D.**

2.4.2 Each travelling standard is supplied with its shipping container, which is sufficiently robust to ensure safe transportation.

2.4.3 The artefacts will be accompanied by a suitable customs ATA Carnet. Care should be taken with the timing of the ATA Carnet, which only lasts for one year.

2.5. Costs

2.5.1 Each laboratory is responsible for the cost of shipping to the next participant including any customs charges and insurance.

2.5.2 Each laboratory pays its share of the services[5] provided by MBW Calibration AG. The participants will be invoiced by MBW Calibration AG after completion of the comparison.

3. DESCRIPTION OF THE TRAVELLING STANDARDS

3.1. Artefacts

3.1.1 Centro Español de Metrología (CEM) lends one travelling standard per loop for the key comparison. The instruments are state-of-the-art, commercially available chilled-mirror dew-point hygrometers.

3.1.2 Details of travelling standards:
The two travelling standards are new and of the same type:

Model:	MBW 373 HX
Size (in packing case):	75 x 55 x 58 cm
Weight (in packing case):	40 kg
Manufacturer:	MBW Calibration AG
Owner:	Centro Español de Metrología (CEM)
Electrical supply:	230 V / 50 Hz
Electrical connection:	Instrument socket IEC/EN 60320-2-2 (socket C14/plug C13) The instrument is supplied with a Schuko (Continental Europe) plug Standard CEE 7/VII
Power consumption:	300 W
Tube connectors:	Swagelok® 6 mm
Accessories:	Endoscope, 4-wire cable for resistance measurements (3 m), heated flexible hose with 6 mm Swagelok® connectors, pressure measurement insert, condensation trap, flowmeter, operating manual
Approximate value for insurance and customs declaration:	40 000 EUR

[5] *MBW Calibration AG, will provide technical support on site with the transfer standards or at the factory premises in Switzerland, as applicable.*

Serial numbers of the instruments are:

Loop 1	Loop2
08-1215	08-1216

4. MEASUREMENT INSTRUCTIONS

4.1. Measurement process

4.1.1 All participants should refer to the operating manuals for instructions and precautions for using the travelling standards. Participants may perform any initial checks of the operation of the hygrometers that would be performed for a normal calibration. In the case of an unexpected instrument failure at a participant institute, the Pilot institute should be informed in order to revise the time schedule, if necessary, as early as possible.

4.1.2 Sample gas generated by a participant's standard generator, is introduced into the inlet of a travelling standard hygrometer through the supplied heated flexible hose terminated with Swagelok® 6 mm connectors. The electrical connector of the hose is plugged into the appropriate socket near the gas inlet terminal. For all dew-point temperatures, normal precautions (heating) should be used to protect against condensation in sample lines. Special care has to be taken with the connection between the end of the heated hose and the input terminal of the instrument. This point has to be heated externally to prevent condensation at high dew-point temperatures.

4.1.3 Measurements are carried out at nominal dew-point temperatures of 30 °C, 50 °C, 65 °C, 80 °C, 85 °C, 90 °C and 95 °C (refer to 4.1.4 for limited range at high dew-point temperatures). These values are chosen in accordance with the maximum dew-point, participants can generate.

4.1.4 If the scope of a laboratory does not cover the whole range of this comparison, the laboratory is allowed to limit measurements to the highest nominal dew-point temperature specified in 4.1.3 that is within the scope.

4.1.5 Measurements should be done in rising order of dew-point temperature.

4.1.6 The values of dew-point temperature applied to the travelling standards should be within ± 0.5 °C of the agreed nominal values for the comparison, and ideally closer than this. Deviations greater than this may increase the uncertainty in the comparison, for a particular result.

4.1.7 The measurements are to be performed at a system absolute pressure not to exceed 108 kPa. Participants should take into account that the flow which has to be adjusted for a constant volumetric at the conditions of the mirror depends strongly on the system pressure and the ambient pressure. Please note that the supplied rotameters are calibrated for use at 1013.25 hPa and 20 ºC. it is recommended that all measurements are performed at the same nominal system pressure that is applicable to the laboratory conditions. For laboratories

at a suitable altitude above sea level, it is recommended that the nominal system pressure be set to 101.3 kPa and for other laboratories at the most convenient value up to 105.0 kPa.

4.1.8 If the type of generator used (e.g. two pressure generator) requires a precise pressure measurement at the point of condensation (mirror), pressure should be measured as close as possible to the outlet terminal of the hygrometer. The hygrometers are **NOT** equipped with a gas pump, so the outlet of the measuring cell is directly connected to the rear outlet terminal. The remaining pressure drop between the point of condensation and the point of pressure measurement shall be determined as accurately as possible. A possible value for this pressure drop found during the initial tests in the Pilot laboratories is approximately 18 Pa at a flow rate of the wet gas of 0.5 l/min. This should be verified with own measurements by each participant. For this purpose, a special adaptor has been provided to be inserted instead of the endoscope to act as a pressure measurement port.

Attention: Great care should be placed when inserting or removing this so as not to damage the internal o-ring seal in the endoscope port. It should be inserted or removed slowly whilst turning slightly to avoid pinching the O-ring.

A 6 mm connector is also available at the top of the the 12 mm tee at the instrument outlet (see Fig. 1) in order to connect for measurement of pressure drop between head and exit.

Important: For the purpose of this comparison the reference point for all measurements is taken as the point of condensation (mirror). Therefore, the applied reference dew-point temperature should be given for this condition, making due allowance for any pressure drops between the point of saturation and the point of condensation.

4.1.9 Special care has to be taken to avoid condensation and subsequently plugging by water in the outlet lines. A suitable heating and tubes with a greater inner diameter while measuring high dew-point temperatures will help prevent this fault.

4.1.10 Due to dew-point temperatures above ambient temperature the condensing water from the outlet of the hygrometer must be separated before entering the variable area flowmeter (rotameter) e.g. by a condensation trap (use hoses or tubes with large inner diameter). Doing this, the water content exceeding saturation conditions at room temperature is removed. This requires a correction of the flow rate indicated by the variable-area flow meter and the laboratory's flow measurement [6]. Further examples are given in **Appendix G**. Participants should contact the pilot in advance of receiving the instruments if they require assistance in determining the values for their exact laboratory

[6] *Mitter H, Böse N, Benyon R and T. Vicente, "Pressure drop considerations in the characterization of dew-point transfer standards at high temperatures". Int. Journal of Thermophysics (2012), Vol. 33, Issue 8-9, pp 1726-1740*

conditions. The following table shows this correction assuming saturation condition at 20 °C (room temperature), volume expansion, according to the system pressure of 101.3 kPa and temperature of the heated head and tube and is calculated for a wet gas flow of 0.5 l/min.

Dew-point temperature °C	Head temperature °C	Volume of water %	Indicated flow rate after the condensation trap l/min
30	60	4.2	0.44
50	80	12.3	0.38
65	95	24.9	0.31
80	110	47.1	0.21
85	115	57.4	0.17
90	115	69.5	0.12
95	115	83.7	0.06

Table 2: Example of indicated flow rate after the condensation trap for the selected dew-point for a system pressure of 101.3 kPa, room temperature 20 ºC.

4.1.11 A suitable condensation trap and variable-area flowmeter (rotameter) has been provided[7]. This should be connected to the instrument outlet directly (see Fig. 1).

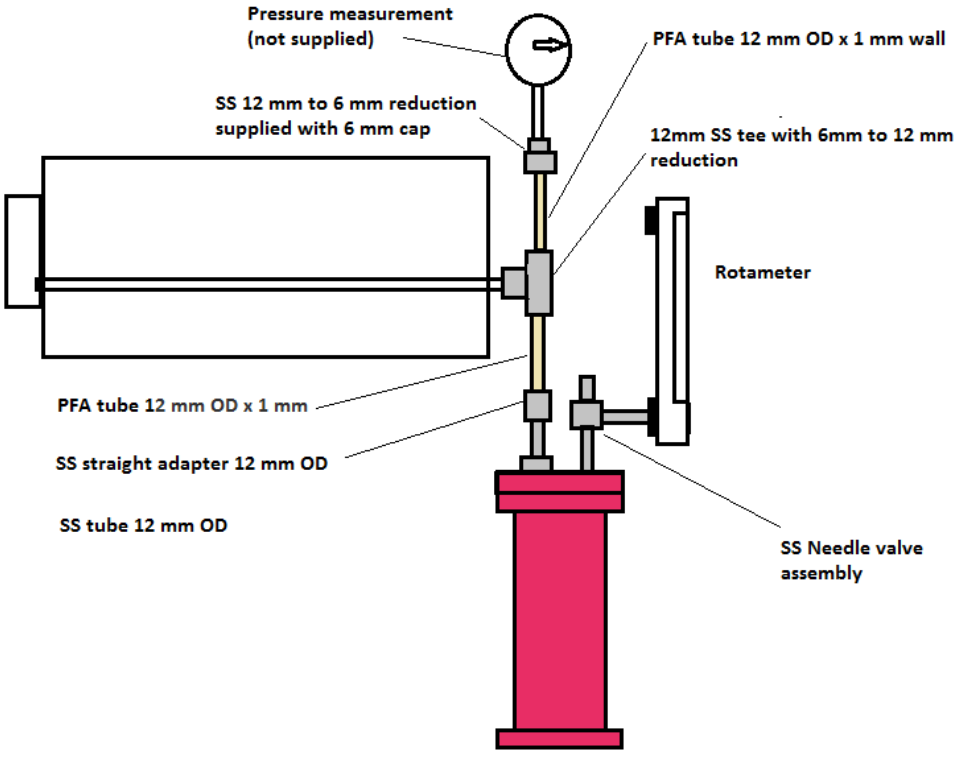

Fig. 1: Schematic of connection of condensation trap with pressure measurement port

[7] *NOTE: Participants may use their own condensation trap if this is more convenient with their generation system.*

4.1.12 Once the flow has been set, the flowmeter should be removed[8] and purged with dry gas. Care must be taken not to touch the needle valve setting whilst removing the flowmeter.

4.1.13 Four sets of measurements are carried out at each generated nominal dew-point temperature. The condensate should be cleared and the mirror cleaned if necessary. The flow after the condensation trap should be readjusted. Where relevant (e.g. significant contribution due to lack of reproducibility of the reference value), values should be taken after returning from another value). This is to reduce the effect of any irreproducibility of the travelling standards [9].

4.1.14 The condensate on the mirror should be cleared and re-formed for each value or repetition of dew-point temperature performing a "Manual Mirror Check" (fixed function key at the bottom bar). The "Automatic Mirror Check" must be disabled (Menu Keys: "Control Setup" → "Mirror Check").

4.1.15 Operation with the travelling standards

Before any humidity measurements, initial actions should be taken:

1) Read the manual "Operating Instructions" delivered by the manufacturer (a copy of the manual is in the transport case).

2) At a volumetric flow rate of 0.5 l/min, the flow-rate indications of the hygrometer, the rotameter and the laboratory flow meter are compared to each other (at a pressure corresponding to the sample gas pressure during dew-point temperature measurements). It is highly recommended to carry out the test in the generator system used in the comparison. In a case of strongly fluctuating sample gas flow, the flow indicator of the hygrometer may show incorrect value. For this test, the dew-point temperature should not exceed room temperature to avoid condensation.

3) When the hygrometer is in a standby mode (i.e. mirror temperature control is switched off), the dew-point temperature indication, resistance of a PRT embedded in the mirror, measured with an external bridge or multimeter, and mirror temperature reading from the RS-232 port are recorded during ten minutes (at least ten measurements). This result should be sent to the Pilot, together with the results of the measurement indicated in section **5.2**, as soon as possible, in order to check the condition of the transfer standard**.**

[8] *NOTE: This is to avoid condensation in the flow meter at higher dew-point temperatures after accumulating water in the condensation trap that could lead to wetting of the flow meter and consequent change the flow through the instrument. Also, sometimes flowmeters tend to oscillate with a back-effect on the instrument.*

[9] *NOTE: It is assumed that the reproducibility of the reference generator is already known. The characterization of the transfer standards has shown that the principal contribution due to lack of reproducibility is the flow setting after the condensation trap and the existence of contamination on the mirror.*

4) Set the hygrometer ready for cleaning with “Mirror Cleaning”.

5) Remove the endoscope carefully following the instructions.

6) Open the measuring head carefully according to the instructions given in the operating manual.

7) Clean the mirror surface using a suitable lint-free tissue or cloth or cotton tips with distilled or de-ionised water preceded by initial cleaning with pure ethanol of p.a. grade if necessary. As the last act of the cleaning procedure it is advantageous to rinse pure distilled water over the mirror which is collected with a cloth below the mirror.

8) Close the measuring head carefully according to the instructions given in the operating manual.

9) Replace the endoscope carefully.

10) Press “OK” for successfully performed mirror cleaning.

Dew-point temperature measurements:

1) Clean the mirror if needed according to the instructions above (no sample gas flow).

2) Set the heater control for the measuring head and the inlet tube to ‘Fixed Mode’ with the target value 30 K **above** the nominal dew-point temperature (Menu Keys: “Control Setup” → “Heater”→”Fixed Mode Target”) and switch on the Heater with the fixed function key at the bottom bar. **Note:** The maximum selectable head temperature is 115 °C. This applies also for dew-point temperatures of 90 °C and above.

3) Wait until the head temperature has stabilized to the pre-set value. To watch this stabilization process, the ‘head temperature’ and the ‘external tube temperature’ should be displayed each on a display line.

4) Set the flow rate of wet sample gas at 0.5 l/min[10] according to an indication by the supplied variable-area flow meter taken from the table 2 in section 4.1.9.

5) **Important:** Press and hold the 0-key (the numerical button for 0) for about 3 seconds until a short beep sounds. This is a special need with both transfer standards to indicate a clean mirror at the right temperature. We have decided to switch off the AUTOLAMP parameter in the instrument setup as this process of manual setting the reflected light intensity to zero gives more stable results over a long period.

[10] *NOTE: Volumetric flow-rate at the measurement head conditions (temperature and pressure).*

6) Start measurements with “Dew/Frost Control” key at the bottom bar (Fixed Function Keys).

7) A homogenous condensate should appear on the mirror; if not, the condensate should be cleared and re-formed with “Mirror Check” (Fixed Function Keys). If necessary, the mirror is cleaned again according to the instructions above. If you experience an oscillating layer thickness with oscillation of the indicated value at very high dew-point temperatures, a new cleaning process may be necessary.

8) After appropriate time of stabilisation, measurements are carried out. The process of collecting data is described below (chapter 4.2). At this time the head temperature and the tube temperature must not increase or decrease.

9) Before changing the sample gas dew-point temperature, make sure that the head temperature and the tube temperature are high enough for the new desired dew-point (see instructions 2 above).

10) Before measuring at the next measurement point, the condensate should be cleared and re-formed with “Mirror Check” (Fixed Function Keys)

4.1.16 Participants should avoid lengthy additional measurements, except those necessary to give confidence in the results of this comparison.

4.1.17 The travelling standards used in this comparison must not be modified, adjusted, or used for any purpose other than described in this document, nor given to any party other than the participants in the comparison. **Important:** Instrument parameters available in the Extended-Access-Menu or via command line on the serial interface of the instrument, must **NOT** be amended without prior written permission of the Pilot.

4.1.18 The Pilot will make an assessment of any drift in the travelling standards during the comparison, based on measurements at the Pilot laboratory at the beginning and end of the comparison period. If drift is found, this will be taken into account in the final analysis of the comparison results.

4.1.19 If poor performance or failure of a travelling standard is detected, the Pilot of the loop will propose a course of action, subject to agreement of the participants.

4.2. Data collection

4.2.1 In the travelling standards, there are two 100-ohm platinum resistance thermometers (PRT) embedded beneath the surface of the chilled-mirror to measure the dew/frost-point temperature. One is used for system measurement and control. The resistance of the other one is measured via a Lemo connector in the rear panel. Dew-point temperature readings used primarily in this comparison are obtained from the resistance of the second PRT. The current applied to the PRT should be nominally 1 mA. The resistance of the PRT should be measured using a calibrated multi-meter or a resistance

bridge, and then converted to a corresponding dew-point temperature. The calculation of the temperature is done according to IEC 60751 and is described in **Appendix E.**

Note: The internal parameters also of the first PRT used for the display and the data communication via RS-232 have been set to the nominal values according to IEC 60751. No individual calibration coefficients are stored in the instruments.

4.2.2 Each measured value (incl. its standard uncertainty) is obtained calculating the mean and standard deviation of at least 10 readings of the resistance of the PRT recorded during 10 to 20 minutes.

4.2.3 Participants may apply their own criteria of stability for acceptance of measurements according to their normal calibration procedures.

4.2.4 As a supporting measurement, the digital display readings (and/or digital signal through a serial port in the rear panel) for dew-point temperature, head temperature, flow rate and head pressure in the travelling standard should be monitored. The mean and standard deviation of a set of at least 10 readings, taken over the same period as the dew-point temperature measurements should be reported.

4.2.5 Values reported for dew-point temperatures produced by a participant's standard generator should be the value applied to the instruments, after any allowances for pressure and temperature differences between the point of realisation (laboratory standard generator or reference hygrometer) and the point of use (travelling standards).

5. REPORTING OF MEASUREMENT RESULTS

5.1 Participants must report their measurement results of four reproduced measurements, within three weeks of completing their measurements to the Pilot (refer to section 2.2.4).

5.2 The participants shall report to the Pilot the first measurement at a nominal dew-point temperature of 30 ºC within 48 h of it being measured, together with the initial tests performed in **4.1.14**, to check the correct performance of the transfer standard(s).

5.3 The Pilot shall accumulate data continually and should analyse the results for possible anomalies in the travelling standard. If problems arise, the Pilot should consult with the participant that submitted the data as soon as possible, and certainly before the distribution of Draft A of the Report of the comparison.

5.4 The parameter to be compared between the laboratories in this comparison is the difference found between the travelling standards and the laboratory dew-point temperature standard. Note that the values of dew-point temperature reported are “arbitrary” values calculated from the measured resistance output, because of the use of the generalised IEC 60751 relationship. The travelling standards are used simply as comparators.

5.5 Participants should report results to the Pilot in terms of dew-point temperature. The main measurement results comprise:

- values of dew-point temperature applied to the travelling standard, and associated standard uncertainty
- values measured using the travelling standard (and the associated uncertainties derived from standard deviation of the set of readings)
- values of difference between applied dew-point and measured dew-point temperature.

Participants shall submit their results in electronic form, using the Excel template provided in **Appendix F**. Use of this format, including calculations of means and differences, allows participants to see clearly the values and uncertainties of the parameters they are submitting for comparison.

5.6 From the data measured by each participant, results will be analysed in terms of differences between applied and measured dew-point temperatures. In each case, the difference will be taken between the applied (realised) value and the mean (mid-point) between the hygrometer values.

5.7 In addition, the difference between the hygrometer reading on all occasions will be analysed and will serve as a check of consistency.

5.8 The participants should report the conditions of realisation and measurement, as background information to support the main results. These conditions may include, pressure and temperature in saturator or reference hygrometer, pressure difference between saturator or reference hygrometer and travelling standards, measurement traceability, frequency of AC (or DC) resistance measurement, and other items. A template for reporting conditions of measurement is included in the Excel workbook provided in **Appendix F**.

5.9 Participants should provide a description of the operation of their dew-point facilities used in the comparison.

5.10 Participants should also provide an example plot of equilibrium condition (resistance versus time) at a nominal dew-point temperature of 50 °C, over at least one hour.

5.11 Any information obtained relating to the use of any results obtained by a participant during the course of the comparison shall be sent only to the Pilot laboratory and as quickly as possible. The Pilot laboratory will be responsible for coordinating how the information should be disseminated to other

participants. No communication whatsoever regarding any details of the comparison other than the general conditions described in this protocol shall occur between any of the participants or any party external to the comparison without the written consent of the Coordinator. The Coordinator will in turn seek permission of all the participants. This is to ensure that no bias from whatever accidental means can occur. Draft B is the first public version.

5.12 If a participant significantly delays reporting of results to the Pilot, then a deadline will be agreed among the participants. If that deadline is not met, then inclusion of those results in the comparison report will not be guaranteed.

6. UNCERTAINTY OF MEASUREMENT

6.1 The uncertainty of the key comparison results will be derived from:

- the quoted uncertainty of the dew-point temperature realisation (applied dew-point temperature)
- the estimated uncertainty relating to the short-term stability of the travelling standard at the time of measurement
- the estimated uncertainty due to any drift of the travelling standard over the period of the comparison (estimated by the Pilots)
- the estimated uncertainty in mean values due to dispersion of repeated results (reflecting the combined reproducibility of laboratory standard and travelling standards)
- the estimated uncertainty due to non-linearity of the travelling standards in any case where measurements are significantly away from the agreed nominal value
- the estimated covariance between applied (laboratory standard) and measured (travelling standard) values of dew-point temperature (if found significant)
- any other components of uncertainty that are thought to be significant.

6.2 Participants are required to submit detailed analyses of uncertainty for their dew-point standards. Uncertainty analysis should be according to the approach given in JCGM100 (2008): *Evaluation of measurement data - Guide to the expression of uncertainty in measurement*. A list of the all significant components of the uncertainty budget[11] should be evaluated, and should support the quoted uncertainties. Type B estimates of uncertainty may be regarded as having infinite degrees of freedom, or an alternative estimate of the number of degrees of freedom may be made following the methods in the Guide. A template for reporting uncertainty of measurement is included in the Excel workbook provided in **Appendix F**. Individual institutes may add to the template any additional uncertainties they consider relevant.

[11] *For example, see J. Nielsen, J. Lovell-Smith, M.J. de Groot, S. Bell, Uncertainty in the Generation of Humidity, CCT/03-20 (BIPM, Sèvres Cedex, France, 2003)*

6.3 The Pilot laboratories will collect uncertainty budgets as background information to the uncertainties quoted by participants for the comparison measurements. The Pilots and the Coordinator will review the uncertainty budgets for consistency among participants.

6.3 The uncertainty budget stated by the participating laboratory should be referenced to an internal report and/or a published article.

7. BILATERAL EQUIVALENCE

7.1 Bilateral equivalences at each dew point will be calculated from differences D_{ij} between participants *i* and *j*, where

$$Dij = R_i - R_j \quad , \tag{1}$$

The bilateral degree of equivalence (DoE) is determined as

$$(D_{ij}, U_{ij}) = (D_{ij}, ku(D_{ij})) \, , \tag{2}$$

where the coverage factor k=2 provides a coverage probability of 95 % for sufficiently large effective number of degrees of freedom of $u(D_{ij})$[12].

In this case, $u(D_{ij})$ is given by

$$u^2(D_{ij}) = u^2(x_i) + u^2(x_j) + u^2_{drift}, \tag{3}$$

where u^2_{drift} is the uncertainty in the comparison due to drift of the hygrometer at a given dew point value. For simplicity, u^2_{drift}, is assigned a single generalised value at each dew point, irrespective of whether participants measured in immediate succession or separated in time. If drift is observed then then clause 8.4 will be applied.

The DoE will be calculated for each pair of participants at each nominal measurement point.

8. THE KEY COMPARISON REFERENCE VALUE (KCRV)

8.1 The outputs of the key comparison are expected to be:

- Results of individual participants for comparison of the hygrometers against their dew-point temperature reference in terms of mean values for each hygrometer at each measured value, estimated standard uncertainty of each mean result and estimated standard uncertainty of comparison process (e.g.

[12] *Cox, M., The evaluation of key comparison data, Metrologia* ***39*** *(2002) 589-595*

effect of long-term stability and non-linearity of the travelling standards) if necessary.

- Estimates of bilateral equivalence between every pair of participants at each measured dew-point temperature.
- A key comparison reference value (KCRV) for each nominal value of dew-point temperature in the comparison. The KCRV will be calculated as a weighted mean of all valid results.
- Estimates of equivalence of each participant to the KCRV. This might be expressed in terms of the Degree of Equivalence (DOE) given as a difference and its uncertainty ($\Delta \pm U$), in °C.

8.2 In the field of dew-point standards, the KCRV does not have any absolute significance with respect to an SI unit. It is calculated only for purposes such as the presentation and inter-relation of key comparison data for the MRA.

8.3 In this comparison and other corresponding RMO comparisons, a reference value is calculated for each nominal value of dew point, treating them as separate data populations for this purpose.

For each nominal dew point value, a key comparison reference value (KCRV) will be calculated as the weighted mean, y, of results

$$y = \frac{x_1/u^2(x_1) + \ldots + x_N/u^2(x_N)}{1/u^2(x_1) + \ldots + 1/u^2(x_N)}, \quad (4)$$

this method of calculation has been agreed by CCT Working Group 6 and applied successfully in CCT-K6. For comparison, values of arithmetic mean and median will also calculated. The uncertainty in weighted mean due to dispersion will be calculated from

$$\frac{1}{u^2(y)} = \frac{1}{u^2(x_1)} + \ldots + \frac{1}{u^2(x_N)}. \quad (5)$$

After collection of participant results, data will be checked for outliers, and calculation of the weighted mean will be made both with and without the outlying results. Values of arithmetic mean and median will also be calculated. As well as the uncertainty in weighted mean due to dispersion, an additional uncertainty in KCRV due to drift of the travelling standard will be include, if necessary, as defined in the next section.

8.4 The Pilots will make an assessment of any drift in the travelling standards during the comparison. The assessment will be based on initial and final measurements done by the Pilot. If drift is found, this will be taken into account in the final analysis of the comparison results. If the drift is small compared with uncertainty values reported by the participants, an estimate for the drift may be set to zero with a standard uncertainty calculated according to the ISO Guide. In a case of a significant drift, the effect is taken into account by assigning a time-dependent value to KCRV, or by other suitable method so that the

estimates of equivalence can be meaningfully calculated between results taken at different times.

8.5 If a travelling standard fails or performs poorly during the comparison, the Coordinator and Pilots will propose a course of action, subject to agreement of the participants.

8.6 A chi-squared test will be carried out on the results with and without any identified outliers, as a measure of the consistency of the data and uncertainties.

Discrepant results will be identified using the criterion:

$$\left|R_{lab} - R_{KCRV}\right| > 2\sqrt{u^2(R_{lab}) - u^2(R_{KCRV})} \quad (6)$$

The decision whether to exclude marginally-outlying data will be based on the impact on the KCRV.

Appendix A. DETAILS OF PARTICIPATING INSTITUTES

E+E Elektronik (BEV/E+E) Austria
Address: Langwiesen 7, A-4209 Engerwitzdorf, Austria
Contact: Dr Helmut Mitter
Phone: +43 7235 605 320
Fax: +43 7235 605 383
E-mail: helmut.mitter@epluse.at

Instituto Nacional de Técnica Aeroespacial (INTA) Spain
Address: Centro de Metrología y Calibración, Ctra. a Ajalvir, km. 4
ES-28850 Torrejón de Ardoz
Contact: Dr Robert Benyon
Phone: +34 915 201 711
Fax: +34 915 201 645
E-mail: benyonpr@inta.es

Istituto Nazionale di Ricerca Metrologica (INRiM) Italy
Address: Strada delle Cacce, 73, I-10135 – Torino
Contact: Dr Vito Fernicola
Phone: +39 011 3977 337
Fax: +39 011 3977 347
E-mail: v.fernicola@inrim.it

Korea Research Institute of Standards and Science (KRISS) R. of Korea
Address: 267 Gajeong-Ro Yuseong-Gu Daejeon 305-340
Contact: Dr. Byung Il Choi
Phone: +82 428685275
Fax: +82 428685290
Email: cbi@kriss.re.kr

National Institute for Standards and Technology (NIST) United States of America
Address: Bldg. 221, Rm. B131. 100 Bureau Dr.
Gaithersburg, MD 20899
Contact; Dr. Christopher Meyer
Phone: +1 301 975 4825
Fax: +1 301 548 0206
E-mail: christopher.meyer@nist.gov

National Metrology Centre (NMC-A*STAR) Singapore
Address: 1 Science Park Drive. PSB Building.
Singapore 118221
Contact Dr. Wang Li
Phone: 65 6279 1959
Fax: 65 6279 1996
Email: wang_li@nmc.a-star.edu.sg

National Metrology Institute of Japan (NMIJ), AIST Japan

Address: AIST Tsukuba Central 3,
Tsukuba 305-8563
Contact: Dr Hisashi Abe
Phone +81 29 861 6845
Fax: +81 29 861 4068
Email: abe.h@aist.go.jp

National Physical Laboratory (NPL) United Kingdom

Address: Hampton Road, Teddington, Middlesex, TW11 0LW
Contact: Dr Stephanie Bell
Phone: +44 20 8943 6402
Fax: +44 20 8943 6306
Email: Stephanie.Bell@npl.co.uk

Physikalisch-Technische Bundesanstalt (PTB) Germany

Address: Bundesallee 100, D-38116 Braunschweig
Contact: Dr.-Ing. Regina Deschermeier
Prof. Dr. Volker Ebert
Phone: +49 531 592 3241
+49 531 592 3200
Fax: +49 531 592 69 3241
E-mail: regina.deschermeier@ptb.de
volker.ebert@ptb.de

VNIIFTRI East Siberian Branch (VNIIFTRI) Russia

Address: Borodina ul. 57.
Irkutsk. 664056. Russia
Contact: Dr Mihail A. Vinge
Tel: +7 3952 468303
Fax: +7 3952 463848
E-mail: vma@niiftri.irk.ru
dep15@niiftri.irk.ru

Appendix B. PROVISIONAL TIME SCHEDULE FOR THE COMPARISON

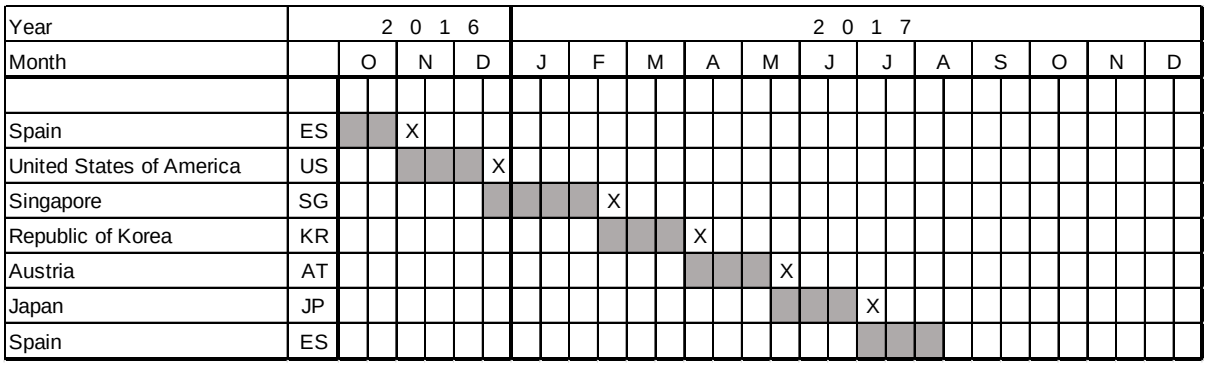

Figure 1: Comparison scheme of loop 1 (One column corresponds to two weeks; ■ = measurement, X = measurement / transportation).

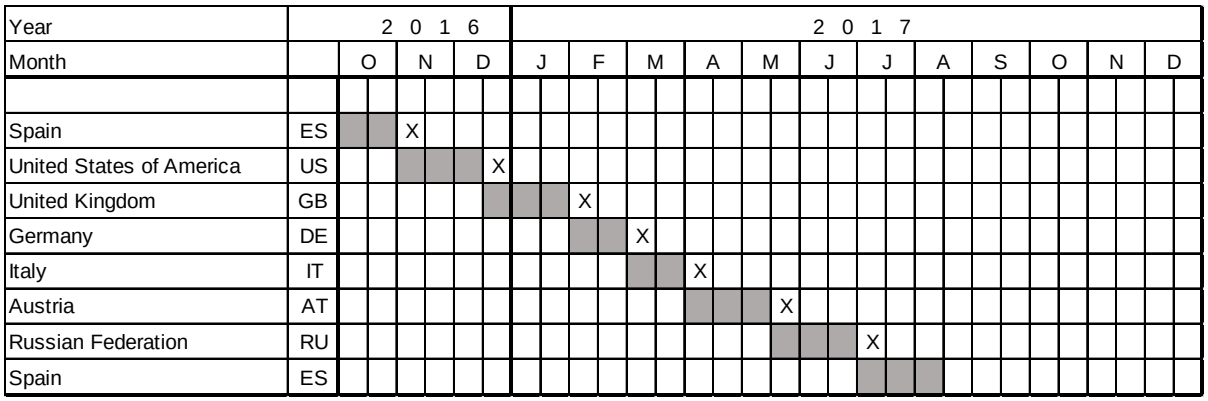

Figure 2: Comparison scheme of loop 2 (One column corresponds to two weeks; ■ = measurement, X = measurement / transportation).

Activity	**Start Month**	**Provisional date**
Draft of technical protocol completed by the Coordinator and sent to participants		Nov. 2016
All comments received from participants		Nov. 2016
Submission of a revised protocol to participants for unanimous approval		Nov. 2016
Submission of revised protocol to CCT/WG6 and TC THERM Chairman		Nov. 2016
Travelling standards characterized by the Pilots		Jan. 2009 – Nov 2016
The first set of key comparison measurements according to the protocol at the Pilot laboratories	INTA: Month 1 NIST: Month 2	Oct. 2016 Nov 2016
Travelling standards sent to participant by Co-Pilot	Month 3	Dec. 2016
Completion of measurements	Month 11 approx.	Aug. 2017
Draft A ready	Month 13 approx.	Oct. 2017
Deadline for comments on draft A	Month 14	Nov. 2017
Draft B ready and submitted to CCT/WG.KC	Month 15	Dec. 2017

Appendix C. PACKING / UNPACKING INSTRUCTIONS

CCT-K8

PACKING / UNPACKING INSTRUCTIONS

Table of contents

1	INTRODUCTION	2
2	UNPACKING INSTRUCTIONS	2
	2.1 Unpacking	2
	2.2 Assembly of condensation trap	5
3	PACKING INSTRUCTIONS	6
	3.1 Preparation of the transfer standard	6
	3.2 Disassembly of the condensation trap	6
	3.3 Packing	6

1. INTRODUCTION

Each instrument is packed in a ZARGES aluminium case that has 10 removable layers of shock-absorbent foam. The layers of foam should be handled with great care to avoid separation of the pre-formed segments.

IMPORTANT:
PACKING & UNPACKING SHOULD ONLY BE PERFORMED BY QUALIFIED LABORATORY PERSONNEL

2. UNPACKING INSTRUCTIONS

2.1 Unpacking

Place transport box in the laboratory at a location close to the point of use and clear an area on a bench/table large enough to take all the contents (hygrometer, condensation trap and accessories). Keep the supplied pallet for despatch. Open the case, releasing the two fastners on one side (it will be necessary to cut the tie wraps blocking the fastners.
Step 1: Remove layer 1 that is the top cover. This exposes layer 2.

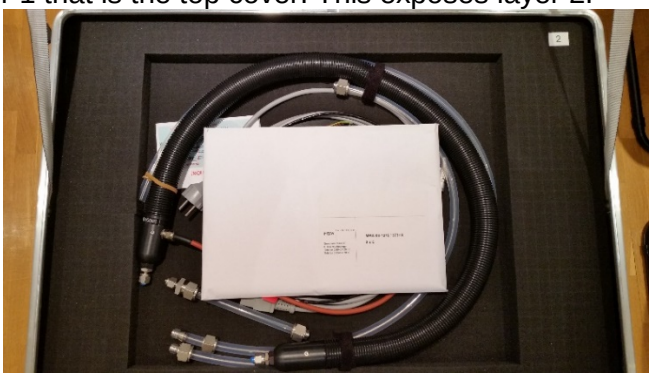

Fig.1: Layer 2

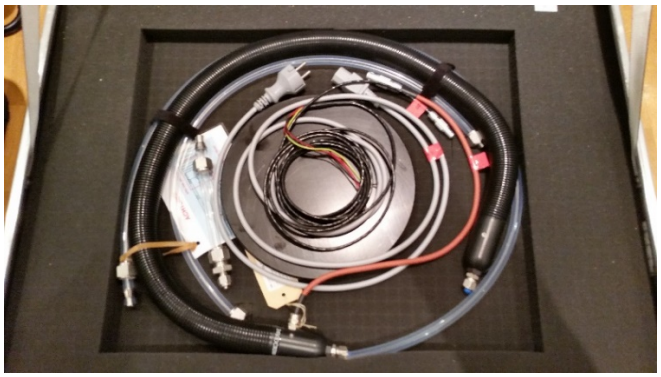

Fig.2: Layer 2 (with instrument operation manual removed)

This has the following contents, that should be removed:

a) Instrument operation manual in an envelope.
b) Shielded cable with LEMO connector for 2nd PRT measurements.
c) Mains cable fitted with European Schuko.
d) 24 V MBW SS heated hose terminated in LEMO connector (for use at inlet if required).
e) 75 cm PFE 12 mm OD tube fitted with 12 mm Swagelok nuts.
f) 100 cm PFE 12 mm OD tube fitted with 12 mm Swagelok nut one end.
g) Short PFE 12 mm OD tube fitted with 12 mm Swagelok nut on one end and a Swagelok 12 mm to 6 mm connector with a 6 mm cap on the other. (For use with condensation trap).
h) Condensation trap support base.

Step 2: Successively remove layers 2 to 6, being careful not to tear the foam and remove the transfer standard. This is best done by two persons, one taking care of the foam. The instrument has two handles that can only be fully opened when the instrument is out of the box, so care has to be taken when removing the instrument. Do not hold by the measuring head.

Fig.3: Layer 5

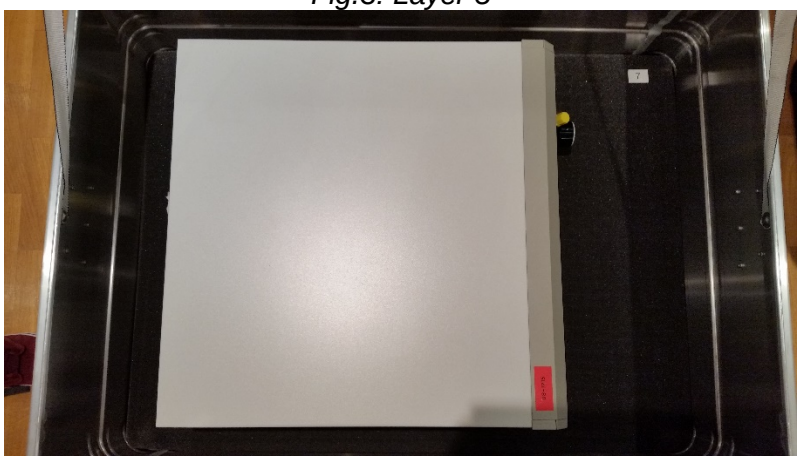

Fig.4: Layer 7

Step 3: Successively remove layers 7 to 10. Once layer 9 has been removed, the condensation trap main body will be visible.

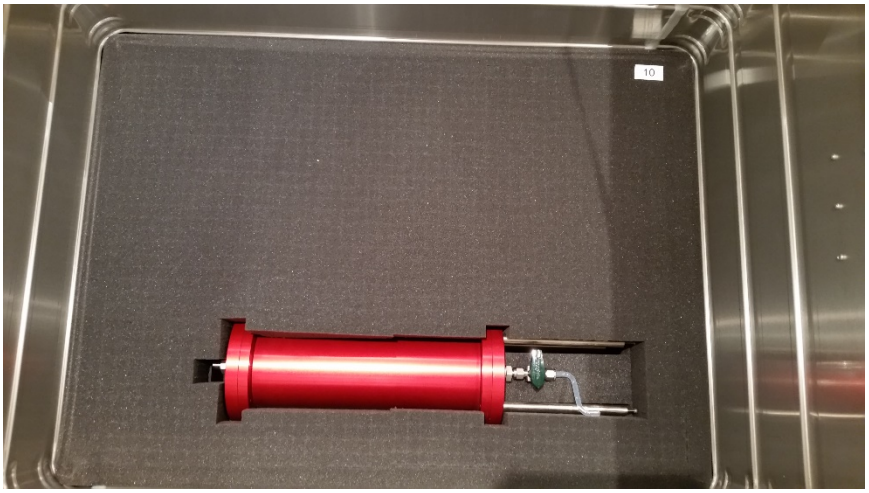

Fig.5: Layer 10

Once layer 10 has been removed, the bottom layer (that should not be removed) is visible:

Fig.6: Bottom layer

It contains:

a) Box of lint-free tissues.
b) Swagelok box that contains [Swagelok SS tee 12 mm with adaptor to 6 mm to connect to instrument outlet, a Swagelok SS 12 mm to 6 mm adaptor to be used as alternative instead of tee if more convenient in instrument set-up, a spare SS 12 mm nut, 12 mm ferrules and insert, a spare LEMO connector for PRT measurement, a SS needle valve assembly with two short lengths of SS tube with 6 mm Swagelok fittings for use with condensation trap] and a ¼" Swagelok connector with o-ring and support ring and a spare o-ring (only to be used if the laboratory needs to have the instrument with ¼" inlet instead of 6 mm). Four SS adaptors from 6 mm to ¼" Swagelok.
c) Spare blank head in red bubble wrap bag.[13]
d) Endoscope case that contains, endoscope, MBW insert for pressure measurement terminated in 6 mm Swagelok fitting, ¼"cap, ¼" nut, set of ¼" nylon ferrules (see Fig. 7).
e) ABB Flowmeter with 6 mm Swagelok at inlet and yellow and red caps (to be removed prior to use).
f) Stainless Steel 12 mm OD insert exit tube for condensation trap.
g) 50 cm PFE 12 mm OD tube fitted with 12 mm Swagelok nuts.
h) Main body of condensation trap.

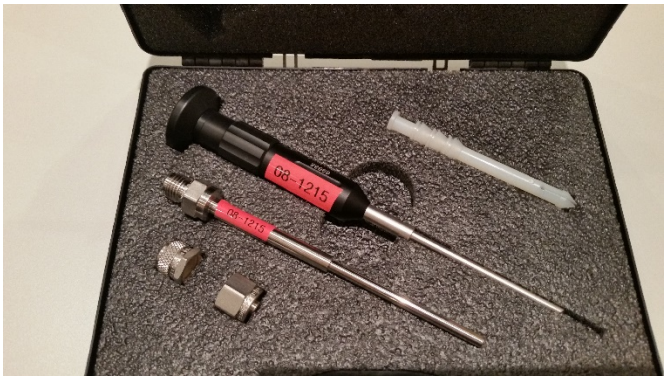

Fig.7: Contents of endoscope case

[13] *The spare head is provided forr use in case of troubleshooting or failure of endoscope, photodiode or detector in the main measuring head.*

2.2 Assembly of condensation trap

Assemble the condensation trap as follows:

a) Attach the base to the four stainless steel legs of the condensation trap using the Allen screws and washers. The base gas a stand-off so that the screw heads do not touch the work bench. Place the condensation trap in the vertical position (see Fig. 8).
b) Insert the stainless-steel exit insert tube into the 12 mm bore-through coupling and hand tighten the 12 mm Swagelok nut and then tighten just under ¼ turn. (the end with the 12 mm straight connector should protrude from the condensation trap
c) Connect the needle valve assembly and hand tighten the 6 mm Swagelok on the condensation trap end and then tighten just under ¼ turn. Check that the needle valve Swagelok couplings are tight (just under ¼ turn from hand tight).
d) Remove the yellow and red plastic protection caps at the inlet and outlet and attach the flowmeter inlet to the needle valve, keeping the flowmeter vertical. Tighten the 6 mm Swagelok nuts to just under ¼ turn from hand tight.

Fig.8: Condensation trap assembled with flowmeter

3. PACKING INSTRUCTIONS
3.1 Preparation of the transfer standard

Once the instrument has been purged with dry gas at the end of the calibration, switch off the instrument and unplug the mains cable from the mains supply and the instrument.
Turn off the generator gas supply to the instrument. Open the condensation trap drain valve and allow the instrument head to depressurize.
Carefully remove the endoscope and place it in its case, together with the pressure measurement insert, the nylon ferrules, the ¼" Swagelok nut, ¼" and Swagelok cap (see Fig. 7). Close the endoscope case.
Place the yellow screw on cap on the endoscope port on the measurement head.
Disconnect the gas lines at the outlet and inlet of the instrument and place the yellow screw on caps on the inlet and outlet Swagelok connectors.
Unplug the heated line LEMO connector.

3.2 Disassembly of the condensation trap

The following instructions are to be followed to prepare the condensation trap for packing:

a) Ensure the condensation trap is empty by opening the drain valve.
b) Remove the flowmeter by loosening the 6 mm Swagelok nut at the flowmeter inlet and place the yellow and red plastic protection caps at the inlet and outlet, respectively.
c) Remove the needle valve assembly by loosening the 6 mm Swagelok on the trap end. (*The needle valve Swagelok nuts should not be loosened and the valve assembly should be the valve and the two short lengths of 6 mm tube with their Swagelok nuts and ferrules*).
d) Disconnect the PFE inlet tube assembly from the condensation trap inlet Swagelok 12 mm adaptor.
e) Remove the stainless steel exit insert tube (that should retain its 12 mm adaptor) by loosening the 12 mm Swagelok nut on the condensation trap end.
f) Remove the condensation trap base by loosening the four stainless steel screws and replacing them afterwards in the four support legs of the condensation trap.
g) Disconnect the two 12 mm nuts on the ends of the 12 mm tee (leave the 12 mm to 6 mm adapter on the short length with its 6 mm cap untouched).

3.3 Packing

Step 1: Open the case and carefully remove layers 1 to 9 of the packaging foam until the bottom unnumbered layer is visible. Place the following in the corresponding cut out sections[14] (refer to figure 6):

a) Box of lint-free tissues.
b) Swagelok box that contains [Swagelok SS tee 12 mm with adaptor to 6 mm to connect to instrument outlet, a Swagelok SS 12 mm to 6 mm adaptor to be used as alternative instead of tee if more convenient in instrument set-up, a spare SS 12 mm nut, 12 mm ferrules and insert, a spare LEMO connector for PRT measurement, a SS needle valve assembly with two short lengths of SS tube with 6 mm Swagelok fittings for use with condensation trap] and a ¼" Swagelok connector with o-ring and support ring and a spare o-ring (only to be used if the laboratory needs to have the instrument with ¼" inlet instead of 6 mm).

[14] *Note: As each element is placed in the box, please tick it off on the despatch form in the measurement protocol*

c) Spare blank head in red bubble wrap bag.
d) Endoscope case that contains, endoscope, MBW insert for pressure measurement terminated in 6 mm Swagelok fitting, ¼"cap, ¼" nut, set of ¼" nylon ferrules (see Fig. 7).
e) ABB Flowmeter with 6 mm Swagelok at inlet and yellow and red caps (to be removed prior to use).
f) Stainless Steel 12 mm OD insert exit tube for condensation trap (including 12 mm adaptor).
g) 50 cm PFE 12 mm OD tube fitted with 12 mm Swagelok nuts.
h) Main body of condensation trap.

Step 2: Place layer 10 (see Fig. 5).
Step 3: Place layers 9, 8 and 7 and put the transfer standard in place (check it has the yellow caps on inlet, outlet and endoscope port (see Fig. 4).
Step 4: Place layers 6 and 5 and put the transfer standard in place (see Fig. 3).
Step 5: Place layers 4, 3 and 2 and place the following components in the cut out (see Fig. 1 & 2).
a) 24 V MBW SS heated hose terminated in LEMO connector (for use at inlet if required)
b) 75 cm PFE 12 mm OD tube fitted with 12 mm Swagelok nuts.
c) 100 cm PFE 12 mm OD tube fitted with 12 mm Swagelok nut one end.
d) Short PFE 12 mm OD tube fitted with 12 mm Swagelok nut on one end and a Swagelok 12 mm to 6 mm connector with a 6 mm cap on the other. (For use with condensation trap).
e) Condensation trap support base
f) Shielded cable with LEMO connector for 2nd PRT measurements.
g) Mains cable fitted with European Schuko plug.
h) Instrument operation manual in an envelope.

Step 6: If you are in an EU member state and the destination is also an EU member State then place the ATA carnet on top of the instrument manual.
Step 7: Place layer 1 and close the case. Place tie-wraps on the two fasteners.
Step 8: If the ATA carnet is to be used then place it in a large envelope marked "ATA CARNET" And fix to the outer top surface of the case.
Step 9: Clearly label the outside of the case in at least two places with the destination[15] and origin address and contact details (be sure to remove the old labels from the previous shipment). Please ensure all the shock indicators are attached and are not in the RED alarm condition. Otherwise replace with new ones.
Step 10: Fix the aluminium transport case to a standard pallet suitable for international shipment. If the laboratory is shipping two instruments in their transport case these should be fitted on one large pallet side by side and never shipped with two separate pallets (See Fig. 9).

Fig.9: Details of cases on pallet

[15] *Please check current details with next participant as defined in the measurement protocol.*

Appendix D. FORM FOR REPORTING ON RECEIPT OF TRAVELLING STANDARDS

TO: *(Pilot Laboratory)*

Dr. Robert Benyon

Fax: 00 34 91520 1645 **E-mail**: benyonpr@inta.es

FROM: *(Participating Laboratory)*

Fax: **E-mail:**

We confirm having received the travelling standard of the CCT Comparison of Dew-point Temperature (CCT/K8):

☐ Loop 1: S/N: 08-1215;

☐ Loop 2: S/N: 08-1216;

on: _____ (date)

After visual inspection

☐ No damage has been noticed;

☐ The following damage must be reported (attach photograph):

Have the hygrometer transportation packages been opened during transit ? e.g., Customs …

☐ No

☐ Don't know (no seals applied)

☐ Yes: Please give details:

Is there any damage to the transportation packages?

☐ No

☐ Yes: Please give details (attach photograph):

Are there any visible signs of damage to the instruments?

☐ No

☐ Yes: Please give details (attach photograph):

Do you believe the travelling standards are functioning correctly?

☐ Yes

☐ No: Please indicate your concerns:

PACKING LIST

Received	Items	Dispatched
	Instrument operation manual in an envelope	
	Shielded cable with LEMO connector for 2nd PRT measurements	
	Power cord with Standard CEE 7/VII plug	
	24 V MBW SS heated hose terminated in LEMO connector (for use at inlet if required) and terminated in 6 mm Swagelok	
	24 V MBW SS heated hose terminated in LEMO connector (for use at inlet if required) and terminated in ¼" Swagelok	
	75 cm PFE 12 mm OD tube fitted with 12 mm Swagelok nuts	
	100 cm PFE 12 mm OD tube fitted with 12 mm Swagelok nut one end	
	Short PFE 12 mm OD tube fitted with 12 mm Swagelok nut on one end and a Swagelok 12 mm to 6 mm connector with a 6 mm cap on the other. (For use with condensation trap).	
	Condensation trap support base	
	Dew-point hygrometer MBW 373 HX S/N: _____* with 2 yellow caps on gas inlet and outlet and endoscope port.	
	Box of lint-free tissues	
	Swagelok box that contains: • Swagelok SS tee 12mm with adaptor to 6 mm to connect to instrument outlet, a • Swagelok SS 12mm to 6 mm adaptor • Spare SS 12 mm nut, 12 mm ferrules and insert • Spare LEMO connector for PRT measurement • SS needle valve assembly with two short lengths of SS tube with 6 mm Swagelok fittings for use with condensation trap • SS Swagelok Tube Fitting, Male Connector, 1/4 in. Tube OD x 1/8 in. Male ISO Parallel Thread, Straight Shoulder (SS-400-1-2RS) with o-ring, support ring and spare o-ring. • Two SS Swagelok Tube Fittings, Reducer, 1/4 in. x 6 mm Tube OD SS-400-R-6M with fitted 6mm nut and ferrules. • 6 mm Plug SS-400-P • ¼" Plug SS-6M0-P	
	Spare blank head in red bubble wrap bag	
	Endoscope case that contains: • Endoscope: S/N: _____* • MBW insert for pressure measurement terminated in 6 mm Swagelok fitting • ¼"cap, ¼" nut, set of ¼" nylon ferrules.	
	ABB Flowmeter with 6 mm Swagelok at inlet and yellow and red caps.	
	Stainless Steel 12 mm OD insert exit tube for condensation trap	
	50 cm PFE 12 mm OD tube fitted with 12 mm Swagelok nuts	
	Main body of condensation trap	
	Zarges K470 IP 65 Aluminium transport case	

*) Please add serial number

Laboratory: _____

Date: _____ Signature: _____

Appendix E. IEC 60751 RELATIONSHIP

Based on the international standard IEC 60751:2008, a nominal resistance-temperature characteristic of the PRT in the travelling standard can be defined as follows:

$$R_t = R_0(1 + At + Bt^2)$$

where:

t = Temperature (ITS-90) in °C,
R_t = Resistance of the PRT at temperature t in Ω
R_0 = Nominal resistance of 100 Ω at 0 °C,
A = 3.9083×10^{-3} °C^{-1} and
B = -5.775×10^{-7} °C^{-2}

Solving the quadratic equation, the temperature can be calculated with

$$t = -\frac{A}{2B} - \sqrt{\frac{A^2}{4B^2} - \frac{R_0 - R_t}{BR_0}}$$

Appendix F. TEMPLATE FOR SUBMISSION OF RESULTS

The template for submission of results is available in electronic form only (Excel workbook). It consists of three worksheets (Results, Conditions and Uncertainty). It will be sent to the participants during the comparison.

Appendix G. EXAMPLES OF FLOW-METER SETTINGS

The following table summarises the flowmeter settings for a laboratory temperature of 22 ºC and ambient pressure of 980 hPa and 1013.25 hPa as a function of system pressure.

Ambient conditions		**System pressure [hPa]**		**1013.25**			**1030**			**1050**		
Temp. [ºC]	**Pressure [hPa]**	**dew-point temp. [°C]**	**head temp. [ºC]**	**(1)**	**(2)**	**(3)**	**(1)**	**(2)**	**(3)**	**(1)**	**(2)**	**(3)**
22	**1013.25**	**30**	**60**	0.44	0.44	**0.44**	0.44	0.44	**0.45**	0.44	0.45	**0.46**
		50	**80**	0.38	0.38	**0.38**	0.38	0.38	**0.39**	0.38	0.39	**0.40**
		65	**95**	0.31	0.31	**0.31**	0.31	0.32	**0.32**	0.31	0.32	**0.33**
		80	**110**	0.21	0.21	**0.21**	0.21	0.22	**0.22**	0.22	0.22	**0.23**
		85	**115**	0.17	0.17	**0.17**	0.17	0.17	**0.18**	0.17	0.18	**0.18**
		90	**115**	0.12	0.12	**0.12**	0.12	0.13	**0.13**	0.13	0.13	**0.13**
		95	**115**	0.06	0.06	**0.06**	0.07	0.07	**0.07**	0.08	0.08	**0.08**
22	**980**	**30**	**60**	0.44	0.45	**0.46**	0.44	0.46	**0.46**	0.44	0.47	**0.47**
		50	**80**	0.38	0.39	**0.40**	0.38	0.40	**0.40**	0.38	0.41	**0.41**
		65	**95**	0.31	0.32	**0.32**	0.31	0.33	**0.33**	0.31	0.34	**0.34**
		80	**110**	0.21	0.22	**0.22**	0.21	0.22	**0.23**	0.22	0.23	**0.23**
		85	**115**	0.17	0.17	**0.17**	0.17	0.18	**0.18**	0.17	0.19	**0.19**
		90	**115**	0.12	0.12	**0.12**	0.12	0.13	**0.13**	0.13	0.14	**0.14**
		95	**115**	0.06	0.07	**0.07**	0.07	0.07	**0.07**	0.08	0.08	**0.08**

(1) Volume flow after condensation
(2) Volume flow after needle valve (there occurs some expansion from system pressure to ambient which changes the flow)
(3) Volume flow indicated by the flow meter (here the calibration parameters 1013.25 hPa and 20 °C are corrected to the real conditions ambient temperature and pressure.

Appendix H. GUIDE ON USE OF SWAGELOK FITTINGS

For the correct use of the instruments it is important to distinguish between metric and fractional measurements of connectors and couplings and to correctly tighten them for reproducible, leak-free operation.

Intermix/Interchange with Other Manufacturers' Components

The critical interaction of precision parts is essential for reliability and safety. Components of other manufacturers should not be intermixed with the Swagelok fittings supplied.

Metric Swagelok Tube Fittings

Metric tube fittings have a stepped shoulder on the body hex.

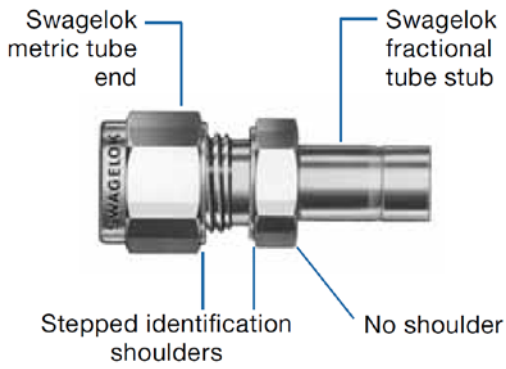

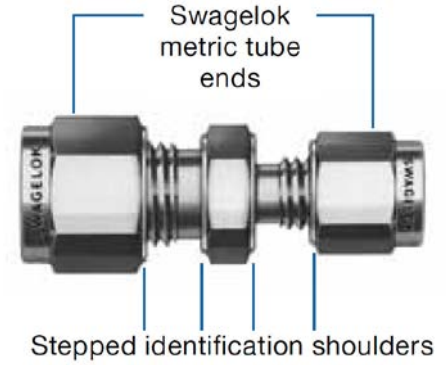

Shaped fittings, such as elbows, crosses, and tees, are stamped MM for metric tubing and have no step on the forging.

Safety Precautions

- Do not bleed system by loosening fitting nut or fitting plug.
- Do not assemble and tighten fittings when system is pressurized.
- Make sure that the tubing rests firmly on the shoulder of the tube fitting body before tightening the nut.
- Do not mix materials or fitting components from various manufacturers—tubing, ferrules, nuts, and fitting bodies.
- Never turn fitting body. Instead, hold fitting body and turn nut.
- Avoid unnecessary disassembly of unused fittings.

Swagelok Tube Fittings Up to 1 in./25 mm

These instructions apply both to traditional fittings and to fittings with the advanced back-ferrule geometry.

1. Fully insert the tube into the fitting and against the shoulder
rotate the nut finger-tight.

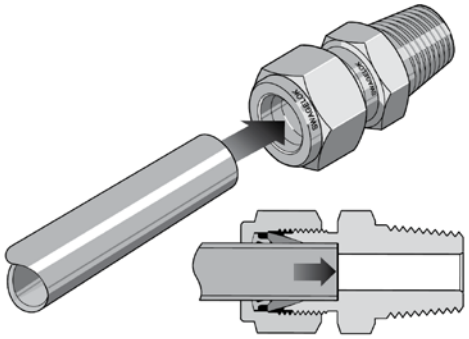

2. Mark the nut at the 6 o’clock position.

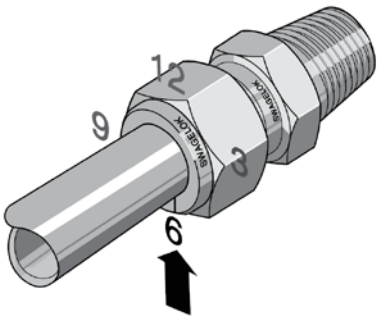

3. While holding the fitting body steady, tighten the nut one and one quarter turns to the 9 o’clock position.

For 1/16, 1/8, and 3/16 in.; 2, 3, and 4 mm tube fittings, tighten the nut threequarters turn to the 3 o’clock position.

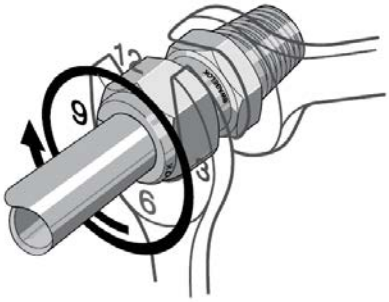

Reassembly—All Sizes

You may disassemble and reassemble Swagelok tube fittings many times.
Always depressurize the system before disassembling a Swagelok tube fitting.

Prior to disassembly, mark the tube at the back of the nut; mark a line along the nut and fitting body flats.
Use these marks to ensure that you return the nut to the previously pulled-up position.

Insert the tube with preswaged ferrules into the fitting until the front ferrule seats against the fitting body.

While holding the fitting body steady, rotate the nut with a wrench to the previously pulled-up position, as indicated by the marks on the tube and flats. At this point, you will feel a significant increase in resistance. Tighten the nut slightly.

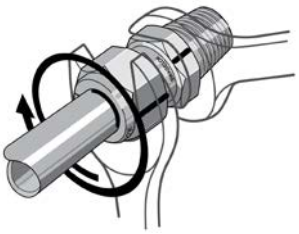

Appendix I. DOCUMENT REVISION HISTORY

The following table includes the document revision history. Document version is identified by date.

Date	Description	Changes
10/11/2016	First draft sent to participants and CCT-WG/Hu.	
26/11/2016	Second draft sent to participants	Addressing comments of PTB, BEV/E+E and NMIJ.
14/12/2016	Revised version submitted to CCT WG.KC	Addressing comments of CCT. WG-KC Additional section on Swagelok fittings
21/12/2016	Revised version submitted to CCT WG.KC	Addressing comments of CCT. WG-KC Clarification of spare head and section 4.1.13
22/02/2017	Final version approved by CCT WG.KC	Section 4.1.13 reverted to that of 14/12/2016 (including footnote)